



**HAL**  
open science

# Linear energy relations for biomass transformation under heterogeneous catalysis : a fast prediction of polyalcohol dehydrogenation on transition metals

Jérémie Zaffran

► **To cite this version:**

Jérémie Zaffran. Linear energy relations for biomass transformation under heterogeneous catalysis : a fast prediction of polyalcohol dehydrogenation on transition metals. Other. Ecole normale supérieure de lyon - ENS LYON, 2014. English. NNT : 2014ENSL0891 . tel-00992665

**HAL Id: tel-00992665**

**<https://theses.hal.science/tel-00992665>**

Submitted on 19 May 2014

**HAL** is a multi-disciplinary open access archive for the deposit and dissemination of scientific research documents, whether they are published or not. The documents may come from teaching and research institutions in France or abroad, or from public or private research centers.

L'archive ouverte pluridisciplinaire **HAL**, est destinée au dépôt et à la diffusion de documents scientifiques de niveau recherche, publiés ou non, émanant des établissements d'enseignement et de recherche français ou étrangers, des laboratoires publics ou privés.

## THÈSE

en vue de l'obtention du grade de  
**Docteur de l'Université de Lyon, délivré par  
l'École Normale Supérieure de Lyon**

**Discipline: CHIMIE**

**Laboratoire de Chimie**

**École Doctorale de Chimie de Lyon**

présentée et soutenue publiquement le 30 avril 2014

par Monsieur Jérémie ZAFFRAN

**Linear energy relations for biomass transformation under  
heterogeneous catalysis:**

*A fast prediction of polyalcohol dehydrogenation on  
transition metals*

*Directeur de thèse: M. Philippe SAUTET*

Devant la commission d'examen formée de :

- Mme Céline CHIZALLET, *IFP Energies Nouvelles*, Examineur
- M. Peijun HU, *Queen's University of Belfast*, Rapporteur
- Mme Carine MICHEL, *ENS Lyon*, Co-encadrant
- M. Jean-François PAUL, *Université de Lille 1*, Rapporteur
- M. Philippe SAUTET, *ENS Lyon*, Directeur

*A mes parents,  
Leur enfant reconnaissant...*

## **Remerciements Personnels**

Je dédie cette thèse à l'ensemble des membres de ma famille, à tout ceux qui ont espéré et qui y ont cru. Mes pensées vont d'abord à mon père, décédé l'an dernier, trop tôt pour voir aboutir ce projet qui lui tenait tant à cœur. A ma mère, pour s'être investi tant financièrement que moralement, ainsi que pour avoir su me raffermir et m'épauler dans les moments de doutes et de difficultés rencontrés au cours de cette aventure. Je n'oublie bien sûr pas mes petits frères Nathaniel et Emmanuel, et leurs familles respectives, pour leur soutien psychologique à de nombreux égards ces dernières années, ainsi que pour avoir partagé avec moi cet instant de bonheur.

## **Acknowledgments**

I warmly acknowledge my supervisor Philippe Sautet for his guidance, his moral support and his encouragement all along this thesis. Carine Michel is also acknowledged for her precious instructions and her help especially in the use of the various computation software programs. Françoise Delbecq's advice, and the many discussions we had with her were extremely fruitful for the achievement of this work. I thank Paul Fleurat-Lessart and David Loffreda for their help in VASP code and in the computation of transition states. This work would not have been possible without Christian Melkonian in the technical staff and without the various components of the whole axis of theoretical chemistry. I finally acknowledge few of our experimental collaborators, especially Joanna Matras-Michalska and Agnieszka Ruppert from Lodz University Of Technology (Poland), and also Catherine Pinel from Ircelyon (France). To conclude, this thesis was financially supported by "Agence Nationale de la Recherche" (ANR), and the computational resources were provided by PSMN and GENCI.

**Linear energy relations for biomass transformation under heterogeneous catalysis:  
*A fast prediction of polyalcohol dehydrogenation on transition metals***

Keywords: biomass, glycerol, polyalcohols, alcohol dehydrogenation, metallic catalysts, Brønsted-Evans-Polanyi type relationships, DFT

## **Abstract**

Biomass valorization is an interesting alternative to fossil resources, which is frequently performed via heterogeneous catalysis. Designing new catalysts is a challenging task that can be significantly accelerated *in silico*. However, biomass molecules are often complex and highly oxygenated, hence rendering calculations more difficult and time consuming. Among these compounds, polyols are particularly important. We developed linear relations of the Brønsted-Evans-Polanyi (BEP) type from the DFT study of C-H or O-H bond dissociation elementary steps for a family of monoalcohol molecules on metallic catalysts (Co, Ni, Ru, Rh, Pd, Ir, Pt). Such relations aim at predicting activation energies from reaction energies. The accuracy of the obtained linear energy models is better than 0.10 eV on the sampling set. Then, the relations were applied for the prediction of the dehydrogenation elementary steps of glycerol, chosen as a prototype of polyalcohols, with an accuracy better than 0.10 eV and with a systematic error around  $\pm 0.10$  eV for Rh. Keeping in mind that the main difference between glycerol and monoalcohols comes from intramolecular H-bonds present in the former, we designed linear relations for water-assisted dehydrogenation of monoalcohols. These new relations allowed us improving the prediction of glycerol reactivity and eliminating the systematic deviation in the case of OH bond breaking. Even if in this study we only focused on glycerol dehydrogenation, similar methods may be applied to other polyols with other chemical reactions, and considerably speed up the computational design of solid catalysts. This work paves the way for the development of novel numerical techniques to address the issue of biomass conversion.

## Relations d'énergie linéaires pour la transformation de la biomasse en catalyse hétérogène:

### *Une méthode de prédiction rapide de la déshydrogénation des polyalcools sur les métaux de transition*

Mots-clefs: biomasse, glycérol, polyalcools, catalyseurs métalliques, déshydrogénation des alcools, relations de type Brønsted-Evans-Polanyi, DFT

## Résumé

La valorisation de la biomasse est une alternative intéressante aux ressources fossiles, et s'effectue fréquemment en catalyse hétérogène. L'élaboration de nouveaux catalyseurs est une tâche ardue qui peut être considérablement accélérée *in silico*. Cependant, les molécules de la biomasse sont souvent complexes et hautement oxygénées, rendant ainsi les calculs plus difficiles et coûteux en temps. Parmi ces composés, les polyols sont particulièrement importants. Nous avons développé des relations du type Brønsted-Evans-Polanyi (BEP) à partir d'une étude DFT menée sur une famille de monoalcools concernant les dissociations des liaisons C-H et O-H sur des catalyseurs métalliques (Co, Ni, Ru, Rh, Pd, Ir, Pt). Ces relations ont pour but de prédire l'énergie d'activation d'une étape élémentaire à partir de son énergie de réaction. La précision obtenue par ces modèles linéaires est supérieure à 0.10 eV pour l'échantillon considéré. Ces relations ont ensuite été appliquées aux étapes élémentaires de la déshydrogénation du glycérol, choisi comme polyol prototype. On observe une erreur moyenne inférieure à 0.10 eV et une erreur systématique de l'ordre de  $\pm 0.10$  eV sur Rh. Etant donné que la principale différence entre les monoalcools et le glycérol, vient des liaisons H intramoléculaires présentes dans celui-ci, nous avons mis en place des relations linéaires pour prédire la déshydrogénation des monoalcools assistée par l'eau. Ces nouvelles relations nous ont permis d'améliorer la prédiction de la réactivité du glycérol et même d'éliminer la déviation systématique dans le cas de la rupture de la liaison OH. Même si dans cette étude nous nous sommes focalisés en particulier sur la déshydrogénation du glycérol, des méthodes similaires pourraient être appliquées à d'autres polyols avec d'autres réactions chimiques. La recherche de catalyseurs solides se trouvant ainsi grandement facilitée, ce travail pave la route pour le développement de nouvelles techniques numériques pour aborder la question de la conversion de la biomasse.

<b>Introduction</b> .....	<b>9</b>
<b>Chapter 1: Review of the literature</b> .....	<b>15</b>
<b>1 On alcohol reactivity under heterogeneous catalysis</b> .....	<b>15</b>
1.1 Glycerol hydrogenolysis .....	15
1.2 Simple alcohol dehydrogenation .....	18
<b>2 Fast prediction of activation energies</b> .....	<b>21</b>
2.1 From DFT to linear energy relations.....	21
2.2 BEP relation: basics .....	22
2.3 Various types of BEP relation.....	24
2.4 BEP type relations for dehydrogenation reactions in the literature.....	29
<b>3 Basics of Statistics</b> .....	<b>31</b>
3.1 Linear regression: the issue of the restricted size samples .....	31
3.2 Tools for error analysis.....	32
3.3 From sample to population .....	34
<b>Conclusion</b> .....	<b>36</b>
<b>Chapter 2: Predicting polyalcohol reactivity from simple alcohols</b> .....	<b>40</b>
<b>Chapter 3: Prediction of monoalcohol dehydrogenation on transition metals</b> ...	<b>47</b>
<b>Introduction</b> .....	<b>47</b>
<b>1 Monoalcohol dehydrogenation on transition metals: basics</b> .....	<b>48</b>
1.1 Selection of a representative subset of reactions .....	48
1.2 Adsorption of alcohol dehydrogenation intermediates and products .....	50
1.3 Thermodynamics and kinetics.....	56
<b>2 Global BEP-type relations</b> .....	<b>59</b>
2.1 Statistical analysis .....	59
2.2 Early and late TS: the impact on BEP-type relations.....	62
<b>3 On the quality of the BEP predictions</b> .....	<b>65</b>
3.1 Reaction dependent models.....	65
3.2 Metal dependent models .....	67
<b>Conclusion</b> .....	<b>71</b>
<b>Chapter 4: Water-assisted dehydrogenation of monoalcohols on transition metals</b> ....	<b>72</b>
<b>Introduction</b> .....	<b>72</b>
<b>1 Thermodynamics and reactivity</b> .....	<b>72</b>
1.1 Configuration of water and co-adsorbates on metallic surfaces.....	73
1.2 Water impact on monoalcohol reactivity.....	75
<b>2 Linear energy relations for water-assisted dehydrogenation</b> .....	<b>79</b>
2.1 Metal and reaction dependent water effect .....	80
2.2 On the quality of the BEP predictions.....	82
2.3 The consequences of water co-adsorption on the TS nature .....	84
<b>Conclusion</b> .....	<b>85</b>
<b>Chapter 5: Using BEP relations to address polyol reactivity on Rh and Pt</b> .....	<b>86</b>
<b>Introduction</b> .....	<b>86</b>
<b>1 Predicting polyol reactivity: the tools and their limitations</b> .....	<b>87</b>
1.1 Glycerol conversion on metallic catalysts: context of the project .....	87
1.2 Improving the prediction of CH and OH dissociation barriers for glycerol .....	90
1.3 Using the BEP relation to predict dehydrogenation paths.....	92
<b>2 Predicting polyol dehydrogenation products on Rh and Pt</b> .....	<b>96</b>
2.1 Glycerol dehydrogenation on Pt.....	96
2.2 1,2-PDO dehydrogenation .....	98
<b>3 Glycerol conversion into lactic acid: Rh or Pt?</b> .....	<b>101</b>
<b>Conclusion</b> .....	<b>103</b>

<b>Summary and perspectives .....</b>	<b>104</b>
<b>Appendix 1: Supplementary Information related to Chapter 2 .....</b>	<b>107</b>

# Introduction

---

From energy needs to organic material synthesis, petroleum has a central role in modern society. However, fossil resources are limited by definition and their exploitation is responsible for the emission of various undesirable gases and especially of carbon dioxide, a well-known greenhouse gas. Faced with this situation, biomass is an interesting alternative. This term refers to « *every material produced by the growth of microorganisms, plants or animals* ». <sup>1</sup> Biomass is abundant and its transformation gives access to many key products for chemical industry. Nevertheless, the few conversion processes already available are still expensive and many efforts are required to develop efficient technologies and to make biomass feedstock competitive comparatively to crude oil. <sup>2</sup> Among the huge variety of valuable molecules, polyols and glycerol in particular are especially important. Indeed, due to their high functionalization those species are real platform structures potentially leading to many chemicals and building blocks useful in polymer manufacture for example. <sup>3,4</sup> The only condition is to understand and to master their reactivity. However, biomass behavior is fundamentally different from petroleum and hence sets new challenges for chemists. Unlike to hydrocarbons, which contain limited functionality, biomass-derived compounds are highly oxygenated and excessively functionalized such as carbohydrates. While in petroleum-derived feeds functional group must be added selectively to produce chemical intermediates, carbohydrates must be selectively deoxygenated in order to be valuable. Besides, petroleum processes are usually conducted at high temperature and in vapor phase. On the contrary, biomass is usually treated at mild temperature and in aqueous or organic liquid phase. <sup>5</sup> As a result, biomass transformation requires a better understanding of those reactions and the development of new efficient catalysts. Computational chemistry tools can considerably facilitate this task. However, designing catalysts *in silico* is particularly hard especially for heterogeneous catalysis with such complex molecules. Indeed, due to the size of these systems but also to their different chemical functions and to their flexibility, they can adopt a huge number of conformations. As a consequence, calculations are extensive and extremely time-consuming mainly for transition states optimizations. Hence, it is a necessity to look for new methods to accelerate the research procedure.

Glycerol is a triol, and despite the limited size its skeleton (only three carbon atoms), this system is still associated to a considerable space of configurations both in the gas phase<sup>6</sup> and on surfaces<sup>7</sup>. Its most stable conformation in the gas phase is represented in **Figure 0-1**. All those conformers are stabilized by intramolecular hydrogen bonds occurring between OH groups and constitute local energetic minima, leading to a very complex potential energy surface.

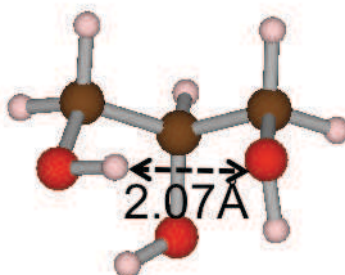


**Figure 0-1: Ball & sticks representation of the most stable conformation of glycerol in the gas phase.** Brown balls are C, red ones are O and pink ones are H. Optimization performed VASP software using PW91 functional.

One important reaction used to transform glycerol is hydrogenolysis, which produces many added value products. This process is mainly carried out on metallic catalysts in liquid phase,<sup>2,3,8,9,10</sup> and it was evidenced that dehydrogenation is the first step of glycerol hydrogenolysis on Rh.<sup>11</sup> However, even if one restricts the study of glycerol reactivity to the first and to the second step of the dehydrogenation reaction, many pathways are still imaginable. Indeed, under the assumption that two successive dehydrogenations cannot occur on the same atomic center, one counts sixteen potential pathways of glycerol transformation, each of them proceeding through a radical intermediate (see **Figure 0-2**). Moreover, it is unclear whether the reactive structure is the most stable conformation or not, and all reactants and products must be adapted to the different transition state structures of the paths to which they are connected. It stems from these considerations that a terrific amount of conformations are necessary to study only two elementary steps and this just for a simple triol conversion. Polyol reaction networks are thus very complex and one needs an efficient tool in order to screen quickly the multiple reaction steps on one given catalyst. Repeating the operation on various solid surfaces allows identifying best catalysts for a given reaction.

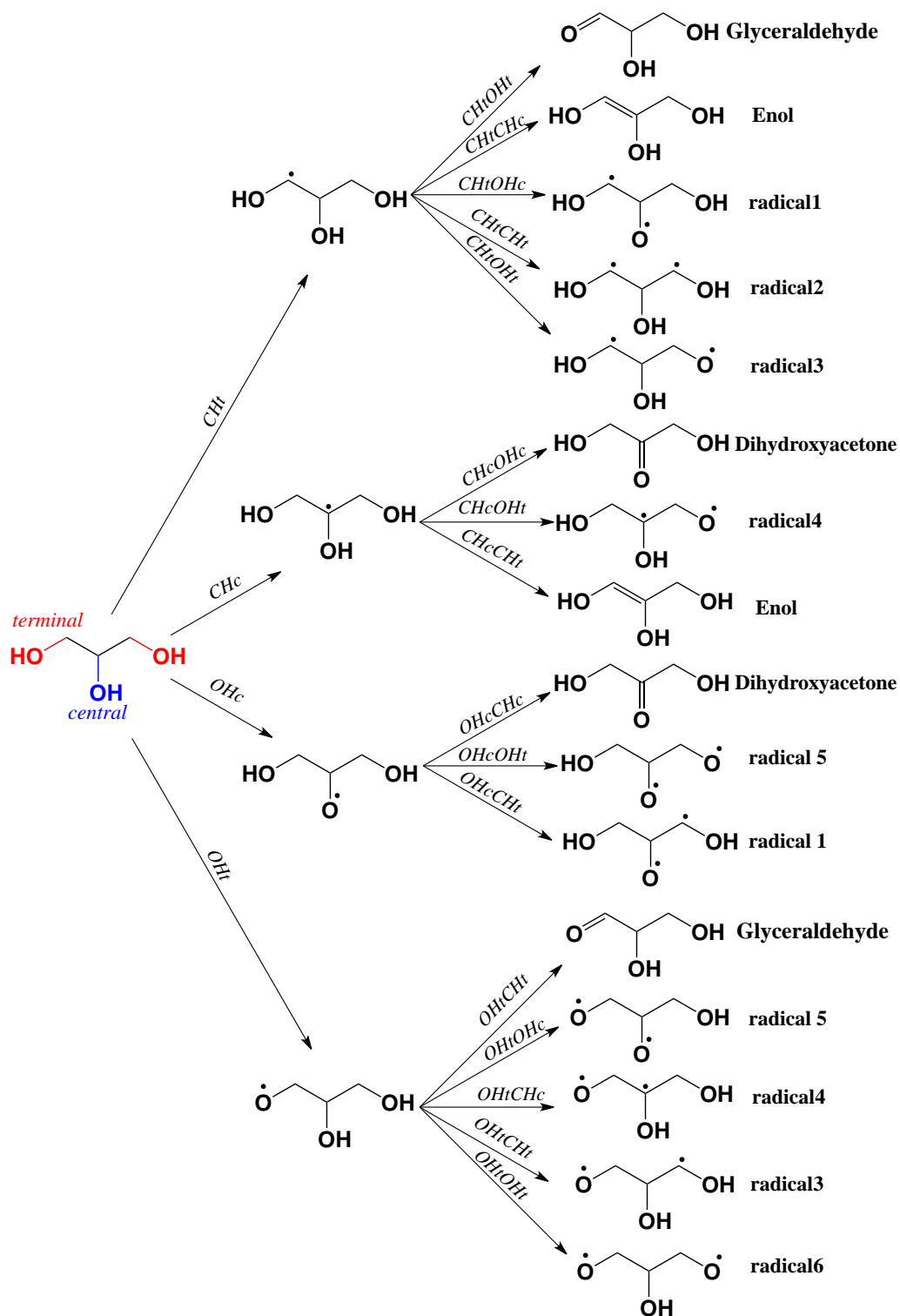


**Figure 0-2: Reaction network for glycerol dehydrogenation (first and second steps).** The *c* index (CHc/OHc) denotes central groups and the *t* index (CHt/OHt) terminal groups. Several pathways may give the same products, but their configurations on the surface depend on the path from which one they are produced. That is why, even if only nine final different products are depicted here, a very large number of conformers must be calculated.

Studying reactivity requires probing as deeply as possible a potential energy surface, with its multiple wells, peaks and cols. Several approximations may be used to prevent first principle calculations and thus to save a precious time. Three of them are of primary importance namely Group Additivity (GA), Linear Scaling Relation (LSR) and Brønsted-Evans-Polanyi (BEP) correlations.<sup>12</sup> The first one determines binding energy of molecules in the gas phase. The second one, LSR, is based on a linear relation between binding energies on solid surfaces of atoms and of molecular fragments constituted by these atoms, giving thus access to adsorption energy of chemical compounds with various sizes. And finally, the BEP correlation aims at deducing for any elementary act, activation energy from a thermodynamic quantity such as reaction energy (see **Figure 0-3**). Those relations are established from DFT calculations on a restricted sample of points. Then, the results provided by these three relations may be integrated into a microkinetic model to conclude about the optimal conditions to conduct a reaction. As a consequence, combining those approximations is a powerful method to accelerate the search for new catalysts and more generally to study the kinetics of a reaction. The approach has been widely used for diatomics and simple molecules.<sup>13,14,15</sup> Nevertheless, such studies are less frequent for large structures, and it may be well adapted to use the same method to predict complex molecule reactivity. For small hydrocarbons and simple alcohols decomposition, typical average errors of BEP type relations predictions vs. DFT calculations range from 0.10 to 0.20 eV according to the screened reactions and surfaces but also to the different authors.<sup>16,17</sup> Such relations that are set from polyols like glycerol lead to similar errors but obviously they are much longer to elaborate.<sup>18</sup>

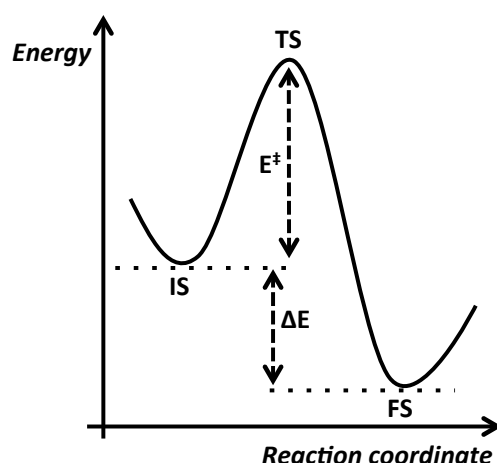


**Figure 0-3:** Generally scheme of an elementary act. The step starts by an initial state (IS) progressing toward a transition state (TS) and finishing with a final state (FS).  $E^\ddagger$  is the activation energy and  $\Delta E$  is the reaction energy

In this thesis, our objective is to establish simple linear energy relations in order to predict polyol reactivity on transition metals, combining thus DFT calculations and BEP-type relations. The originality of this work is to directly apply to a complex alcohol such relationships that are designed for monoalcohols. Taking glycerol dehydrogenation as a prototype system, we will firstly validate the procedure on Rh (111) surface and then we will extrapolate the linear energy relations to other metals. Afterwards, we will strengthen our predictive models by considering the monoalcohol dehydrogenation assisted by a water molecule. In such a way, we will simulate the H bond effect occurring between the OH groups present in polyols. This manuscript is structured in five chapters. Chapter 1 is devoted to a review of the literature concerning alcohols decomposition over metallic catalysts and their corresponding BEP type relations. In chapter 2, we will establish such relations for monoalcohols dehydrogenation on Rh (111) and we will apply them on glycerol. In chapter 3, we will extrapolate those relations to monoalcohols dehydrogenation on several other transition metals. Hydrogen bond effect will be considered in chapter 4, with water-assisted dehydrogenation in monoalcohols. And finally the so-established predictive models will be used in chapter 5 to screen a part of the reaction network of the glycerol hydrogenolysis on some metallic catalysts.

---

<sup>1</sup> IUPAC Recommendations, Pure and Applied Chemistry **1992**, *64*, 143

<sup>2</sup> J. Birtill, G. Centi and R.A. Van Santen, « *Catalysis for Renewables: From Feedstock to Energy Production* », John Willey & Sons: Weinheim **2007**

<sup>3</sup> A. M. Ruppert, K. Weinberg and R. Palkovits, *Angew. Chem. Int. Ed.* **2012**, *51*, 2564 – 2601

<sup>4</sup> M. Pagliaro, R. Ciriminna, H. Kimura, M. Rossi and C. Della Pina, *Angew. Chem. Int. Ed.* **2007**, *46*, 4434 – 4440

<sup>5</sup> J. N. Chheda, G. W. Huber and J. A. Dumesic, *Angew. Chem. Int. Ed.* **2007**, *46*, 7164 – 7183

<sup>6</sup> C. S. Callam, S. J. Singer, T. L. Lowary, C. M. Hadad, *J. Am. Chem. Soc.* **2001**, *123*, 11743-11754

<sup>7</sup> D. Coll, F. Delbecq, Y. Aray, P. Sautet, *Phys. Chem. Chem. Phys.* **2011**, *13*, 1448.

<sup>8</sup> E. P. Maris, W. C. Ketchie, M. Murayama and R. J. Davis, *J. Catal.* **2007**, *251*, 281 - 294

<sup>9</sup> J. Chaminand, L. Djakovitch, P. Gallezot, P. Marion, C. Pinel and C. Rosier, *Green Chem.*, **2004**, *6*, 359–361

<sup>10</sup> C. Zhou, J. N. Beltramini, Y. Fan and G. Q. Lu, *Chem. Soc. Rev.* **2008**, *37*, 527–549

<sup>11</sup> F. Auneau, C. Michel, F. Delbecq, C. Pinel and P. Sautet, *Chem. Eur. J.* **2011**, *17*, 14288 – 14299

- 
- <sup>12</sup> J. E. Sutton and D. G. Vlachos, *J. Catal.* **2013**, *297*, 202–216
- <sup>13</sup> T. Bligaard, J. Norskov, S. Dahl, J. Matthiesen, C. Christensen and J. Sehested, *J. Catal.* **2004**, *224*, 206-217
- <sup>14</sup> A. Michaelides, Z. Liu, C. Zhang, A. Alavi, D. King and P. Hu, *J. Am. Chem. Soc.* **2003**, *125*, 3704-3705
- <sup>15</sup> R. A. Van Santen, M. Neurock and S. G. Shetty, *Chem. Rev.* **2010**, *110*, 2005-2048
- <sup>16</sup> S. Wang, V. Petzold, V. Tripkovic, J. Kleis, J. G. Howalt, E. Skulason, E. M. Fernandez, B. Hvolbaek, G. Jones, A. Toftelund, H. Falsig, M. Bjorketun, F. Studt, F. Abild-Pedersen, J. Rossmeisl, J. K. Norskov and T. Bligaard, *PCCP* **2011**, *13*, 20760-20765
- <sup>17</sup> J. E. Sutton and D. G. Vlachos, *ACS Catal.* **2012**, *2*, 1624-1634
- <sup>18</sup> B. Liu and J. Greeley, *J. Phys. Chem. C* **2011**, *115*, 19702-19709

# Chapter 1: Review of the literature

---

Biomass reactivity has been extensively studied in the literature during the last decades, both experimentally and theoretically. Polyalcohols occupy a large part in this chemistry and various techniques are available to simplify calculations of such complex compounds. In this chapter, we will review some important works on alcohol reactivity, including glycerol, considered as a model polyol, and monoalcohols. Then we will focus on the Brønsted-Evans-Polanyi relationship from its funding principles to some of its recent applications. This method allows a considerable timesaving in the computation of activation energies for large systems. Finally, we will present some basics of Statistics, since such considerations are tightly related to linear energy relations.

## 1 On alcohol reactivity under heterogeneous catalysis

Many processes are available in industry to transform alcohol. Hydrogenolysis is one of them. It is generally performed on metallic catalysts, and leads to various products according to the metal selectivity and activity. Environmental parameters such as the solvent nature, the operating temperature, the pH of the solution or the nature of the support are also determining for the reaction. Several common points exist between complex alcohols like glycerol and monoalcohols.

### 1.1 Glycerol hydrogenolysis

#### 1.1.1 Short review of some experimental works

Glycerol is a by-product of biodiesel production easily obtained from vegetable oils. It can be considered as a real platform molecule providing its selective functionalization is possible.<sup>1,2</sup> Hydrogenolysis of glycerol, which typically consists of a bond scission under H<sub>2</sub> atmosphere, can be performed using various types of catalysts (see **Table 1-1**). Metals and alloys have often been used supported over different materials.<sup>2</sup> Polyol hydrogenolysis mechanism combines both dehydration and dehydrogenation steps. The main challenge is the selective breaking of C-O or C-C bonds. Noble metals, such as Rh and Ru, are usually very active for

this task, but not always selective. They can split the glycerol skeleton into a huge variety of products and by-products as ethylene glycol (EG), lactic acid (LA) and various small hydrocarbons. To the opposite, Cu, which is not efficient for C-C breaking, is very selective to propanediols.<sup>3</sup> The catalyst activity and to a certain extent also its selectivity, are closely related to the metal environment. The pH of the solution, but also the acidity of the support can highly impact the reaction. Indeed, it was shown that alkaline medium enhances Pt activity,<sup>4</sup> and that an acidic support favors the dehydration steps, hence affecting the catalyst selectivity.<sup>5</sup> To conclude, let us mention that bimetallic combinations are also used for glycerol conversion. Such catalysts are very active and tend to diminish the C-C bond breaking, and thus favoring dehydrogenation reactions.<sup>6</sup>

Catalysts	Main product	Selectivity (%)	Conversion (%)	Ref.
<b>Raney Cu</b>	1,2-PDO	78	85	7
<b>Cu/ZnO</b>	1,2-PDO	100	19	8
<b>Cu/C</b>	1,2-PDO	85	43	9
<b>Cu/Al<sub>2</sub>O<sub>3</sub></b>	1,2-PDO	94	34	10
<b>Ru/ Al<sub>2</sub>O<sub>3</sub></b>	1,2-PDO	47	34	11
<b>Ru/TiO<sub>2</sub></b>	1,2-PDO	47	66	11
<b>Ru/C</b>	EG	47	40	12
<b>Ru/C, NaOH</b>	LA	34	100	12
<b>Pd/Fe<sub>2</sub>O<sub>3</sub></b>	1,2-PDO	94	100	13
<b>Pt/sulfated ZrO<sub>2</sub></b>	1,3-PDO	84	67	14
<b>Ru-Re/SiO<sub>2</sub></b>	1,2-PDO	45	51	15
<b>Pt-Re/C</b>	1,3-PDO	34	20	16
<b>Ni-Ce/C</b>	1,2-PDO	63	77	17

**Table 1-1: Some important metal supported catalysts used for glycerol conversion.** For each catalyst we presented the selectivity of the main product and the conversion of glycerol. PDO: propanediol, EG: ethylene glycol, LA: Lactic Acid

### 1.1.2 Theoretical contributions and importance of dehydrogenation

Many theoretical groups are also involved in the study of glycerol hydrogenolysis. Sautet and co-workers showed that dehydration intermediates are strongly adsorbed on transition metals, hence rendering the reaction much more exothermic on solid surfaces than in the gas phase.<sup>18</sup>

They also evidenced that the relative stability of the various intermediates depends on the metal nature, which is responsible for the different selectivity of the catalysts. Besides, according to Greeley and Liu, while noble metals are in general very active in glycerol decomposition, some of them such as Pt and Pd are more selective towards C-C bond activation than C-O bond.<sup>19</sup> They also explained in the same paper that Cu is very selective towards C-H/O-H scissions, in agreement with the previous experimental section. The metal oxide support has also an important role in the catalyst selectivity, since it determines the proportion of 1,2-PDO vs. 1,3-PDO on Cu catalyst.<sup>20</sup>

In tight collaboration with experimentalists, Sautet's group of research is involved in an ongoing project aiming at producing LA from glycerol. Various complex mechanisms are conceivable depending on the catalyst and the experimental conditions, the first step being either dehydration or dehydrogenation. Considering Rh catalyst, Auneau *et al.*<sup>21</sup> evidenced from DFT calculations that dehydration step is kinetically disfavored comparatively to dehydrogenation. Some of their experimental observations, performed on Rh/C catalyst in alkaline medium, confirmed this conclusion. They showed in particular that glycerol conversion is significantly enhanced under He atmosphere comparatively to H<sub>2</sub>. They finally proposed the following mechanism (see **Figure 1-1**). After a first dehydrogenation step, glycerol is transformed into glyceraldehyde (GAL), which is dehydrated in basic conditions into an enol. The latter, unstable in solution, spontaneously evolves towards pyruvaldehyde (PAL) giving finally either LA or 1,2-PDO through acetol intermediate. Hydrogenation/dehydrogenation steps thus occur at various stages of the mechanism and this is the starting point of this thesis. Due to the particular importance of this reaction, we will exclusively deal in the following with C-H and O-H dissociations.

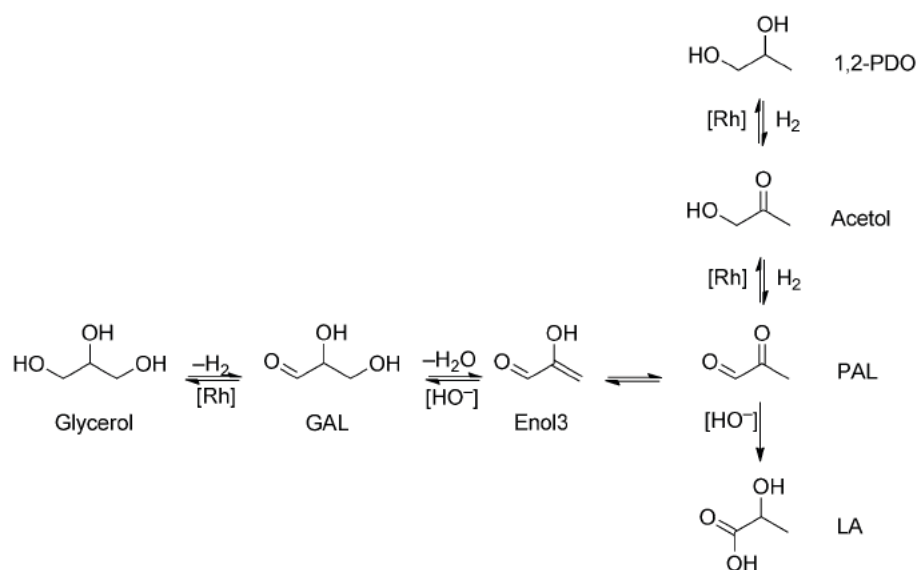


**Figure 1-1: Glycerol conversion into lactic acid.** GAL: glyceraldehyde, PAL: pyruvaldehyde, LA: Lactic Acid. (Figure taken from Ref.21)

## 1.2 Simple alcohol dehydrogenation

### 1.2.1 Metal catalyzed dehydrogenation in the gas phase

Dehydrogenation is a key reaction occurring in many chemical processes of biomolecule transformation, such as steam reforming. This technique allows the production of hydrogen gas, through the decomposition of various kinds of molecules. It is especially used for monoalcohols and in particular for ethanol and generally performed in the gas phase. Many DFT studies focused on ethanol reforming.<sup>22,23,24</sup> As for glycerol hydrogenolysis, this reaction is also catalyzed by transition metals. According to Wang *et al.*,<sup>25</sup> the catalyst activity is related to its redox properties, which is directly correlated to the electronic density of states (DOS). An efficient metallic catalyst should present a broad and high DOS around the Fermi level. In such conditions, the metal can act as an electron reservoir, accepting or donating electrons to the adsorbates. This can explain why noble metals such as Rh, Pt, Ir or Pd (presenting an extended DOS) are especially active and why others such as Cu, Ag or Au (presenting a contracted DOS) are much less active.<sup>25</sup> In spite of their poor activity, the latter catalysts are very selective towards C-H and O-H breaking (as for glycerol). Thus the carbon skeleton is barely attacked and the reaction may stop after few dehydrogenation steps. To the opposite, for Ir or Pt, the reaction can hardly end before the complete decomposition of the molecule, producing not only hydrogen gas but also coke and carbon monoxide. These

theoretical conclusions are also observed experimentally not only on ethanol but also on methanol and can probably be extended to many other simple alcohols.<sup>26,27</sup>

## 1.2.2 Water-assisted dehydrogenation

The water promoting effect on dehydrogenation was already demonstrated experimentally,<sup>28</sup> and explained theoretically<sup>29</sup> on catalytic alcohol oxidation on Pt. In the DFT framework, we mainly distinguish two ways to deal with the solvent. In the first one, the aqueous solvent is modeled by multilayers of water molecules, arranged in a hexagonal structure similarly to ice.<sup>30,31</sup> Several water molecules are weakly adsorbed at the interface metal/solvent, and establish H-bonds with other adsorbed molecules or with molecules belonging to the solvent layers. Let us call it the “multilayers model”. In the second method, one considers a co-adsorbed system with only one water molecule and one alcohol molecule, connected together by a H-bond.<sup>32</sup> This is called “micro-solvation model”. We observed that both models lead to consistent results, with the only difference that on certain metals, OH activation barriers are slightly lower for the micro-solvation model than for the multi-layer model. In this thesis we only used the micro-solvation model to treat the solvent.

In the micro-solvation model, the configuration of the species on the surface is determinant for reactivity, as developed by Michel *et al.*<sup>32</sup> In their study, they considered water-assisted dehydrogenation on Rh. Ethanol and water can adopt two distinct configurations depicted in **Figure 1-2**. In the first one, the water molecule is linked to the metal, while EtOH is H-bonded with water and not directly connected to the surface. This configuration is designed as “EtOH acceptor”, since the ethanol molecule accepts the H-bond. In the second adsorption mode, it is the opposite. Now, EtOH is adsorbed and the water molecule is H-bonded to EtOH. This configuration is designed as “EtOH donor”, since the ethanol molecule donates the H-bond. Concerning OH scission in EtOH, only the configuration “EtOH acceptor” presents the O-H bond in the optimal position toward the metal. In such a conformation, the structure is pre-organized to undergo the OH scission. That is why OH breaking is activated by water. To the opposite, the CH bond is not well positioned with respect to the metal, hence the CH inhibition. In fact, CH is only slightly inhibited in both configurations, and the water effect on CH breaking activation barriers is much lower than for OH dissociations. In the following of this thesis, water-assisted dehydrogenation of alcohols will be exclusively considered under the “alcohol acceptor” configuration.

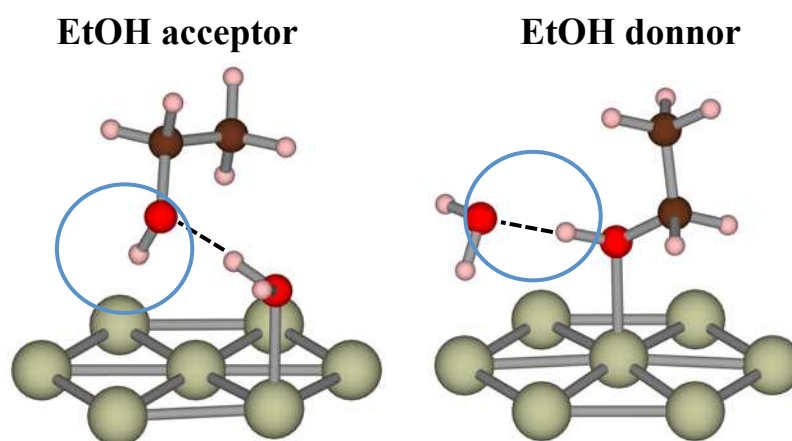


**Figure 1-2: The two configurations of EtOH-H<sub>2</sub>O on Rh (111).** In “EtOH donor” configuration, the ethanol OH bond is engaged in an H-bond with water, hence rendering its scission not favorable. In “EtOH acceptor”, the ethanol OH bond points towards the surface, whereas CH bonds points in the opposite direction. That is why in ethanol OH breaking is activated and CH breaking is inhibited. Greenish: Rh; Red: O; Brown: C, Pink: H

As a conclusion, we saw that simple alcohols and glycerol dehydrogenation proceeds on similar metallic catalysts. All the metals do not exhibit the same efficiency, and their activity is related to the adsorption strength of molecules on their surfaces. This relation between thermodynamics and kinetics is one important concept of Chemistry that has been extensively debated during the last century. Its founding principles and its various usages are presented in the next section.

## 2 Fast prediction of activation energies

Solid catalyst design can be considerably speeded up owing to computational tools. Nevertheless, transition states calculation is hard and tedious task. Various techniques are available in the literature in order to bypass this difficulty, but their accuracy is a major issue.<sup>33</sup>

### 2.1 From DFT to linear energy relations

In a multiscale-modeling framework, one distinguishes mainly three stages: the microscopic level, the mesoscopic level and the macroscopic level.<sup>34</sup> The size of the studied system, the time scale of the phenomenon that is described and the accuracy that is required determine the modeling techniques to use. At the meso- and macroscale, one deals with the global behavior of all the system components. The goal is to optimize the reaction rates and the reactor performance. The various parameters that are necessary for this task, such as activation energies or reaction energies, are estimated at the microscopic scale (see **Figure 1-3**). *Ab initio* calculations, and especially DFT, are particularly important since they give directly access to rare events such as transition states (TS). However, the computational cost of those methods is high, mainly because of the TS optimization. Whether only few days are necessary to reach a TS for small molecules dissociation (diatomics, small hydrocarbons, alcohols with one or two carbon atoms...), many weeks of calculations may be required for more complex systems (polyols with three carbon atoms or more, long and non linear hydrocarbon chains...). This is even more complicated since large and flexible structures can adopt a huge number of configurations.

In order to avoid massive and time-consuming DFT calculations, it is important to find methods to quickly get the main parameters that are required to model a chemical reaction network. Several linear energy relations are available in heterogeneous catalysis to facilitate this search. Firstly, thermochemistry of species in the gas phase can be fast estimated with the method of Group Additivity (GA).<sup>35,36</sup> Secondly, adsorption energies can be easily deduced using the Linear Scaling Relation (LSR).<sup>37</sup> Finally, activation energies for elementary acts are predictable from reaction energies owing to the Brønsted-Evans-Polanyi (BEP) relation.<sup>38,39,40</sup> These three relations combined together, constitute an easy way to design microkinetic models.<sup>41</sup> Such models allow determining the most abundant products deriving from a

complex mechanism, and the optimal catalysts to use for the target reaction. However, all of these predictive methods are affected by some statistical errors depending on the molecules, on the reactions, on the catalysts and on various other parameters. When using those techniques to study reactivity in heterogeneous catalysis, it is a necessity to know how accurate they are and to control the error generated by the models. In this thesis, we exclusively focused on BEP type relations standing for alcohol dehydrogenation on metallic catalysts.

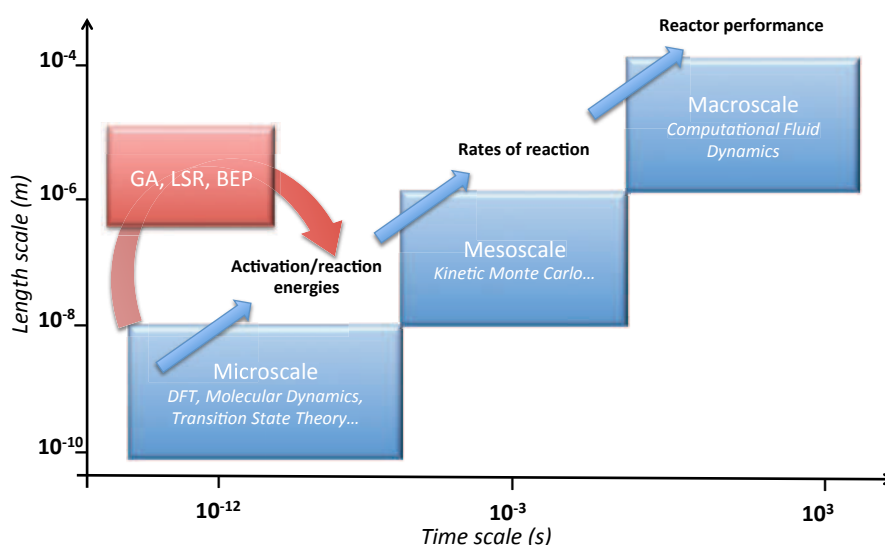


**Figure 1-3:** Global scheme of some major modeling techniques for heterogeneous catalysis. Linear energy relations allow avoiding massive DFT calculations.

## 2.2 BEP relation: basics

The question to know whether a mathematical relation between activation energies and reaction energies exists or not, was debated for a long time. At the beginning of the last century, some chemists evidenced the existence of a relation between thermodynamics and kinetics experimentally. Bell<sup>39</sup> and Brønsted<sup>38</sup> were able to link the strength of an acid catalyst and the rate constant of a given chemical reaction. Then, Evans and Polanyi<sup>40</sup> proved that activation energy and reaction energy could be connected by a simple linear relation. Due to these pioneer works, this relation is designed by the initials of their author names, “B.E.P”. During the second part of the 20<sup>th</sup> century, such relations were often used by experimentalists in homogeneous catalysis in various fields.<sup>42,43</sup> However, in the last decade, owing to novel achievements in computational chemistry and to the development of efficient calculation

supercomputers, some theoreticians, such as Liu and Hu,<sup>44</sup> started to investigate BEP relationship for heterogeneous catalysis.

Several theoretical justifications underlie the principle of this relation. One of them is recalled in a recent review by Van Santen *et al.*<sup>45</sup> During an elementary act, the system progresses from an initial state (IS) toward a final state (FS) through a transition state (TS). IS and FS can be viewed as the minimum of a harmonic potential (see **Figure 1-4**), crossing each other at the TS point. One understands easily that while shifting the two harmonic potential one with respect to the other (*i.e.* stabilizing or destabilizing the reactant or the product), the crossing point (*i.e.* the TS energy) is also more or less affected, hence a relation between activation energy and reaction energy. We will admit that this relation is linear, of the type:

$$E^\ddagger = \alpha \cdot \Delta E + \beta \quad \text{Equation 1-1}$$

Where  $E^\ddagger$  and  $\Delta E$  are the activation and reaction energies, respectively. This equation is fitted from a set of data with various  $\Delta E$  and  $E^\ddagger$ .  $\alpha$  and  $\beta$  are the correlation parameters.  $\alpha$  is also called “transfer coefficient” and is a feature of the TS.  $\beta$  is the intrinsic activation barrier, depending on the reaction and on the catalyst.<sup>46</sup>

The transfer coefficient has a physical meaning when it is comprised between 0 and 1. When it is close to 0, the product is more stabilized than the reactant (blue line in **Figure 1-4**). In that case the TS is called “early” because its geometry is close to the IS. To the opposite when the transfer coefficient is close to 1, the product is destabilized with respect to the reactant. Then, the TS is called “late” because its geometry is close to the FS (red line in **Figure 1-4**). Let us mention that those early/late considerations, directly stemming from Hammond postulate,<sup>47</sup> only stand when the force constants of the IS and FS harmonic wells (*i.e.* the opening of the parabolas) are equal to each other. In the following we will consider that in first approximation this condition is always verified, and that every TS can be characterized as early or late. Furthermore, let us mention that according to Hu and co-workers,<sup>48</sup> BEP relationships can be gathered in various classes with respect to their corresponding chemical reactions. Dehydrogenations belong to class I and are generally related to late TS, especially for CH dissociations.

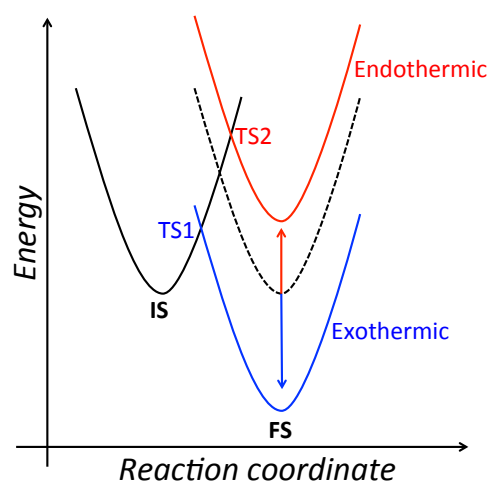


**Figure 1-4: Scheme of an energetic reaction profile.** In an exothermic reaction (blue line) the FS potential is shifted down, hence stabilizing the FS. In this situation the TS (TS1) is geometrically closer to the IS than the FS. In an endothermic reaction (red line) the FS potential is shifted up, hence destabilizing the FS. In this situation the TS (TS2) is geometrically closer to the FS than the IS.

## 2.3 Various types of BEP relation

There are various ways to correlate kinetics and thermodynamics. In the classical manner one connects activation energies and reaction energies. This is the so-called BEP relation. Four directions may be considered for one given reaction: dissociation/association (diss/assoc) and exothermic/endothermic (exo/endo). Each of them is associated to one given BEP relation. Apart from the traditional BEP, one can also correlate the TS energy either with the FS or with the IS energy. This is called a Transition State Scaling (TSS) relation. The four directions described above for the BEP still stand for the TSS, but now another subtlety must be taken into account: the energetic reference. Indeed, energies can refer either to the IS or to the FS in the gas phase. The general notation that we adopted is TSS-diss.FS/FS, “diss” denotes the dissociation direction, the first “FS” denotes the thermodynamics state connected to the TS, and the second “FS” denotes the gas reference. Finally, we count in total twelve BEP-type relations (see **Figure 1-5**): four classical BEP and twelve TSS (TSS-diss.FS/FS is equivalent to TSS-assoc.IS/IS).<sup>49,50,51</sup>

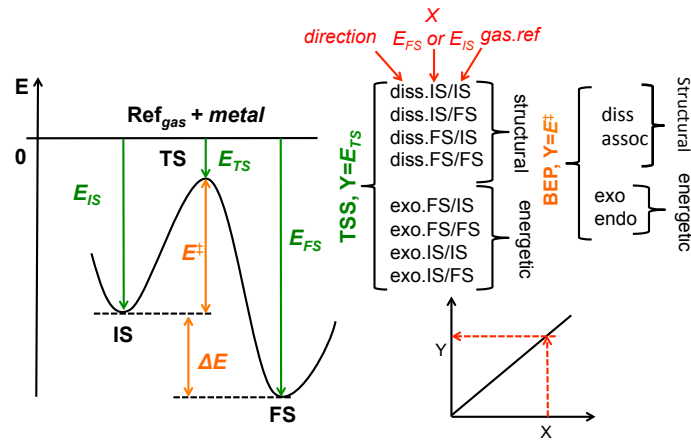


**Figure 1-5: Summary of the 12 BEP type relations, for a generic reaction step.** These relations can be gathered according to structural considerations (dissociation/association) or to energetic considerations (exothermic/endothermic). IS: Initial State, FS: Final State, diss: dissociation, assoc: association, exo: exothermic, endo: endothermic

However, all these relations are not fundamentally different and underlie the same idea, meaning a correlation between kinetics and thermodynamics. Thus, it is important to evidence their similarities and their discrepancies starting from their mathematical expressions. Let us focus firstly on the influence of the reaction direction on the BEP relation. Equation 1-2 and Equation 1-3 give the BEP relation in the dissociation and in the association direction, respectively:

$$E_{diss}^{\ddagger} = \alpha_{diss}^{BEP} \cdot \Delta E_{diss} + \beta_{diss}^{BEP} \quad \text{Equation 1-2}$$

$$E_{assoc}^{\ddagger} = \alpha_{assoc}^{BEP} \cdot \Delta E_{assoc} + \beta_{assoc}^{BEP} \quad \text{Equation 1-3}$$

Where  $E_{diss}^{\ddagger}$  and  $\Delta E_{diss}$  are the activation and reaction energies in the dissociative direction, respectively.  $\alpha_{diss}^{BEP}$  and  $\beta_{diss}^{BEP}$  are the parameter of the corresponding correlation. (Similarly for the association direction.)

Splitting the activation energy and reaction energy in Equation 1-2, we get:

$$E_{TS} - E_{IS} = \alpha_{diss}^{BEP} \cdot (E_{FS} - E_{IS}) + \beta_{diss}^{BEP} \quad \text{Equation 1-4}$$

where  $E_{TS}$ ,  $E_{FS}$  and  $E_{IS}$  are respectively the energies of the IS, FS and TS in the dissociative direction.

Subtracting  $E_{FS}$  from both sides of Equation 1-4, we get:

$$E_{TS} - E_{FS} = (1 - \alpha_{diss}^{BEP}) \cdot (E_{IS} - E_{FS}) + \beta_{diss}^{BEP}$$

$$\Leftrightarrow E_{assoc}^{\ddagger} = (1 - \alpha_{diss}^{BEP}) \cdot \Delta E_{assoc} + \beta_{diss}^{BEP} \quad \text{Equation 1-5}$$

where,  $E_{assoc}^{\ddagger}$  and  $\Delta E_{assoc}$  are respectively activation and reaction energies in the associative direction.

Identifying Equation 1-3 and Equation 1-5, the correlation parameters of the BEP relation in the association direction and in the dissociation direction are thus related as follows:

$$\begin{cases} \alpha_{assoc}^{BEP} = 1 - \alpha_{diss}^{BEP} \\ \beta_{assoc}^{BEP} = \beta_{diss}^{BEP} \end{cases} \quad \text{Equation 1-6}$$

It stems directly from these considerations, that BEP.assoc and BEP.diss have identical error distributions. Similar conclusions are obtained for BEP.exo and BEP.endo.

Now let us compare together BEP and TSS relations regardless of the direction and the energetic reference. A general expression of the BEP and the TSS relation are respectively presented in Equation 1-7 and Equation 1-8:

$$E^{\ddagger} = \alpha^{BEP} \cdot \Delta E + \beta^{BEP} \quad \text{Equation 1-7}$$

$$E_{TS} - E_{Ref} = \alpha^{TSS} \cdot (E_{FS} - E_{Ref}) + \beta^{TSS} \quad \text{Equation 1-8}$$

where  $E_{TS}$ ,  $E_{FS}$  and  $E_{IS}$  are respectively the absolute energies of TS, FS and IS, and  $E_{Ref}$  the energetic reference (including both the gas phase and the bare slab energy).\*

While splitting all the terms of Equation 1-7, one obtains:

---

\* In this chapter, we took care to mention explicitly the energetic reference in all the TSS expressions. But in the following, the energetic reference will be only reminded in the generic designation (TSS-diss.FS/FS) and not in the equation ( $E_{TS} = \alpha \cdot E_{FS} + \beta$ )

$$(E_{TS} - E_{Ref}) - (E_{IS} - E_{Ref}) = \alpha^{BEP} \cdot [(E_{FS} - E_{Ref}) - (E_{IS} - E_{Ref})] + \beta^{BEP}$$

$$\Leftrightarrow (E_{TS} - E_{Ref}) = \alpha^{BEP} \cdot (E_{FS} - E_{Ref}) + \beta^{BEP} + (1 - \alpha^{BEP}) \cdot (E_{IS} - E_{Ref}) \quad \text{Equation 1-9}$$

Identifying Equation 1-8 and Equation 1-9:

$$\left\{ \begin{array}{l} \alpha^{BEP} = \alpha^{TSS} \\ \beta^{TSS} = \beta^{BEP} + (1 - \alpha^{BEP}) \cdot (E_{IS} - E_{Ref}) \end{array} \right. \quad \text{Equation 1-10}$$

As a result, we can see that when the transfer coefficient ( $\alpha^{BEP}$ ) is close to 1, BEP and TSS correlation parameters are equal to each other. Let us mention that this conclusion is still valid when the transfer coefficient is close to 0, but in that case the TSS correlates the TS energy with the IS energy. For other values of the transfer coefficient,  $\beta^{TSS}$  is no more constant and both FS and IS impact the TS energy.

Concerning the quality of the predictions, one can ask if BEP and TSS give predictions of similar accuracy. Let  $\mathcal{E}_{BEP}$  be the error stemming from the BEP relation and  $\mathcal{E}_{TSS}$  the error stemming from the TSS relation. Again this proof is valid regardless the direction of the reaction of the energetic reference.

$$\mathcal{E}_{BEP} = E^\ddagger - \widehat{E}^\ddagger \quad \text{Equation 1-11}$$

$$\mathcal{E}_{TSS} = E_{TS} - \widehat{E}_{TS} \quad \text{Equation 1-12}$$

where  $E^\ddagger$  is the DFT-calculated activation energy and  $\widehat{E}^\ddagger$  is the BEP-predicted activation energy (and similarly for  $E_{TS}$  and  $\widehat{E}_{TS}$ ).

In order to find a relation between  $\mathcal{E}_{BEP}$  and  $\mathcal{E}_{TSS}$ , let us substitute Equation 1-7 in Equation 1-11. Then, when one decomposes activation and reaction energies with respect to TS, IS and FS energies, one gets:

$$\begin{aligned} \varepsilon_{BEP} &= \left( (E_{TS} - E_{Ref}) - (E_{IS} - E_{Ref}) \right) - \left( \alpha^{BEP} \cdot \left( (E_{FS} - E_{Ref}) - (E_{IS} - E_{Ref}) \right) + \beta^{BEP} \right) \\ \Leftrightarrow \quad \varepsilon_{BEP} &= (E_{TS} - E_{Ref}) - \left( \alpha^{BEP} \cdot (E_{FS} - E_{Ref}) + \beta^{BEP} \right) + (1 - \alpha^{BEP}) \cdot (E_{IS} - E_{Ref}) \\ \Leftrightarrow \quad \varepsilon_{BEP} &= \mathcal{E}_{TSS} + (1 - \alpha^{BEP}) \cdot (E_{IS} - E_{Ref}) \end{aligned} \quad \text{Equation 1-13}$$

Hence, when the transfer coefficient ( $\alpha^{BEP}$ ) is close to 1, BEP and TSS errors are similar. Again, let us mention that for a transfer coefficient close to 0, this conclusion is still valid providing one considers the TSS connecting the TS energy and IS energy. For any other transfer coefficient, one can expect some discrepancies between BEP and TSS errors. As a result, we can say in agreement with Sutton *et al.*,<sup>46</sup> that TSS is an approximation of the BEP valid under certain assumptions. Both of these relations should be equivalent for reactions with early TS ( $\alpha^{BEP} \rightarrow 0$ ) or with late TS ( $\alpha^{BEP} \rightarrow 1$ ). Let us mention that with an analogous reasoning we could show that the energetic reference has no influence on the quality of the TSS relation, providing the transfer coefficient is close to 0 or to 1.

Even if TSS and BEP can be equivalent regarding their error distributions, one must highlight few differences. TSS links a TS either with an IS or with an FS. Hence, in order to have a TSS of good quality all the TS must have the same nature, either early or late. TSS relations are thus very sensitive to the TS geometry, and require a set of TS with very similar structures. To the opposite, in the BEP framework both FS and IS are taken into account, since activation energy is correlated to reaction energy. As a result, BEP tolerates some discrepancies up to a certain point between the TS geometries. Even if BEP and TSS are equivalent in a certain limit, potentially BEP should be valid in a larger window.<sup>57</sup> However, even for BEP relation it is necessary to focus on a certain range of energies, else TS structures become too much different.<sup>61</sup> In conclusion, two factors are important to establish a satisfying BEP type relation: to focus on a restricted energetic range, and to use a set of structures with similar geometry.

## 2.4 BEP type relations for dehydrogenation reactions in the literature

Since the 2000's, BEP type relations have been extensively investigated in the literature on various kinds of systems in heterogeneous catalysis. We will focus here especially on some papers related to CH and OH scission on metallic surfaces (see **Table 1-2**).

Ref.	Reactions	Molecules	Type of BEP	Metals	Facets
52	CH	Ethylene	BEP	Pd, Pd/Re, Pd/Au, Pd/Ru	(111)/(0001)
53	OH	Water	BEP	Au, Ni, Cu, Pt, Pd, Ag, Ir, Pd, Rh	(111), (211), (110)
54	OH	Water	BEP	Ru, Co, Rh, Ir, Ni, Pd, Pt	(111)/(0001)
55	CH/OH together	Methanol	TSS	Pt	(111)
56	CH/OH together	Glycerol	TSS	Pt	(111)
57	CH/OH together	Water, Small hydrocarbons	BEP/TSS	Au, Ag, Pt, Pd, Re, Ir, Ru, Rh, Cu, Ni, Co, Mn, Fe	(111), (211)
58	CH/OH separately	Ethanol	BEP/TSS	Pt	(111), (211)
59	CH/OH separately	Methane, Ethane, Methanol, Ethanol, Ethylene glycol	BEP/TSS	Pt	(111)
60	CH/OH separately	Acrolein	TSS	Pt	(111)
61	CH/OH separately	Furan derivatives, some small species	BEP/TSS	Pd	(111)

**Table 1-2: Some important BEP type relations available in the literature for catalytic dehydrogenation on transition metals.** In the second column, we present the dissociated/associated bond (either CH or OH). Some authors treat CH and OH scissions in a unique linear energy relation, and others treat them with two distinct relations.

Even if Pt (111) was studied in a majority of papers, the concept of the BEP relation is not limited to this catalyst. Potentially it is possible to get predictions on activation energies (or

TS energies) with a satisfying accuracy for any transition metal. The typical average error is around 0.15 eV for OH and 0.20 eV for CH.<sup>57</sup> Likewise, the concept of the BEP relation should also be valid whatever the facet that is considered. Even if many works were performed on close-packed surfaces, some authors showed that linear energy relations are in general unaffected on open surfaces in the case of dehydrogenation reactions (only slightly for OH scission).<sup>57,62</sup> Concerning the coverage effect, Sutton *et al.* evidenced that the correlation parameters are insensitive to the coverage both for CH and OH dissociations.<sup>59</sup>

BEP type relations were mainly established on small species during the last decade. It is only recently that those relations were investigated on large and complex molecules such as acrolein,<sup>51</sup> glycerol<sup>56</sup> or furans.<sup>61</sup> Once those linear energy relations established, they were used to predict the reactivity of similar systems (*i.e.* equivalent in size and in chemical functions) on one given surface,<sup>63</sup> or on different metal catalysts.<sup>64</sup> However, designing linear energy relations may be long and tedious, especially for large molecules. It can be extremely attractive to establish such relations quickly on small molecules, such as methanol, and to apply them directly on bigger systems, such as glycerol. Besides, it is not obvious that a BEP type correlation established on one given metal is transferable to any other metals. In order to be sufficiently predictive, a linear energy model should be built on a set of various different metals. And this is the originality of this thesis, to predict glycerol reactivity from BEP type relations, established for the dehydrogenation of simple alcohols on several transition metals.

Linear energy relations are intrinsically related to statistics, and it is necessary to master this tool before to address this issue. Statistics will allow us to define rigorously our predictive models, and to know to what extent it is possible to be confident in their predictions. This is the object of the last section of this chapter.

### 3 Basics of Statistics

Various statistical tools are necessary to analyze a linear regression.<sup>65,66</sup> However, the number of points used to establish it is an important issue. Small sample sizes require a particular interest and this is the object of this part. Let us mention that all the statistical analysis in this thesis were performed with the R software.<sup>67</sup>

#### 3.1 Linear regression: the issue of the restricted size samples

A sample is a size limited set of representative individuals extracted from a global population. Various quantities may be measured on each individual, and sometimes it is possible to correlate them together. A linear regression is obtained from a linear fit between a set of dependent variables and a set of independent or explanatory variables. In the BEP paradigm the dependent variables are the various DFT-calculated activation energies,  $\{E_1^\ddagger, E_2^\ddagger, \dots, E_n^\ddagger\}$ , and the explanatory variables are the reaction energies  $\{\Delta E_1, \Delta E_2, \dots, \Delta E_n\}$ . This mathematical relation or statistical model can be used to predict any quantity  $E_i^\ddagger$  from another quantity  $\Delta E_i$  with a given error  $\varepsilon_i$ . Such errors are by definition random and thus unpredictable (in contrast with systematic errors). They are also called “residual errors” or “residues”, and are defined such that:

$$\varepsilon_i = E_i^\ddagger - \widehat{E}_i^\ddagger \quad \text{Equation 1-14}$$

where  $E_i^\ddagger$  is the DFT calculated activation energy and  $\widehat{E}_i^\ddagger$ , the model predicted activation energy.

Usually, the quality of a given model is assessed by the coefficient of determination  $R^2$ , such that:

$$R^2 = 1 - \frac{\sum_i \varepsilon_i^2}{\sum_i (E_i^\ddagger - \overline{E_i^\ddagger})^2} \quad \text{Equation 1-15}$$

where  $\overline{E_i^\ddagger}$  is the mean value of all the  $E_{i \in \{1,2,\dots,n\}}^\ddagger$

In principle, a model is as much predictive as  $R^2$  is high. However, this criterion, usually relevant for large ensembles (hundreds individuals), is very questionable for restricted samples (few dozens individuals or less). Indeed, in that case this parameter can be strongly

affected by adding or removing even only one individual. Besides, in such conditions,  $R^2$  is too sensitive to the potential mistakes of sampling. As a result, if only one point is non-representative of the population, or is just not correctly reported, it might be sufficient to considerably lower the coefficient of determination. Since in this thesis we dealt with sets containing sometimes less than ten individuals, it is necessary to find other ways to analyze the quality our linear models.

## 3.2 Tools for error analysis

### 3.2.1 Assessing the quality of a linear model on a given set of points

The quality of a statistic model may be directly assessed by the analysis of the residual errors that it generates. The box-and-whiskers plot (or box plot) is an efficient tool devoted to this task (see **Figure 1-6**). In such a diagram all the residues, obtained for each individual, are represented. 50% of them are contained in the box and all the representative errors are ranged between the two whiskers. The latter interval is called “range of errors” or “error span”. Non-representative errors appear out of the box and its whiskers and are called outliers. The tighter the range of errors, the better the predictive model.

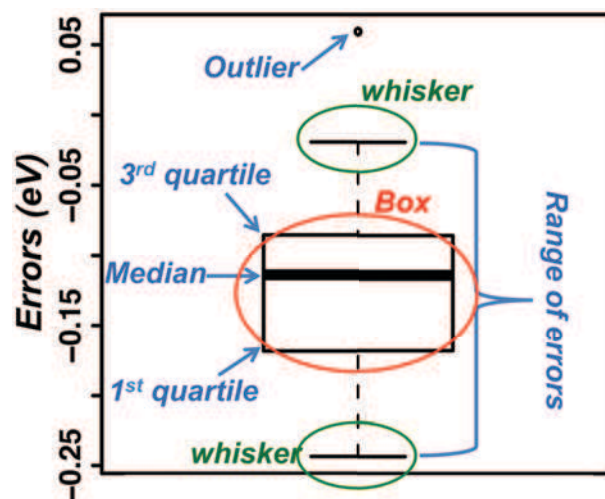


**Figure 1-6: Generic scheme of a boxplot.** The wideness of the box has no signification, only its spread matters. Several features must be considered: the first quartile (25% of the data are contained beyond this point), the median (50% of the data are contained beyond this point) and the third quartile (75% of the data are contained beyond this point)

Aside from this visual tool, two quantitative descriptors are often used: the mean absolute error (MAE) and the maximal absolute error (MAX) defined as follows for a sample containing  $N$  individuals:

$$\begin{cases} MAE = \frac{\sum_i |\varepsilon_i|}{N} \\ MAX = \max_i |\varepsilon_i| \end{cases} \quad \text{Equation 1-16}$$

Let us mention that MAE and MAX can be quite misleading when it exists outliers with a too high magnitude, thus it is important not to ignore the box plot.

### 3.2.2 The systematic deviation and its consequences

The goal of this thesis is to predict glycerol reactivity from linear energy relationships established on monoalcohols. Thus, the linear model that is used to perform predictions does not correspond to the glycerol set of points. Such a situation leads to a systematic deviation, also called “systematic shift” or “mean signed error” (MSE), which is defined as follows:

$$MSE = \frac{\sum_i \varepsilon_i}{N} \quad \text{Equation 1-17}$$

A positive MSE means an underestimation by the model ( $E_i^\ddagger > \widehat{E}_i^\ddagger$ ,  $E_i^\ddagger$  being the DFT activation energy, and  $\widehat{E}_i^\ddagger$ , the BEP estimation), and a negative MSE means an overestimation ( $E_i^\ddagger < \widehat{E}_i^\ddagger$ ).

The question to know if a predictive model established on a given set of points, may be applied or not on different samples is central. For example, in order to predict alcohol reactivity on two different metals, one can ask if it is worth using two distinct BEP relations, *i.e.* one for each metal, or if a unique relationship, common to every metal, is sufficiently predictive. To address this issue, let us consider three different samples  $S0$ ,  $S1$  and  $S2$ , and a linear regression  $\mathcal{M}$  fitted from  $S0$ . We wonder if  $\mathcal{M}$  can be applied on  $S1$  and on  $S2$ . The first condition is that MSE (for  $S1$  and  $S2$ ) must be close to zero (in practice we chose a threshold  $\varepsilon_0=0.05$  eV, *i.e.* approximately a half of the DFT accuracy). If this is verified, the second condition is that MAE and MAX must be as low as possible (in practice on the order

of the DFT accuracy, *i.e.* 0.10-0.20 eV). If both of these conditions are verified,  $\mathcal{M}$  can be used both for  $S1$  and on  $S2$ . Then, if MSE is significantly different from zero, the question is to know if the MSE committed on  $S1$  and on  $S2$  have the same algebraic sign. If yes, and if both MSE have the same magnitude order (in practice we chose a threshold  $\varepsilon_1=2.\varepsilon_0=0.10$  eV), one should test the condition on MAE and MAX. Else, it is not possible to use one unique model for  $S1$  and  $S2$  and two distinct models are necessary. This method is summed-up in the following scheme. Let us mention that other rigorous statistical methods do exist, but inapplicable here due to the limited size of our samples.

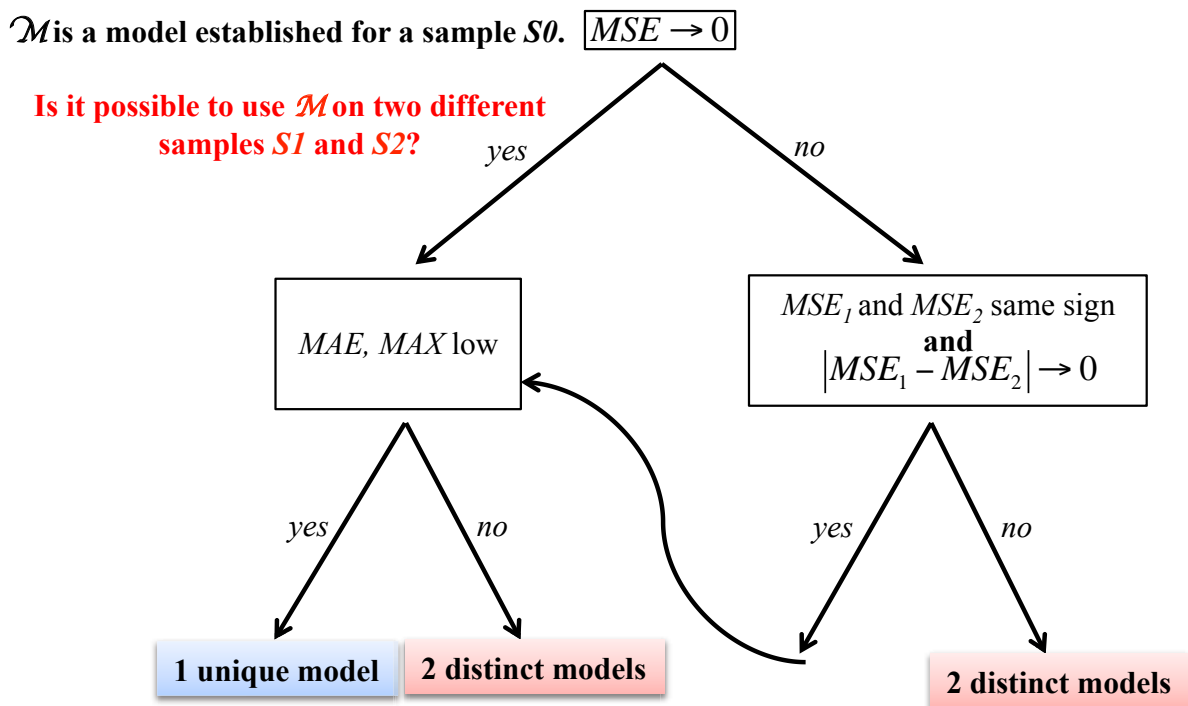


Figure 1-7: Method to decide if a unique model established on a given sample can be applied to two different samples.  $MSE_1$  and  $MSE_2$  are the MSE obtained while applying the model  $\mathcal{M}$  respectively to  $S1$  and  $S2$  samples

### 3.3 From sample to population

In the previous section we presented some tools to describe the effect of a linear regression on one given sample. This is a part of what is called *descriptive statistics*. However it is not straightforward to extrapolate these conclusions to the whole population. The operation consisting using the deductions obtained from one sample, to perform some predictions on one population is called “inference” and gives rise to the field of *inferential statistics*. As a

result the correlation parameters (meaning the slope and the intercept) of a linear regression for a given population (for example the monoalcohol population), are in fact comprised inside a confidence interval surrounding the correlation parameters calculated for the corresponding sample (for example only few typical monoalcohols such as methanol, ethanol and isopropanol). The confidence interval related to the slope or to the intercept is calculated with the following simplified expression:

$$X \in \left[ x - t_{\tau,N} \cdot \sqrt{s_x^2}; x + t_{\tau,N} \cdot \sqrt{s_x^2} \right] \quad \text{Equation 1-18}$$

where  $X$  is the “real” correlation parameter (slope/intercept), meaning the one existing in the population.  $x$  is the correlation parameter that is estimated from the sample.  $s_x^2$  is the variance of the correlation parameter. And  $t_{\tau,N}$  is a the Student coefficient depending of the size of the sample  $N$ , and on the expected confidence level  $\tau$ .

Such intervals are generally calculated for a confidence level of 95%, meaning that a given variable measured on the population has 5% of likelihood to be out of the interval established from the sample analysis. The interval length is directly related to the size of the sample and to the spread of the data. For a fixed error distribution, it is generally tighter for large samples than for restricted samples. A narrow confidence interval shows the robustness of a predictive model.

To sum up various statistical tools are available in order to analyze linear regressions, and to bypass the problem of the small sample size. These methods are based on a precise description of residual errors, and on the calculation of confidence and prediction intervals. However, it is worth mentioning that the concept of linear regression underlies in fact many assumptions. Those hypotheses are related to the normality of the distribution of the variables, and to the sampling method. The last issue is capital since it determines if a sample contains representative individuals or not. However, it is not possible to valid those hypotheses with certainty in our situation, and we will consider in first approximation that they are always verified. In consequence, one must be careful with the conclusions stemming from the use of statistics tools. Despite of the relevance of the statistical analysis proposed in this thesis, it is important to appreciate those results through the prism of Chemistry rather than with a pure mathematical point of view. That is why in the following we will consider that a model is

sufficiently predictive when the residual errors are in the range of the DFT accuracy, meaning around 0.10-0.20 eV.

## Conclusion

As a conclusion, we saw in this chapter that transition metals are often used to catalyze alcohol dehydrogenation, both for polyols and monoalcohols. Their reactivity is strongly influenced by the experimental conditions. Both selectivity and activity of the catalyst may be affected by the pH and the solvent. Some linear energy relations exist in order to easily predict the activation energies of one given reaction for a certain type of molecules and of catalysts. These relations are named BEP-type relations, and correlate in various ways a kinetics value and a thermodynamics value. Recently, they have been extensively used in the literature for heterogeneous catalysis, both for complex and simple molecules. However, such relations may be long to establish in particular for complex systems such as polyols. Therefore, it can be very interesting if it could be possible to predict polyol reactivity from relationships established on monoalcohols. Various statistics tools are necessary to valid the method and to assess the quality of the resulting linear models.

In this thesis we will firstly test the procedure on Rh (111), trying to predict glycerol dehydrogenation from BEP type relations established on a set of monoalcohols. Then, we will look for other BEP type relations related to monoalcohol dehydrogenation on various transition metals. Afterwards, in order to rationalize the intramolecular H-bond effect occurring in polyols, we will consider water impact on the linear relationships. And finally, we will use those relations in order to predict a part of the glycerol reaction network on some transition metals.

---

<sup>1</sup> M. Pagliaro, R. Ciriminna, H. Kimura, M. Rossi and C. Della Pina, *Angew. Chem. Int. Ed.* **2007**, *46*, 4434-4440

<sup>2</sup> A. M. Ruppert, K. Weinberg, and R. Palkovits, *Angew. Chem. Int. Ed.* **2012**, *51*, 2564-2601

<sup>3</sup> C. Montassier, D. Giraud, J. Barbier and J. P. Boitiaux, *Bull. Soc. Chim. Fr.* **1989**, *2*, 148-155.

<sup>4</sup> M. Rose and R. Palkovits, *Macromol. Rapid Commun.* **2011**, *32*, 1299-1311.

- <sup>5</sup> B. Bachiller-Baeza, A. Guerrero-Ruiz and I. Rodriguez-Ramos, *J. Catal.* **2005**, *229*, 439- 445
- <sup>6</sup> L. Ma and D. He, *Top. Catal.* **2009**, *52*, 834- 844
- <sup>7</sup> C. Montassier, D. Giraud and J. Barbier, « *Polyol Conversion by Liquid Phase Heterogenous Catalysis over Metals* », M. Guisnet et al. Elsevier : Amsterdam, **1988**, pp. 165 – 170.
- <sup>8</sup> J. Chaminand, L. Djakovitch, P. Gallezot, P. Marion, C. Pinel and C. Rosier, *Green Chem.* **2004**, *6*, 359-361
- <sup>9</sup> C. Montassier, J. M. Dumas, P. Granger and J. Barbier, *Appl. Catal.A* **1995**, *121*, 231-240
- <sup>10</sup> L. Guo, J. Zhou, J. Mao, X. Guo and S. Zhang, *Appl. Catal. A* **2009**, *367*, 93-98
- <sup>11</sup> J. Feng, H. Fu, J. Wang, R. Li, H. Chen and X. Li, *Catal. Commun.* **2008**, *9*, 1458-1464
- <sup>12</sup> E. P. Maris and R. J. Davis, *J. Catal.* **2007**, *249*, 328–337
- <sup>13</sup> M. G. Musolino, L. A. Scarpino, F. Mauriello and R. Pietropaolo, *Green Chem.* **2009**, *11*, 1511-1513
- <sup>14</sup> J. Oh, S. Dash and H. Lee, *Green Chem.* **2011**, *13*, 2004- 2007
- <sup>15</sup> L. Ma and D. He, *Catal. Today* **2010**, *149*, 148-156
- <sup>16</sup> O. M. Daniel, A. DeLaRiva, E. L. Kunkes, A. K. Datye, J. A. Dumesic and R. J. Davis, *Chem. Cat. Chem.* **2010**, *2*, 1107-1114
- <sup>17</sup> W. Yu, J. Xu, H. Ma, C. Chen, J. Zhao, H. Miao and Q. Song, *Catal. Commun.* **2010**, *11*, 493-497
- <sup>18</sup> D. Coll, F. Delbecq, Y. Aray and P. Sautet, *PCCP*, **2011**, *13*, 1448-1456
- <sup>19</sup> B. Liu and J. Greeley, *PCCP*, **2013**, *15*, 6475-6485
- <sup>20</sup> J. Guan, X. Wang, X. Wang and X. Mu, *Sci. China. Chem.*, **2013**, *56*, 763-772
- <sup>21</sup> F. Auneau, C. Michel, F. Delbecq, C. Pinel and P. Sautet, *Chem. Eur. J.* **2011**, *17*, 14288–14299
- <sup>22</sup> Y. Choi and P. Liu, *Catal. Today*, **2011**, *165*, 64-70
- <sup>23</sup> J. E. Sutton, P. Panagiotopouou, X. Veryldos and D. G. Vlachos, *J. Phys. Chem. C*, **2013**, *117*, 4691-4706
- <sup>24</sup> Y. Ma, L. Hernandez, C. Guadarrama-Perez and P. B. Balbuena, *J. Phys. Chem. A*, **2012**, *116*, 1409-1416
- <sup>25</sup> J. Wang, C. S. Lee and M. C. Lin, *J. Phys. Chem. C*, **2009**, *113*, 6681-6688
- <sup>26</sup> M. Ni, D. Y. C. Leung and M. K. H. Leung, *International Journal of Hydrogen Energy*, **2007**, *32*, 3238-3247
- <sup>27</sup> N. Takezawa and N. Iwasa, *Catal. Today*, **1997**, *36*, 45 - 56
- <sup>28</sup> A. Frassoldati, C. Pinel and M. Besson, *Catal. Today*, **2011**, *173*, 81-88
- <sup>29</sup> S. Chibani, C. Michel, F. Delbecq, C. Pinel and M. Besson, *Catal. Sci. Technol.*, **2013**, *3*, 339-350
- <sup>30</sup> D. D. Hibbitts and M. Neurock, *J. Catal.* **2013**, *299*, 261-271
- <sup>31</sup> P. Vassilev, R. A. van Santen and M. Koper, *J. Chem. Phys.*, **2005**, *122*, 054701
- <sup>32</sup> C. Michel, F. Auneau, F. Delbecq and P. Sautet, *ACS Catal.* **2011**, *1*, 1430-1440
- <sup>33</sup> J. K. Norskov, T. Bligaard, J. Rossmeisl and C. H. Christensen, *Nature Chem.*, **2009**, *1*, 37-46
- <sup>34</sup> M. Saliccioli, M. Stamatakis, S. Caratzoulas and D. G. Vlachos, *Chem. Eng.*, **2011**, *66*, 4319-4355

- <sup>35</sup> S. W. Benson, J. H. Buss, *J. Chem. Phys.*, **1958**, *29*, 546–572
- <sup>36</sup> S. W. Benson, F. R. Cruicksh, D. M. Golden, G. R. Haugen, H. E. Oneal, A. S. Rodgers, R. Shaw and R. Walsh, *Chem. Rev.*, **1969**, *69*, 279–324.
- <sup>37</sup> F. Abild-pedersen, J. Greeley, F. Studt, J. Rossmeisl, T. Munter, P. Moses, E. Skulason, T. Bligaard and J. Nørskov, *Phys. Rev. Lett.*, **2007**, *99*, 016105.
- <sup>38</sup> J. Brønsted, *Chem. Rev.*, **1928**, *5*, 231-338
- <sup>39</sup> R. P. Bell, *Proc. R. Soc. Lond. A*, **1936**, *154*, 414-429
- <sup>40</sup> M. Evans and M. Polanyi, *Trans. Faraday Soc.*, **1938**, *34*, 0011–0023
- <sup>41</sup> J. A. Dumesic, D. F. Rudd, L. M. Aparicio, J. E. Rekoske, A. A. Trevino, « *The Microkinetics of Heterogeneous Catalysis* », American Chemical Society : Washington, DC, **1993**
- <sup>42</sup> L.P. Hammett, « *Physical Organic Chemistry* », McGraw-Hill: New York, **1970**, p 356.
- <sup>43</sup> L. Stryer « *Biochemistry* », W.H. Freeman: San Francisco, **1995**, Chapter 8.
- <sup>44</sup> Z. P. Liu and P. Hu, *J. Chem. Phys.* **2001**, *115*, 4977-4980
- <sup>45</sup> R. A. van Santen, M. Neurock and S. G. Shetty, *Chem. Rev.*, **2010**, *110*, 2005–2048
- <sup>46</sup> J. E. Sutton and D. G. Vlachos, *ACS Catal.* **2012**, *2*, 1624–1634
- <sup>47</sup> G. Hammond, *J. Am. Chem. Soc.*, **1955**, *77*, 334-338
- <sup>48</sup> A. Michaelides, Z. P. Liu, C. J. Zhang, A. Alavi, D. A. King and P. Hu, *J. Am. Chem. Soc.* **2003**, *125*, 3704-3705
- <sup>49</sup> J. Zaffran, C. Michel, F. Auneau, F. Delbecq and P. Sautet, *ACS Catal.*, **2014**, *4*, 464–468
- <sup>50</sup> R. Alcalá, M. Mavrikakis and J. A. Dumesic, *J. Catal.*, **2003**, *218*, 178–190
- <sup>51</sup> D. Loffreda, F. Delbecq, F. Vigné and P. Sautet, *Angew. Chem. Int. Ed.* **2009**, *48*, 8978 –8980
- <sup>52</sup> V. Pallassana and M. Neurock, *J. Catal.*, **2000**, *191*, 301–317
- <sup>53</sup> J. L. C. Fajín, M. N. D. S. Cordeiro, F. Illas and J. R. B. Gomes, *J. Catal.*, **2010**, *276*, 92–100
- <sup>54</sup> C. Michel, F. Göttl and P. Sautet, *Phys. Chem. Chem. Phys.*, **2012**, *14*, 15286–15290
- <sup>55</sup> J. Greeley and M. Mavrikakis, *J. Am. Chem. Soc.*, **2004**, *126*, 3910-3919
- <sup>56</sup> B. Liu and J. Greeley, *J. Phys. Chem. C*, **2011**, *115*, 19702–19709
- <sup>57</sup> S. Wang, V. Petzold, V. Tripkovic, J. Kleis, J. G. Howalt, E. Skulason, E. M. Fernández, B. Hvolbæk, G. Jones, A. Toftelund, H. Falsig, M. Björketun, F. Studt, F. Abild-Pedersen, J. Rossmeisl, J. K. Nørskov and T. Bligaard, *Phys. Chem. Chem. Phys.*, **2011**, *13*, 20760–20765
- <sup>58</sup> H. F Wang and Z. P. Liu, *J. Am. Chem. Soc.*, **2008**, *130*, 10996–11004
- <sup>59</sup> J. E. Sutton and D. G. Vlachos, *ACS Catal.* **2012**, *2*, 1624–1634
- <sup>60</sup> D. Loffreda, F. Delbecq, F. Vigné and P. Sautet, *Angew. Chem. Int. Ed.* **2009**, *48*, 8978 –8980
- <sup>61</sup> S. Wang, V. Vorotnikov, J. E. Sutton and D. G. Vlachos, *ACS Catal.*, **2014**, *4*, 604–612
- <sup>62</sup> J. K. Nørskov, T. Bligaard, B. Hvolbæk, F. Abild-Pedersen, I. Chorkendorff and C. H. Christensen, *Chem. Soc. Rev.*, **2008**, *37*, 2163–2171

<sup>63</sup> S. Laref, F. Delbecq and D. Loffreda, *J. Catal.*, **2009**, *265*, 35–42

<sup>64</sup> B. Liu and J. Greeley, *Phys. Chem. Chem. Phys.*, **2013**, *15*, 6475-6485

<sup>65</sup> C. Spatz, «*Basic Statistics: Tales of Distributions*», 10<sup>th</sup> ed. Wadsworth Cengage learning, **2010**

<sup>66</sup> J. M. Utts and R. F. Heckard, «*Statistical ideas and methods* », Thomson Brooks/Cole: Belmont, **2006**

<sup>67</sup> M. J. Crawley, «*The R book*», 2<sup>nd</sup> ed. John Willey & Sons: West Sussex, **2013**

## Chapter 2: Predicting polyalcohol reactivity from simple alcohols

---

The ultimate goal of this thesis is to elaborate methods to fast predict polyalcohol reactivity. This task can be achieved using linear energy relationships. However, designing such relations on complex molecules is hard and very time-consuming. The process may be significantly accelerated if it was possible to address the reactivity of such species, with BEP-type relations established on simpler molecules. In this chapter, we will demonstrate the validity of this concept. Considering dehydrogenation on Rh (111) as a model reaction, we will predict activation energies for CH and OH scissions in glycerol, taken as a prototype polyol. The prediction is performed *via* linear energy relations established on a set monoalcohol molecules. The statistics tools described in the previous chapter will be continuously used to assess the quality of the estimation of activation barriers. The supplementary information related to the following article can be found in Appendices.

## Linear Energy Relations As Predictive Tools for Polyalcohol Catalytic Reactivity

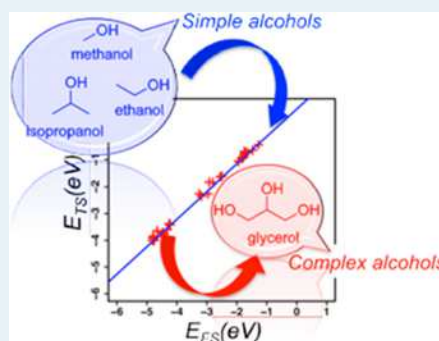
J eremie Zaffran, Carine Michel, Florian Auneau, Fran oise Delbecq, and Philippe Sautet\*

Universit  de Lyon, CNRS and Ecole Normale Sup rieure of Lyon, 46 All e d'Italie, 69364 Lyon Cedex 07, France

**S** Supporting Information

**ABSTRACT:** Molecules extracted from biomass can be complex, and computing their reactivity on a catalyst is a real challenge for theoretical chemistry. We present herein a method to predict polyalcohol reactivity in heterogeneous catalysis. We start from a set of simple alcohol molecules, and we show that an accurate linear energy relationship can be constructed from DFT calculations for the O–H and C–H dehydrogenation reactions. We then show that this relation can then be used for a fast prediction of the reactivity of glycerol. Compared with pure DFT calculations, our method provides results of good accuracy with a systematic deviation of  $\sim 0.1$  eV. We were able to prove that this deviation is caused mainly by intramolecular effects occurring in glycerol and not in simpler molecules.

**KEYWORDS:** Br nsted–Evans–Polanyi type relationships, glycerol, polyols, biomass, monoalcohols, dehydrogenation, DFT



Molecules extracted from biomass set new challenges for heterogeneous catalysis and require the design of improved catalysts.<sup>1,2</sup> The cellulosic fraction of biomass is constituted of polyalcohols, which can be transformed to valuable products (chemicals or fuels) by various types of chemical reactions (dehydrogenation, hydrogenolysis, dehydration, ...).<sup>3</sup> These polyalcohols are associated with a large space of geometric configurations, and they can be involved in a complex network of serial or parallel reactions, which render the study of their reactivity with a solid catalyst complex and tedious. The calculation of their reactions at metal surfaces requires quantum chemical methods to properly describe bond-breaking and bond-forming steps, but these methods are too heavy for a fast exploration of complex reaction networks. It is hence of utmost importance to design methods that are of similar accuracy to quantum chemical approaches but can allow a fast screening of multiple elementary steps.

In this work, we show that transition state energies and reaction barriers for polyalcohols can be efficiently predicted from linear relationships of Br nsted–Evans–Polanyi (BEP) type, linking the desired kinetics quantities with more easily accessible adsorption energy or reaction energy data, which are established here using a set of monoalcohol molecules. Here, we use glycerol as a prototype polyalcohol, and we focus on dehydrogenation reactions on a Rh catalyst, hence involving the C–H and O–H bond-breaking processes. Indeed, it has been demonstrated that dehydrogenation is the first step for glycerol transformation on a Rh catalyst, under H<sub>2</sub> gas pressure or under He.<sup>4</sup> Even if one restrains the reactivity of glycerol to dehydrogenation processes, many pathways are possible by a combination of elementary acts dealing with CH/OH groups in central/terminal positions. In addition, glycerol can adopt a

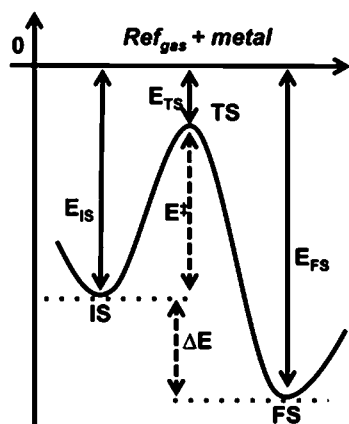
very large number of configurations in the gas phase<sup>5</sup> and on a surface.<sup>6</sup> It is unclear if the most stable configuration will be the most reactive one, and probing all configurations/pathways with first principle approaches such as DFT is, hence, a very tedious and computer-intensive task.

The idea of simple and fast evaluation of activation barriers from reaction thermodynamic data traces back to the pioneering work of Br nsted,<sup>7</sup> Bell,<sup>8</sup> Evans, and Polanyi,<sup>9</sup> as detailed in a recent review.<sup>10</sup> These correlations were initially used to compare molecular reactivity and, in a later stage, to model the kinetics of chemical reactions. They have been applied to heterogeneous catalysis reactions by several authors; however, two alternative methods were considered. Although some authors correlated activation energy with reaction energy,<sup>11–14</sup> in a traditional BEP style, others proposed to correlate the transition state energy with the energy of the initial or the final state of the reaction, a method later referred to as transition state scaling (TSS).<sup>15–19</sup> Only a few papers compare the merits of both correlation methods.<sup>20,21</sup> The situation remains confused on this point because for a single type of correlation, different definitions were used. In this paper, we will explore both TSS (with eight possible definitions) and BEP (with four definitions) correlations to clarify their comparison.

A general catalytic elementary step is shown in Scheme 1. The step starts from the initial state minimum, IS; progresses through the transition state, TS; and finishes at the final state

Received: November 11, 2013

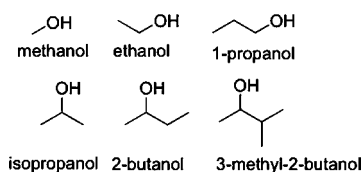
Revised: December 17, 2013

Scheme 1. General Scheme of a Surface Catalytic Elementary Step<sup>a</sup>

<sup>a</sup> $E_{TS}$ ,  $E_{IS}$ , and  $E_{FS}$  are energies of the transition state, the initial state, and the final state, respectively.  $E^\ddagger$  and  $\Delta E$  are activation and reaction energies, respectively.

minimum, FS. The principle of the BEP analysis is to explore the correlation behavior when plotting the activation (or the TS) energy versus the reaction (or FS) energy for a given sample of such reaction steps. The definition of IS and FS is not absolute because it depends on the direction chosen for the reaction. In our case, one can define the direction from the reaction itself, bond dissociation (diss), or association (assoc). Another possibility is to select the direction on an energy criterion, such as for each step choosing the endothermic (endo) or exothermic (exo) direction. This defines four types of BEP analysis, expressing the correlation between the activation energy,  $E^\ddagger = E_{TS} - E_{IS}$ , and the reaction energy,  $\Delta E = E_{FS} - E_{IS}$ . TSS relations correlate intrinsic TS and FS energies so that a reference energy is needed. We use as a reference a state in which all surface fragments are considered in gas phase, and the most stable spin state was chosen in the case of radicals. A TSS relation is, hence, defined by a direction (diss/assoc or exo/endo), a choice of thermodynamic state (either IS or FS), and a choice for the energy reference (again IS or FS). Our general notation is diss.IS/IS, where the last symbol defines the energy reference. Clearly, diss.IS/IS and assoc.FS/FS are identical definitions, such as exo.FS/FS and endo.IS/IS, so that only diss and exo directions will be kept. Eight types of TSS are then defined.

The existence and the quality of the correlation will be studied on a sample of simple alcohol molecules that are displayed in Scheme 2. Six molecules have been chosen with

Scheme 2. Sample of Molecules Used to Establish the BEP Type Relationships<sup>a</sup>

<sup>a</sup>Here are depicted the six monoalcohol molecules generating the 29 elementary CH and OH dissociation steps included for the construction of the linear relations.

several substitution levels and a mixture of primary and secondary alcohols. For each of them, OH and CH bond dissociations have been considered, with a further distinction between CH bonds in the  $\alpha$  or  $\beta$  position with respect to the OH. First and second dehydrogenation reactions have been considered so that a set of dehydrogenated products is formed of various chemical natures (radicals, carbonyls, enols). In total, the sampling set contains 29 bond activations (12 CH $\alpha$ , 7 CH $\beta$ , and 10 OH, see the Supporting Information (SI)).

If we first select the diss.FS/FS, exo.FS/IS, and BEP.diss forms of correlation, which have been previously used in the literature,<sup>11–21</sup> the 29 points  $E_{TS}/E_{FS}$  or  $E^\ddagger/\Delta E$  are displayed in Figure 1. A clear and high-quality linear relation is seen. The statistical analysis of the deviations between DFT values and linear relation values are shown for each correlation as box plots on the inserts of Figure 1. We also report the mean absolute error (MAE) and the maximum error (MAX). Error is defined as “DFT value – linear relation value”. The three chosen correlation definitions give very similar error distributions for the three subsets CH $\alpha$ /CH $\beta$ /OH, in a range from  $\sim -0.1$  to  $+0.1$  eV. This attests to the good quality of these relationships, which is confirmed by a MAE on the order of 0.05 eV (see Table 1) in each case. Note that the range of data is smaller for the BEP definition, giving a less visually appealing correlation (and a larger confidence interval for the slope of the linear relation; see the SI) for a similar distribution of errors. Let us highlight in addition that splitting the sample into three subsets considerably lowers the errors of the linear model, as shown by the MAE/MAX analysis, which is almost divided by 2. Furthermore, predicting CH $\alpha$ /CH $\beta$ /OH by a model established with all the points together leads to nonnegligible systematic errors (see SI Figure S2), significantly degrading the prediction.

From this analysis of the sampling set, the three selected types of correlations are of equivalent and high quality, and the error values after a separation in the three types of bonds is small (MAE  $\sim 0.05$  eV), which is very encouraging for a use of these correlations in predicting reactivity. A similar result was obtained for all 12 types of correlations considered, as seen in Figure 2. When taking all bonds together, only small variations are seen in the MAE between the methods, and hence, all 12 should be evaluated as being of the same general quality (error  $\sim 0.08$  eV). Separation of the set in each type of dissociated bond (CH $\alpha$ /CH $\beta$ /OH) again lowers the error, showing fluctuations around 0.05 eV for the various methods. None, however, is consistently better than the other ones, even if for the specific case of CH $\beta$  dissociation BEP are more accurate than TSS (for box plots, see SI Figure S3). The main point here is to clearly stress that TSS and BEP type relations have a similar (and high) merit,<sup>19</sup> at least for Rh catalysts and the chosen family of monoalcohol molecules.

Our results also show that the choice of the direction of the reaction (either on a chemical or energy base) or of the reference (for TSS modes) is not determinant for the result. This is, of course, reassuring for the robustness of the correlation concept and its usage for a wide range of systems and reactions. The BEP formulation has some practical advantages because the correlated quantities are more directly linked with reaction thermodynamics and kinetics so that trends can more clearly be caught and so that the slope (also called the transfer coefficient) has a simple interpretation in terms of early or late character of the transition state.

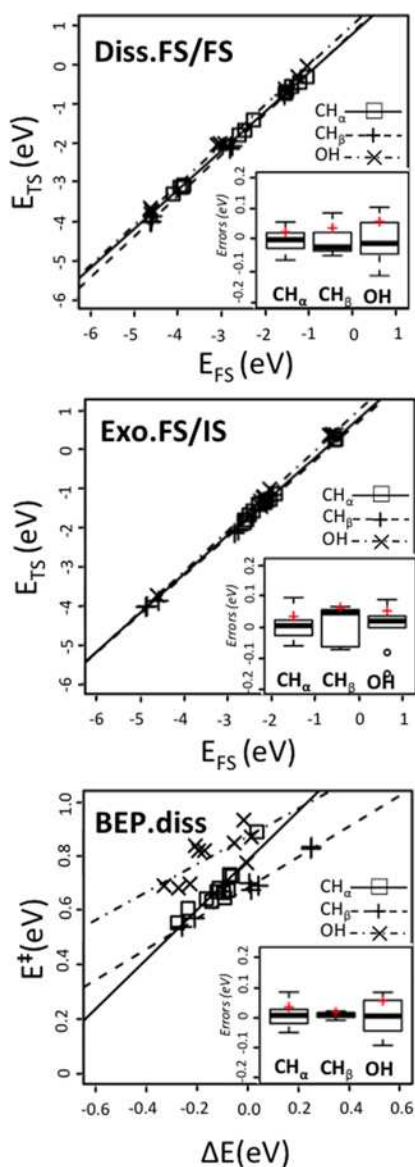


**Figure 1.** Linear relations constructed from first and second dehydrogenation steps of the six monoalcohol molecules of Scheme 1 on Rh(111). Three definitions of the correlation are considered:  $\square$ ,  $\times$ , and  $+$  are the DFT calculated values for  $\text{CH}_\alpha$ ,  $\text{CH}_\beta$ , and OH respectively; and full, dashed, and mixed lines are the corresponding linear relations. At the bottom right corner of each graph, the box plots depict the corresponding error distribution. Red crosses signal mean absolute errors (MAE).

Now that we have established these correlations on the monoalcohol sample set, we turn to the central question: Can we use them to predict the reactivity of glycerol, chosen as a prototype polyalcohol? We have considered all first and second C–H and OH bond dissociations of glycerol on Rh(111). Note that in the case of glycerol, all CH bonds are in  $\alpha$  of an OH group. For simplicity, we focus here on only the three correlation modes already selected for Figure 3 (diss.FS/FS, exo.FS/IS, and BEP.diss), but a complete analysis is provided in the SI (see Figure S4). We calculated the most stable initial and final states for first and second hydrogenation processes on

**Table 1. Error Analysis for Monoalcohol BEP Type Relationships<sup>a</sup>**

	TSS-diss.FS/FS		TSS-exo.FS/IS		BEP.diss	
	MAE	MAX	MAE	MAX	MAE	MAX
all	0.09	0.23	0.08	0.17	0.07	0.18
$\text{CH}_\alpha$	0.03	0.06	0.03	0.09	0.03	0.07
$\text{CH}_\beta$	0.04	0.09	0.06	0.07	0.01	0.02
OH	0.06	0.11	0.05	0.15	0.05	0.10

<sup>a</sup>Here is presented the error analysis (mean absolute error, MAE; maximal absolute error, MAX) for the 29 CH and OH dissociation elementary steps of the considered monoalcohols family on Rh(111). The correlation can be established from the global sample (all), or subfamilies can be considered for each type of chemical bond activated ( $\text{CH}_\alpha$ ,  $\text{CH}_\beta$ , OH).

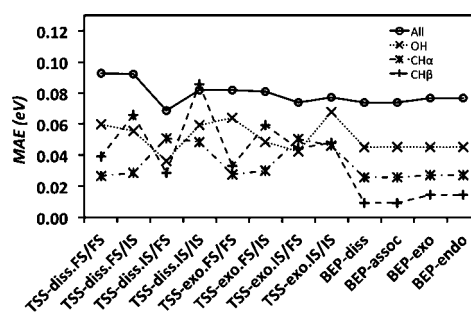


**Figure 2.** Comparison of the 12 considered definitions for the correlations (grouped into 8 TSS and 4 BEP types). MAE is given for the linear relation considering the 3 subsets ( $\text{CH}_\alpha$ / $\text{CH}_\beta$ /OH) separately and the whole set (“All”) of monoalcohol dehydrogenation reactions.

glycerol on Rh(111) and determined the TS linking them. Note that for some reaction steps, we included several TS and their corresponding reactants and products (associated with different conformations of glycerol) to improve the reliability of our statistical analysis (see glycerol structures in the SI and Figure S5).

The 31 (18 C–H and 13 O–H dissociations) points for glycerol are shown in Figure 3, together with their associated linear relation in black and with the correlation lines previously established for the monoalcohol family (in red). This graph clearly shows that the correlation established with the monoalcohol family is already a good model to predict the transition state energy or the activation energy for glycerol. The analysis of the deviation between the points for glycerol and the (red) line from the monoalcohol family quantifies this result (see box plots in Figure 3 and Table 2).

Notice that in this case, we also present the mean signed error (MSE), which is nonzero here because the linear relation is not associated with the sample considered for glycerol. One can clearly notice a systematic deviation, the prediction line underestimating the activation energy (on average, by 0.1 eV) for the CH bonds and overestimating it (by 0.1 eV) for the OH bonds. We will see the consequence of this systematic error on the predictive potential of the method later. The MAE is very close to this MSE and, hence, remains small ( $\sim 0.1$  eV for all three definitions). The error is, hence, reasonably increased with respect to the sampling set, and this gives predictive power to the approach. Points corresponding to metastable configurations of glycerol follow the linear relation within given statistical errors, although the most stable thermodynamic state

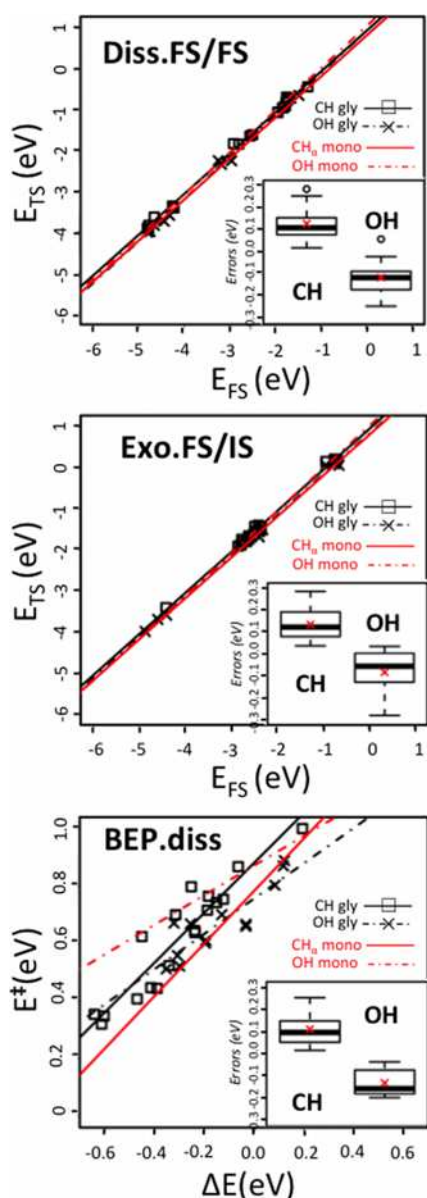


**Figure 3.** Linear relations constructed from first and second dehydrogenation steps of glycerol on Rh(111). Three definitions of the correlation are considered:  $\square$  and  $\times$  are the DFT calculated values for CH and OH bonds, respectively, and full and mixed lines are the corresponding linear relations. In red are recalled the linear relations obtained in the case of the monoalcohol set for the  $\text{CH}_\alpha$  (full line) and the OH (mixed line) bonds. At the bottom right corner of each graph, the box plots depict the corresponding error distributions between the data points and the (red) monoalcohol linear relations. Red crosses signal mean signed errors.

is not always strictly associated with the most stable TS (see Figure S5 in the SI). Again, the two TSS and the BEP approaches have a very similar performance in terms of error. This can be generalized to all 12 correlation types considered in this paper, as shown in Figure S4 in the SI. All definitions give a similar error distribution, with an especially narrow range for the BEP case for OH dissociation and a larger error for the TSS involving the initial state as variable for the CH activation.

The capability to reasonably predict the catalytic reactivity of glycerol from that of simple alcohols is not a straightforward result, and it opens several perspectives. Generally speaking, to our knowledge, the use of BEP-type relations on simple molecules to predict multifunctional ones has not been demonstrated. It has been proposed, however, to predict the influence of substituents in the case of the hydrogenation of unsaturated aldehydes.<sup>22</sup> There are many reasons why glycerol reactivity might be different from that of simple alcohols. The presence of terminal and central OH/CH is equivalent to primary and secondary alcohols, both of which are in the sampling set. One key difference, however, is the presence in glycerol of intramolecular hydrogen bonds that assist the OH dissociation for the H bond acceptor OH.<sup>23</sup> The DFT-calculated TS energy will, hence, be lower for glycerol than for the monoalcohol sample, hence explaining the  $\sim 0.1$  eV systematic error. This effect appears clearly if one considers some water-assisted reactions in the case of dehydrogenation of monoalcohols.

As a simpler H-bonded system, we considered ethanol, interacting with a chemisorbed water molecule through a H-bond, ethanol being the H-bond acceptor.<sup>22</sup> In this configuration, the OH bond scission in ethanol is modified, and the corresponding points are shifted toward the glycerol line in the BEP plots (see Figure S6 in the SI). In contrast, the positive systematic error seen for the CH bond dissociation is not related to the H bond effect. It stems from the constraints that neighboring OH groups in glycerol exert on glycerol. By interacting with the metal surface, they make the adsorbed molecule more rigid; hence, hindering the formation of the optimal C–H transition structure and increasing its energy with respect to the freer situation of monoalcohol sample. However, these effects are not very marked, and on average, the predictive potential remains good.

In the following, we will consider some examples of glycerol dehydrogenation elementary steps focusing on selectivity issues, that is, on the comparison of the barriers between different paths from a given intermediate. This is a severe test in situations for which DFT barriers are close and will highlight the cases in which a prediction is valid and those for which the accuracy might be insufficient. Scheme 3 presents two examples for glycerol or its hydrogenated intermediate on a Rh(111) surface and compares DFT calculated barriers (below arrow) with those predicted by three correlations built from the monoalcohol family (above arrows). The comparison between CH and OH dissociation (first line) is especially difficult because the systematic deviation in the prediction is different, with an overestimation for OH and an underestimation for CH, and because here, the DFT barrier difference is small. The method is, hence, not able to correctly grasp the preferred reaction.

The second elementary reaction starts from dehydrogenated glycerol at the terminal carbon and compares two further OH dissociation steps. The systematic deviation is eliminated because similar reactions are compared and the random error remains, which is inherent to any statistical model. Errors range now between  $\sim 0.1$  and  $\sim +0.1$  eV, which is similar to the results obtained for simple alcohols. In addition, the difference between barriers obtained from the correlations (0.13–0.22 eV) being large enough to safely predict that the reaction on the right, forming glyceraldehyde, is favored.

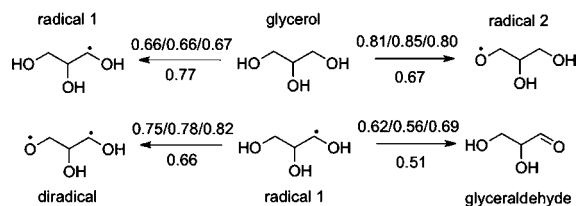
We, hence, showed that linear energy relations established for a sample of monoalcohol molecules on Rh can efficiently be

Table 2. Error Analysis for the Prediction of Glycerol Reactivity<sup>a</sup>

	TSS-diss.FS/FS			TSS-exo.FS/IS			BEP.diss		
	MSE	MAE	MAX	MSE	MAE	MAX	MSE	MAE	MAX
CH	+0.13	0.13	0.28	+0.13	0.13	0.29	+0.11	0.13	0.25
OH	-0.11	0.12	0.24	-0.09	0.10	0.28	-0.13	0.13	0.20

<sup>a</sup>Here is presented the error analysis for predicting glycerol reactivity on Rh(111) from the monoalcohol linear energy relationship using the three main definitions: MSE, mean signed error; MAE, mean absolute error; and MAX, maximal absolute error.

### Scheme 3. Prediction of Activation Energies for Glycerol Dehydrogenation<sup>a</sup>



<sup>a</sup>The first line describes two possible paths for the first dissociation starting from glycerol, and the second line describes two probable routes for the second step starting from “radical 1”. The value below each arrow is the activation energy predicted by DFT, and the three values above are the activation energies predicted from three definitions of the monoalcohol linear energy relationship (TSS-diss.FS/FS, TSS-exo.FS/IS, BEP.diss).

applied to the prediction of reaction barriers for polyalcohol molecules, such as glycerol with a statistical mean absolute error of  $\sim 0.1$  eV. Coupled with other approaches that simplify the evaluation of the adsorption energy of large molecules, as group additivity<sup>24</sup> or scaling relations,<sup>25</sup> this opens a fast and powerful exploration of the complex mechanisms and of the kinetics for the catalytic transformation of molecules extracted from biomass. Small deviations occur from the presence of intramolecular H bonds in the polyalcohol molecule, underestimating (respectively overestimating) the barrier for CH (respectively OH) and, hence, favoring CH dissociation versus OH in the predicted values. It would be certainly important to develop methods to estimate this systematic deviation between the set of CH or OH dissociation steps for glycerol versus monoalcohols because this would allow us to implement a correction on the data and to improve the prediction when comparing dehydrogenation at CH and OH on the polyalcohol. Although this analysis has been performed on a Rh(111) surface, the conclusions should not be specific to that system and extend to other faces or metal, as already proposed for other reaction steps.<sup>18,20</sup> Immediate perspectives aim at generalizing this behavior to other bond cleavages, such as C–C or C–O; other metals; and other types of molecular systems extracted from biomass, such as lignin.

### ■ ASSOCIATED CONTENT

#### Supporting Information

Computational methods and elements of statistics, additional tables and schemes, list of reactions and their corresponding structures used to get the relationships. This material is available free of charge via the Internet at <http://pubs.acs.org>.

### ■ AUTHOR INFORMATION

#### Corresponding Author

\*E-mail: [philippe.sautet@ens-lyon.fr](mailto:philippe.sautet@ens-lyon.fr).

### Notes

The authors declare no competing financial interest.

### ■ ACKNOWLEDGMENTS

We thank PSMN at ENS Lyon, IDRIS-CNRS, and CINES for computational resources. We also acknowledge the support of ANR through the GALAC Project (ANR-10-CD2I-011).

### ■ REFERENCES

- (1) Huber, G. W.; Chheda, J. N.; Barrett, C. J.; Dumesic, J. A. *Science* **2005**, *308*, 1446–1450.
- (2) Chheda, J. N.; Huber, G. W.; Dumesic, J. A. *Angew. Chem., Int. Ed.* **2007**, *46*, 7164–7183.
- (3) Ruppert, A.; Weinberg, K.; Palkovits, R. *Angew. Chem., Int. Ed.* **2012**, *51*, 2564–2601.
- (4) Auneau, F.; Michel, C.; Delbecq, F.; Pinel, C.; Sautet, P. *Chem.—Eur. J.* **2011**, *17*, 14288–14299.
- (5) Callam, C. S.; Singer, S. J.; Lowary, T. L.; Hadad, C. M. *J. Am. Chem. Soc.* **2001**, *123*, 11743–11754.
- (6) Coll, D.; Delbecq, F.; Aray, Y.; Sautet, P. *Phys. Chem. Chem. Phys.* **2011**, *13*, 1448–1456.
- (7) Bronsted, J. N. *Chem. Rev.* **1928**, *5*, 231–338.
- (8) Bell, R. P. *Proc. R. Soc. London, Ser. A* **1936**, *154*, 414–429.
- (9) Evans, M. G.; Polanyi, M. *Trans. Faraday Soc.* **1938**, *34*, 11–23.
- (10) Van Santen, R. A.; Neurock, M.; Shetty, S. G. *Chem. Rev.* **2010**, *110*, 2005–2048.
- (11) Pallassana, V.; Neurock, M. *J. Catal.* **2000**, *191*, 301–317.
- (12) Liu, Z. P.; Hu, P. *J. Chem. Phys.* **2001**, *115*, 4977–4980.
- (13) Michaelides, A.; Liu, Z. P.; Zhang, C. J.; Alavi, A.; King, D. A.; Hu, P. *J. Am. Chem. Soc.* **2003**, *125*, 3704–3705.
- (14) Wang, H. F.; Liu, Z. P. *J. Am. Chem. Soc.* **2008**, *130*, 10996–11004.
- (15) Logadottir, A.; Rod, T.; Nørskov, J. K.; Hammer, B.; Dahl, S.; Jacobsen, C. J. H. *J. Catal.* **2001**, *197*, 229–231.
- (16) Alcalá, R.; Mavrikakis, M.; Dumesic, J. A. *J. Catal.* **2003**, *218*, 178–190.
- (17) Loffreda, D.; Delbecq, F.; Vigné, F.; Sautet, P. *Angew. Chem., Int. Ed.* **2009**, *48*, 8978–8980.
- (18) Chen, Y.; Vlachos, D. G. *J. Phys. Chem. C* **2010**, *114*, 4973–4982.
- (19) Liu, B.; Greeley, J. *J. Phys. Chem. C* **2011**, *115*, 19702–19709.
- (20) Wang, S.; Petzold, V.; Tripkovic, V.; Kleis, J.; Howalt, J. G.; Slulason, E.; Fernandez, E. M.; Hvolbaek, B.; Jones, G.; Toftlund, A.; Falsig, H.; Björketun, M.; Studt, F.; Abild-Pedersen, F.; Rossmeisl, J.; Nørskov, J. K.; Bligaard, T. *Phys. Chem. Chem. Phys.* **2011**, *13*, 20760–20765.
- (21) Sutton, J. E.; Vlachos, D. G. *ACS Catal.* **2012**, *2*, 1624–1634.
- (22) Laref, S.; Delbecq, F.; Loffreda, D. *J. Catal.* **2009**, *265*, 35–42.
- (23) Michel, C.; Auneau, F.; Delbecq, F.; Sautet, P. *ACS Catal.* **2011**, *1*, 1430–1440.
- (24) Saliccioli, M.; Chen, Y.; Vlachos, D. G. *J. Phys. Chem. C* **2010**, *114*, 20155–20166.
- (25) Abild-Pedersen, F.; Greeley, J.; Studt, F.; Rossmeisl, J.; Munter, T. R.; Moses, P. G.; Skulason, E.; Bligaard, T.; Nørskov, J. K. *Phys. Rev. Lett.* **2007**, *99*, 016105.

## *Chapter 2: Predicting polyalcohol reactivity from simple alcohols*

Starting from a model system we evidenced that it is possible to predict the reactivity of complex molecules, such as polyalcohols, from simple molecules. In spite of their high statistical quality, the BEP-type relationships established on monoalcohols lead to systematic errors when they are applied to glycerol. This systematic deviation is not oriented in the same direction for CH and OH dissociations, hence rendering difficult any comparison between them. It is thus important to understand the origin of this shift and to find methods to reduce it. We think that the systematic error observed for CH bond is related to structural constraints present in glycerol and not in simple alcohol, hence hindering the dissociation. To the opposite, for OH bond it is related to intramolecular bonds occurring in glycerol and assisting the bond breaking.

Even if this analysis was performed on Rh, the conclusion must be also applicable to other transition metals. In the following we will develop similar linear relations for monoalcohol dehydrogenation on various metals. Then we will address the question of the H-bond effect and see how it affects the BEP-type relation.

# Chapter 3: Prediction of monoalcohol dehydrogenation on transition metals

---

## Introduction

In the previous chapter, we evidenced that glycerol reactivity on Rh (111) may be deduced from linear energy relations established for monoalcohols on the same surface. Now, we intend to generalize this result to other transition metals, in order to eventually predict polyols reactivity on various metallic catalysts. As previously, we considered a set of dehydrogenation reactions for various monoalcohols on the close packed facet of several metals namely, Co (0001), Ni (111), Ru (0001), Rh (111), Pd (111), Ir (111) and Pt (111). Then, we looked for global BEP-type models valid for all of these metals.

In the first part of this chapter, we will focus on some generalities about monoalcohol reactivity and thermodynamics of their dehydrogenation products on a set of transition metals. Then, the second and the third part will be devoted to the set up of BEP-type relations of good quality to predict  $\text{CH}_\alpha$  and OH dissociations. Let us remind that in glycerol every CH bond is in  $\alpha$  position of an OH function. That is why we did not focus on  $\text{CH}_\beta$  breaking in this chapter.

# 1 Monoalcohol dehydrogenation on transition metals: basics

In order to study the dehydrogenation of monoalcohol molecules on transition metals, we selected a set of reactions from the previous results on Rh (111). Then, we analyzed and compared the stability of reaction intermediates between all the considered metals, before focusing on their reactivity.

## 1.1 Selection of a representative subset of reactions

Aiming at fast predicting alcohol reactivity, we reduced the number of points that are necessary to establish a BEP type relation. Indeed, we decided to focus only on certain characteristic reactions strategically picked from those ones calculated on Rh (see **Figure 3-1**), in order to efficiently scan a large number of metals. Concerning  $\text{CH}\alpha$  dissociations, the sample size is reduced from 12 to 8 points, and from 10 to 7 for OH scissions. Therefore, using this strategy we avoid calculating 42 points (since we saved 4 points for  $\text{CH}\alpha$  and 3 points for OH, and since we considered 6 metals, except Rh), each points including an initial state (IS), a transition state (TS) and a final state (FS).

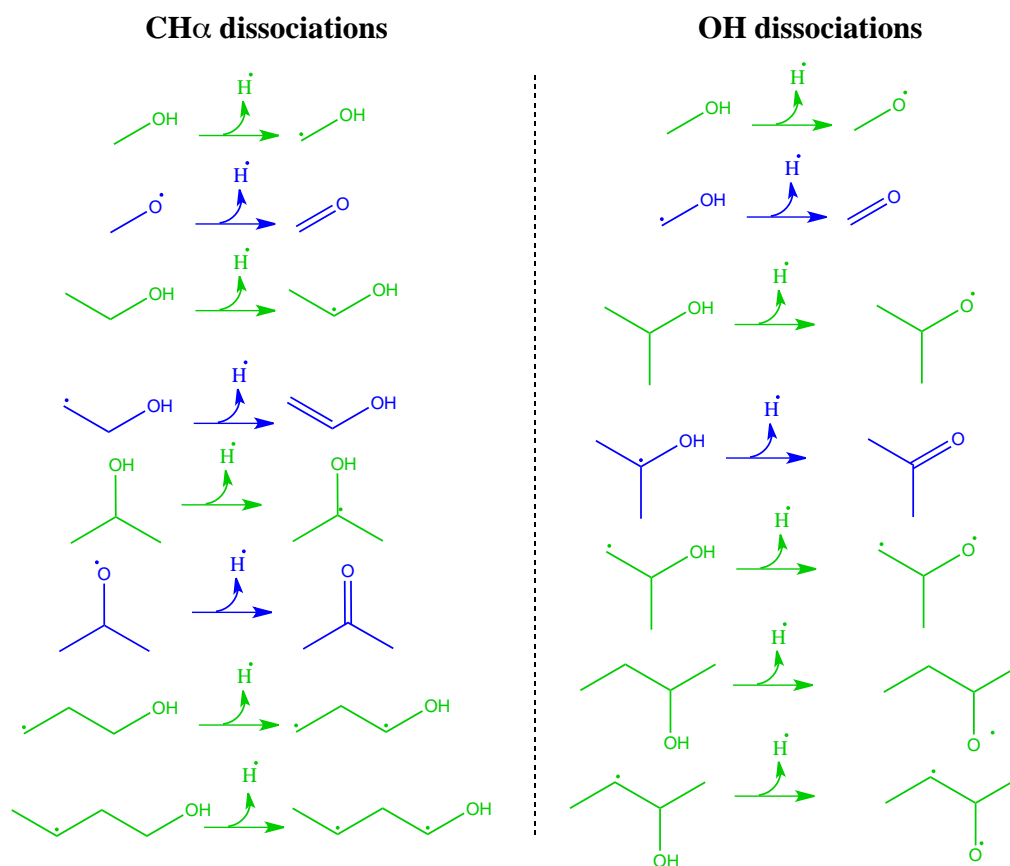


**Figure 3-1:** List of dehydrogenation reactions considered on the various transition metals. Green reactions represent the production of radicals and blue ones represent the formation of carbonyls and enols. All the species, either reactants or products, are adsorbed on the slab.

While sampling this subset of reactions, we tried to be representative on the chemical and on the statistical point of view. On the chemical side, we chose elementary reactions producing closed shell molecules (carbonyls and enols) or radicals (mono and diradicals). All species are chemisorbed on the metal surface, so that the complete system {fragment + surface} is always closed-shell non spin-polarized (except for Co and Ni). Concerning the statistical aspect, we considered two important linear energy relations obtained for Rh namely, the TSS.diss.FS/FS and the BEP.diss. On these two graphics we selected some points such as all the energetic zone is scanned both for the x-axis ( $E_{\text{FS}}$  for the TSS and  $\Delta E$  for the BEP) and the y-axis ( $E_{\text{TS}}$  for the TSS and  $E^\ddagger$  for the BEP). In such a way, assuming that all the points occupy an energetic range rather similar for every metal, we are sure that the largest part of the energetic zone is sampled for BEP and TSS. Besides, we also tried to reproduce the statistical error distributions obtained for Rh with these two relations. We included thus in our sample some

typical points such as the whiskers of the boxplot, meaning the points producing the two extreme errors. The procedure is schemed in **Figure 3-2** in one specific case.

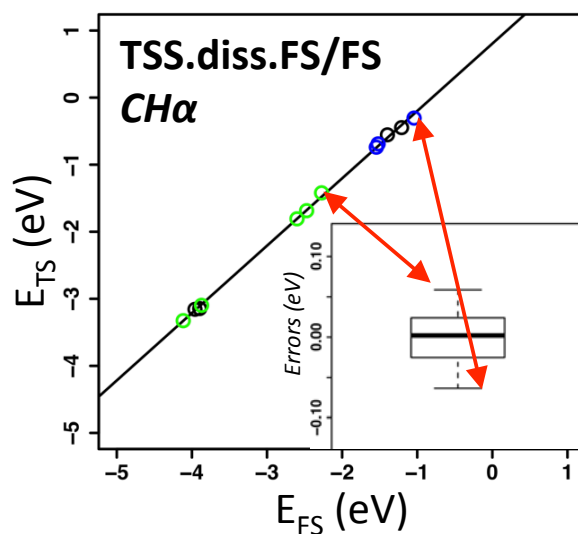


**Figure 3-2:** Selection of the set of reactions from the TSS.diss.FS/FS relation for CH $\alpha$  dissociation on Rh (111). 8 reactions are selected on the 12 initially calculated on Rh. The green points correspond to the mono- and di-radicals formation, and the blue ones to the carbonyls and enols formation. The extreme residual errors are pointed with the double red arrow. The same procedure was repeated on BEP.diss in order to ensure that the whole energetic zone is also scanned for reaction and activation energies. Reactions were selected in the same way for OH dissociations.

Other more rigorous methods exist in statistics to isolate a representative subset of points from a given sample, but the sample we are dealing with is too small to apply them. Accordingly, we will admit that the reactions we extracted are representative, at least on Rh (111), and we will describe these steps on several metals.

## 1.2 Adsorption of alcohol dehydrogenation intermediates and products

### 1.2.1 General description of the adsorption modes

We computed the previous subset of reaction steps for Co, Ni, Ru, Pd, Ir and Pt on the (111) surfaces for *fcc* metals and on the (0001) surface for *hcp* ones (Co and Ru here). Several types of intermediates, reactants and products may be identified and gathered according to their chemical nature. There are alcohols, carbonyls and enols on one side, and hydroxylated alkyl and alkoxy radicals on the other one. All these species have various adsorption modes with

different stability according to the metallic surface. Even if many results are already available in the literature,<sup>1,2,3,4,5,6,7,8</sup> various species such as enols or acetone are difficult to find on every metal. Besides, PW91 functional is not systematically used in the literature for every species, and we should use the same level of calculations in every case in order to be consistent and confident in our results. Thus, we performed extensive computations to find the most stable configurations for all the species that are relevant for our study.

Several trends can be observed in the adsorption of those species on the various metals. Firstly, alcohols always adsorb *via* their OH group in a top position as expected.<sup>1</sup> Concerning the other molecules (carbonyl derivatives and enols), the situation is a bit more confused. In the case of carbonyls, the top-bridge adsorption mode (molecule horizontal, see **Figure 3-3**) is often reported in the literature.<sup>2,3,4,5,6</sup> However, we observed that this configuration can compete with a top position (molecule vertical, see **Figure 3-3**) according to the substitution level of the molecule. Top-bridge and top configurations are equivalent for acetone except for Ir, Pd and Pt where the top adsorption is much more favorable. For weakly substituted carbonyls, top-bridge adsorption is generally favored, except for Pt where formaldehyde is in di-sigma and acetaldehyde is in top. These observations are gathered in **Table 3-1**.

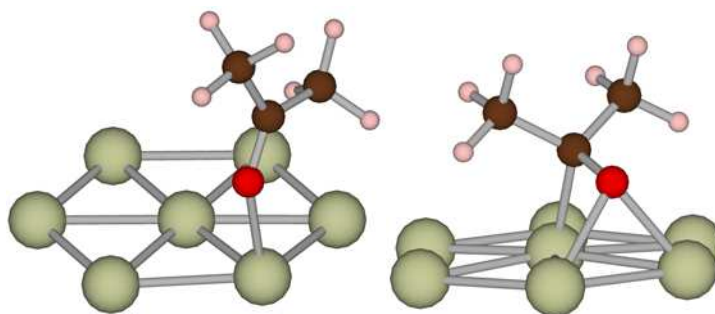


**Figure 3-3:** Acetone adsorption on Rh (111). Top (left) and top-bridge (right) positions are equivalent. (Greenish: Rh, brown: C, red; O and pink: H)

<b>Carbonyl derivative adsorption</b>  <b>R1-CO-R2</b>	<b>Co (0001)</b>	<b>Ni (111)</b>
	$R1=R2=H$ Ct-Ob $R1=H; R2=Me$ Ct-Ob $R1=R2=Me$ Ct-Ob $\leftrightarrow$ Ot	$R1=R2=H$ Ct-Ob $R1=H; R2=Me$ Ct-Ob $R1=R2=Me$ Ct-Ob $\leftrightarrow$ Ot
<b>Ru (0001)</b>	<b>Rh (111)</b>	<b>Pd (111)</b>
$R1=R2=H$ Ct-Ob $R1=H; R2=Me$ Ct-Ob $R1=R2=Me$ Ct-Ob $\leftrightarrow$ Ot	$R1=R2=H$ Ct-Ob $R1=H; R2=Me$ Ct-Ob $R1=R2=Me$ Ct-Ob $\leftrightarrow$ Ot	$R1=R2=H$ Ct-Ob $R1=H; R2=Me$ Ct-Ob $\leftrightarrow$ Ot $R1=R2=Me$ Ct-Ob $\leftrightarrow$ Ot
	<b>Ir (111)</b>	<b>Pt (111)</b>
	$R1=R2=H$ Ct-Ob $R1=H; R2=Me$ Ct-Ob $\leftrightarrow$ Ot $R1=R2=Me$ Ot	$R1=R2=H$ Ct-Ot $R1=H; R2=Me$ Ot $R1=R2=Me$ Ot

**Table 3-1: Adsorption modes of carbonyls of transition metals.** The configuration of the species on the surface depends on the substitution level (i.e. on R1 and R2). Each atom of the C=O bond may be adsorbed in a different position: “t” for “top” and “b” for “bridge”

Concerning enols, these species present a larger variety of configurations on metallic surfaces involving the ethylenic bond and the OH group. We noticed especially that for Rh, Pd, Ir and Pt the di- $\sigma$  mode is the most favorable, and competes with the  $\pi$ -mode for Rh and Ir. In the two latter metals OH is coordinated to the metal, which stabilizes the system. For Co, Ni and Ru we found a particular mode of adsorption, already reported in the literature for ethylene.<sup>7</sup> One C is on a hollow site (or in bridge) and the other one (the one linked to OH) is rather on a top position. For Co and Ru, which are more electrophilic, the OH is also coordinated to a neighboring surface atom. The three main adsorption modes of enols are depicted in **Figure 3-4**, and **Table 3-2** sums up their most stable configuration metal per metal.

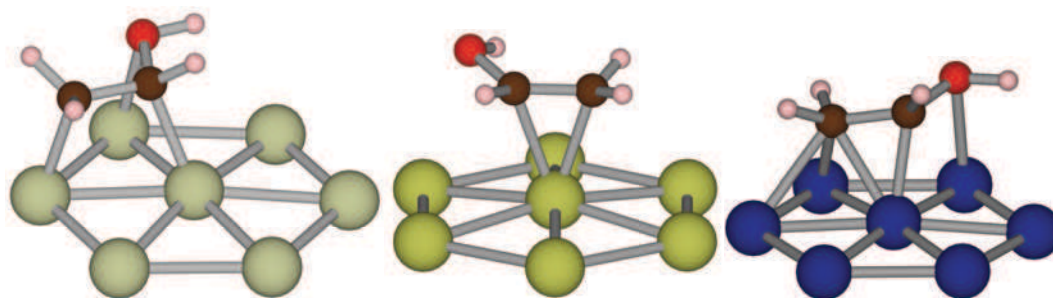


**Figure 3-4: Enol adsorption on Rh (di- $\sigma$ ), Ir ( $\pi$ ) and Co (hollow-top) (from left to right). (Greenish: Rh, yellowish: Ir, blue: Co, brown: C, red; O and pink: H)**

<p><b>Enol adsorption</b></p>	<p><b>Co (0001)</b></p> <p>C<sub>1</sub>h-C<sub>2</sub>t-Ot</p>	<p><b>Ni (111)</b></p> <p>C<sub>1</sub>h-C<sub>2</sub>t</p>
<p><b>Ru (0001)</b></p> <p>C<sub>1</sub>b-C<sub>2</sub>t-Ot</p>	<p><b>Rh (111)</b></p> <p>CC <math>\pi</math>-Ot <math>\Leftrightarrow</math> CC di-<math>\sigma</math>-Ot</p>	<p><b>Pd (111)</b></p> <p>CC di-<math>\sigma</math></p>
	<p><b>Ir (111)</b></p> <p>CC <math>\pi</math> <math>\Leftrightarrow</math> CC di-<math>\sigma</math>-Ot</p>	<p><b>Pt (111)</b></p> <p>CC di-<math>\sigma</math></p>

**Table 3-2: Adsorption modes of enols on transition metals.** Each of the two C atoms of the ethylenic bond occupies a specific site on the surface: “h” for “hollow”, “b” for “bridge” and “t” for “top”. When the OH group is connected to the metal, it is notified by “Ot”. For every configuration a scheme is reported in the table, representing a top view of the molecule (black lines) on the metal (grey triangles).

Regarding now the radical species adsorption, the situation is much less dependent on the substitution level of the structure. We observed that alkoxy radicals bind to the surface with their radical O in a hollow site except for Pt, where it is on a top site. As for the hydroxylated alkyls, they are linked with the metal *via* the radical C in a top position with their OH group connected to the surface (except for Pd and Pt, where OH is desorbed). These results are confirmed by literature.<sup>2,3,4,5,6,8</sup> Let us mention that for Co, Ru and Ni, a configuration that is energetically equivalent (energy difference <0.05 eV) exists for weakly substituted species such as CH<sub>2</sub>OH, in which the C is on the bridge site. Concerning alkyl diradicals, the OH group adsorption is difficult due to “cycle constraints”. Indeed, the adsorption mode of these systems generates considerable torsions and the structure loses in flexibility. As a consequence, in this configuration the OH group cannot approach the surface in an optimal way to establish any bond as represented in **Figure 3-5**.

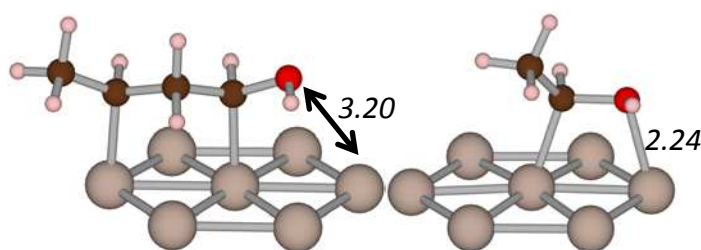


**Figure 3-5:** Example of a di- and mono-radical (respectively left and right) adsorbed on Ru (0001). Due to the cycle torsions induced by the diradical adsorption, the OH group cannot approach enough the surface to bind (left picture). To the opposite, when there is just a unique radical center on the structure (right picture), OH has more freedom to tilt toward the surface and to coordinate. (Grey: Ru, brown: C, red; O and pink: H)

### 1.2.2 Relative stability of the different species

All the different species previously considered do not have the same stability on every metal. Moreover, the order of stability between all these species may also be affected from one metal to the other. In order to address this issue we considered three molecules (iPrOH, MeCOMe and CH<sub>2</sub>CHOH) and two radicals (iPrO and MeCOHMe) adsorbed in their most stable configurations. Then, we computed their adsorption energies according to the following formula:

$$E_{ads}(M@slab) = E(M@slab) - [E(M) + E(slab)] \quad \text{Equation 3-1}$$

where  $E_{ads}(M@slab)$  is the adsorption energy of the species  $M$ ,  $E(M@slab)$  the absolute energy of the species  $M$  bonded to the surface,  $E(M)$  the absolute energy of  $M$  in the gas phase and  $E(slab)$  the absolute energy of the metallic slab.

Adsorption energies are shown in **Figure 3-6** for each of the previous species on the seven metallic surfaces. For information, we also added the adsorption energy of H, since in every reaction the dissociated H atom is considered in a hollow position on a separate slab. One notices firstly that adsorption energies are similar and rather weak on all the metals for acetone and isopropanol, which are both chemisorbed only through the lone pair on the oxygen. Only small variations occur for the enol and similarly for H. However, major differences appear regarding the adsorption of radicals. The strength of adsorption sharply increases (i.e.  $E_{ads}$  decreases) for the alkoxy (iPrO) moving from the right to the left in the periodic table (Pt Ir/ Pd Rh Ru/ Ni Co). These observations are in agreement with the d-band model of Hammer and Norskov.<sup>9</sup> The farther to the left it is, the closer the d-band center is from the Fermi level. Since the d-band is shifted upward, antibonding adsorbate-metal d-states are depopulated. That is why adsorption is stronger on Ru than on Pd. Now, concerning the hydroxylated alkyl (MeCOHMe), we observe a different behavior. Even if adsorption strength increases a bit from Co to Pt, globally the variations are very small in a given period of the classification. This absence of correlation, between the adsorption energies and the d-band center, was also reported by Nakamura and coworkers<sup>10</sup> in the case of methyl adsorption on transition metals on a top position. It was suggested that this adsorption mode is not optimal for the coupling between the adsorbates orbitals and the metal d-band, comparatively to a hollow site. Since in our case, every hydroxylated alkyl was found on a top position, similar considerations might explain the quite even behavior of their adsorption energies.

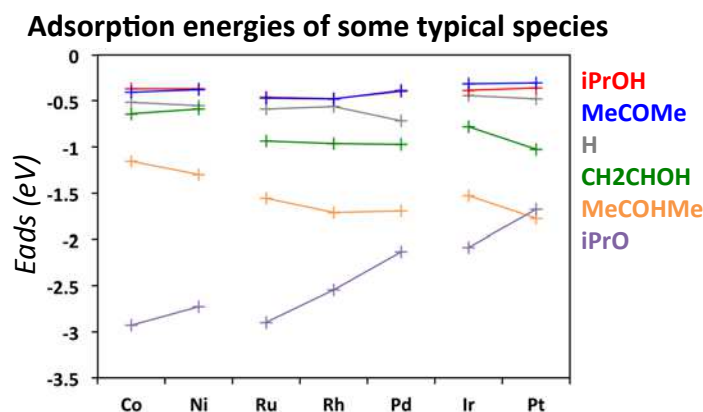


**Figure 3-6:** Adsorption energies of the main reaction intermediates for monoalcohols dehydrogenation on transition metals. Apart from the H atom, three molecules are considered, namely, acetone, isopropanol and one enol, and two radicals, namely an alkoxy (iPrO) and a hydroxylated alkyl (MeCOHMe).

### 1.3 Thermodynamics and kinetics

For each of the seven metals of our set we searched for reaction paths for all the dehydrogenation reactions mentioned in 1.1, starting systematically from the most stable adsorbates. Let us begin by analyzing thermodynamics of the reactions. We used here the statistical tools described in the last part of Chapter 1. Reaction energies for every dehydrogenation reaction are represented in box plots on **Figure 3-7** for each metal. Considering first the CH $\alpha$  dissociations, we can see that reaction energies range from  $\sim -0.70$  eV to  $\sim +0.60$  eV. Dehydrogenation reactions on Pt and Pd catalysts are globally exothermic, whereas on Co and Ni they are rather endothermic. On other metals, reaction energies are smaller in absolute value. Let us mention that enol formation has in general the lowest reaction energies (corresponding to the outliers observed in the left panel of **Figure 3-7** for Co, Ni, Ru and Ru), competing with acetone formation for Pd, Ir and Pt. Regarding now OH dissociations, the trends are reversed. Indeed, Co presents the highest exothermicity with Ni and Ru, while reactions over Ir and especially Pt are endothermic. This result was also observed for ethanol by Lin and coworkers.<sup>11</sup> Lowest reaction energies correspond in general to the formation of carbonyls, competing with alkoxy on Co, Ni and Ru. Finally, CH $\alpha$  scission on Ir and OH scission on Pd are particular cases. Indeed, in both situations reaction energies spread nearly equitably around zero. As a result, there are subsets of exothermic,

endothermic and athermic reactions on these metals, and none of these groups looks negligible or statistically underrepresented.

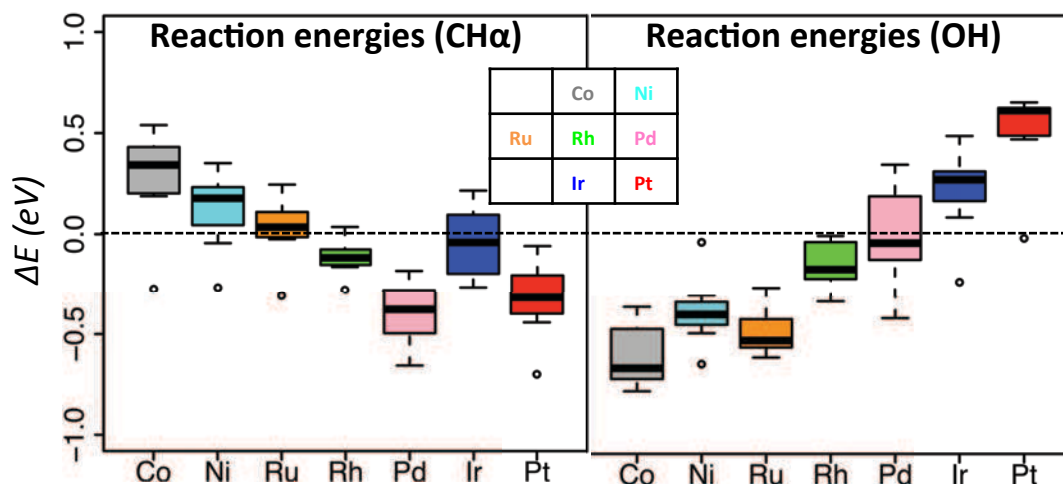


**Figure 3-7:** Box plot representation of the reaction energies for  $CH\alpha$  and  $OH$  scissions on the set of seven transition metals

This behavior can be explained in the light of the conclusions of the previous section. Indeed we showed in **Figure 3-6**, that only adsorption energy of alkoxy radicals exhibits considerable variations along the different metals, steadily decreasing (in absolute value) from Co to Pt. Since for other species the variations are much weaker, we can think that only alkoxy radicals should have a major influence in the evolution of the reaction energies. Concerning  $CH\alpha$  breaking, this species occurs as reactant in the formation of carbonyl derivatives. Since, in that case the reaction energy is defined as the difference between the carbonyl and the alkoxy energies while adsorbed on the surface, and considering that carbonyl and hydrogen adsorption energies are rather even along the metals, we understand that reaction energies decrease from Co to Pt. We can show similarly why the tendency is reversed for  $OH$  breaking, considering now that alkoxy radicals occur as a product of alcohol dehydrogenation.

After addressing the question of thermodynamics, we can deal now with the activation energies (see **Figure 3-8**). Considering first  $CH\alpha$  dissociation, we observe that globally reactions on Co, Ni and Ru present the highest activation energies approximately ranging between 0.8 and 1.2 eV. The lower outliers observed on the left panel of **Figure 3-8** correspond to enol formation on these metals. Activation energies are lower for the other metals of our set, with minimal values of 0.36 eV and 0.11 eV for acetone formation respectively on Ir and Pt. Regarding then  $OH$  dissociations, activation energies are rather

similar for the set of metals, ranging between 0.6 and 1.0 eV. Comparing CH $\alpha$  and OH breaking we can say that on oxophilic metals such as Co, Ni and Ru, OH scission is globally easier than CH scission. On other metals, such as Ir or Pt, CH dissociation is easier than OH dissociation. Besides, all the box plots have not the same broadness according to the reaction and to the metal. This feature is directly related to the selectivity of the catalyst. The tighter the activation barrier distribution, the less selective the catalyst is. This observation is also true for reaction energies. To conclude, it is worth noting that from Co to Pt, activation energies globally evolve as the reaction energies (compare **Figure 3-8** and **Figure 3-7**) for CH $\alpha$  dissociations. This observation highlights the correlation existing between activation energies and reaction energies, and suggests a transfer coefficient (*i.e.* the slope of the BEP.diss relation) close to 1 in that case. To the opposite, such a correlation is not observed for OH scission, activation energies seeming to evolve independently of reaction energies. In this situation, a transfer coefficient close to zero is expected.

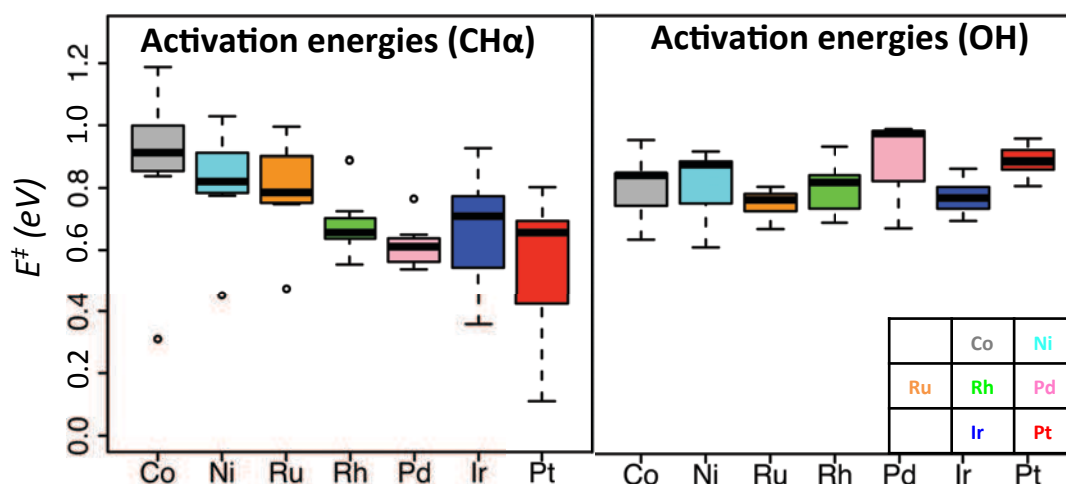


**Figure 3-8:** Box plot representation of the activation energies for CH $\alpha$  and OH scissions on the set of seven transition metals

## 2 Global BEP-type relations

In this part we will establish BEP type relations for monoalcohols dehydrogenation on the previous set of metals. Such relations can be ultimately used to perform a screening of metallic catalyst efficiency in alcohol dehydrogenation. As a consequence, it may be very useful to find a global relationship valid on a whole set of metals, rather than one relation specific to each metal individually. As we did on Rh in Chapter 2, we will look for a linear energy relation for OH dissociations and subsequently for CH $\alpha$  breaking.

### 2.1 Statistical analysis

#### 2.1.1 OH breaking

In order to assess the quality of the linear relations for OH dissociations on the set of monoalcohol molecules over transition metals, we can first look at the mean absolute error (MAE) and the maximum error (MAX) for some representative BEP type relations. We established a global predictive model considering the whole set of OH dissociations on the seven transition metals. The total sample thus contains 49 points. Apart from the BEP.diss relation (frequently used in the literature), we also focused on two TSS connecting the TS energy with the initial state, namely TSS.diss.IS/IS and TSS.exo.IS/IS, and on two TSS connecting the TS with the final state, the TSS.diss.FS/FS and the TSS.exo.FS/FS. In accordance with the conclusions of the first chapters, we assumed that the influence of the choice of gas reference is negligible. All the results are gathered in **Table 3-3**.

OH	TSS.diss.FS/FS	TSS.exo.FS/FS	TSS.diss.IS/IS	TSS.exo.IS/IS	BEP.diss
<i>MAE</i>	0.30	0.17	0.08	0.12	0.08
<i>MAX</i>	0.68	0.46	0.20	0.40	0.18

**Table 3-3:** *MAE and MAX in eV, while using one global model for all metals to predict OH scissions. The model is built considering the set of OH dissociations in the framework of 5 BEP type relations.*

The first conclusion stemming from this table is that the TSS relations connecting the TS energy with the final state energy gives rather bad predictions. However, the TSS relations connecting the TS with the initial state, look better and especially the TSS.diss.IS/IS. Despite of an acceptable average error, the TSS.exo.IS/IS presents a high maximal error. As a result,

two modes of correlation particularly stand out, namely TSS.diss.IS/IS and the classical BEP.diss. For these two relations one observes an MAE on the order of 0.10 eV and a MAX on the order on 0.20 eV. These two BEP type relations are depicted on **Figure 3-9** with their corresponding equations and error distributions.

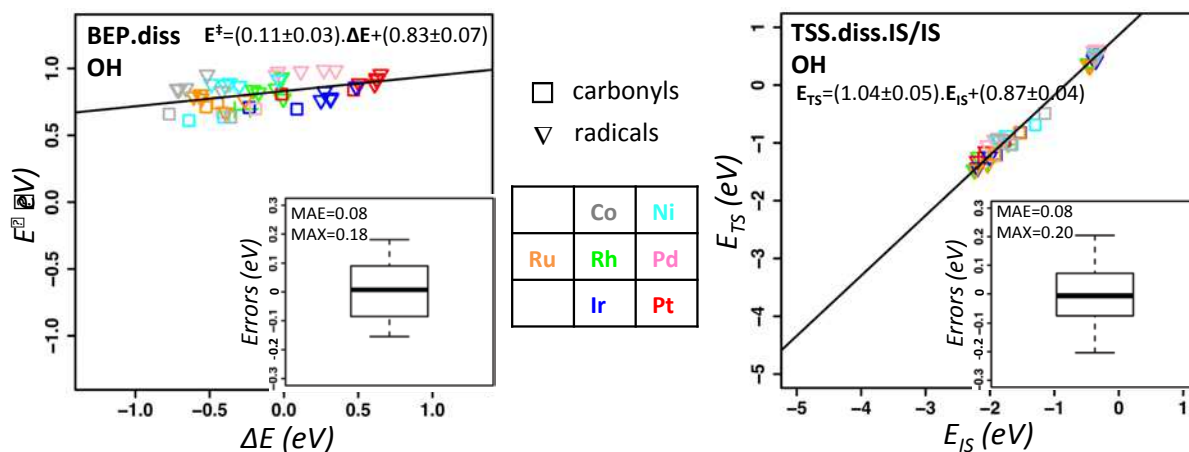


**Figure 3-9: BEP.diss and TSS.diss.IS/IS relations for OH dissociations in monoalcohols on various transition metals and their corresponding error distributions.** The global model is obtained considering all the metals together (represented in various colors). The different symbols represent the formation of species with a different chemical nature.

At a first glance, all the points seem well integrated in the global model. We can see that in the two kinds of relations error distribution is tight, with errors ranging from about -0.20 eV to +0.20 eV. Besides, the confidence interval of the correlation parameters (slope and intercept) is very narrow in both cases proving the robustness of the statistical model. Let us highlight that the low value of the slope in the BEP relation has some implications on the nature of the TS that will be detailed in the following. If one considered the reaction in the hydrogenation direction instead of the dehydrogenation, the slope would be close to 1 but residual errors would be exactly identical.

### 2.1.2 CH $\alpha$ breaking

Again, in order to find a satisfying predictive model for CH $\alpha$  dissociations, we start by analyzing MAE and MAX for the linear relations previously mentioned. A global linear model is obtained by conducting a linear regression within the whole set of CH $\alpha$  reactions on the seven transition metals (56 reactions). All the results are summed up in **Table 3-4**.

$CH\alpha$	TSS.diss.FS/FS	TSS.exo.FS/FS	TSS.diss.IS/IS	TSS.exo.IS/IS	BEP.diss
<i>MAE</i>	0.11	0.11	0.14	0.11	0.09
<i>MAX</i>	0.55	0.44	0.59	0.52	0.30

**Table 3-4: MAE and MAX in eV for a global model including all metals to predict  $CH\alpha$  dissociations.** The model is built considering the set of  $CH\alpha$  dissociations in the framework of 5 BEP type relations.

In this table one observes no major difference between the TSS in the prediction of  $CH\alpha$  dissociations. Indeed all the MAE are very close to each other and the MAX are especially high, higher than 0.50 eV. Only the classical BEP.diss, with an MAE at 0.09 eV and a MAX at 0.30 eV, seems to lead to more acceptable errors. BEP.diss relation is plotted below in **Figure 3-10** with its error distributions. Let us mention that concerning TSS.diss.FS/FS, the highest errors are due to Pd, the MAX shifting from 0.55 eV for the global model, to 0.27 eV when excluding Pd.

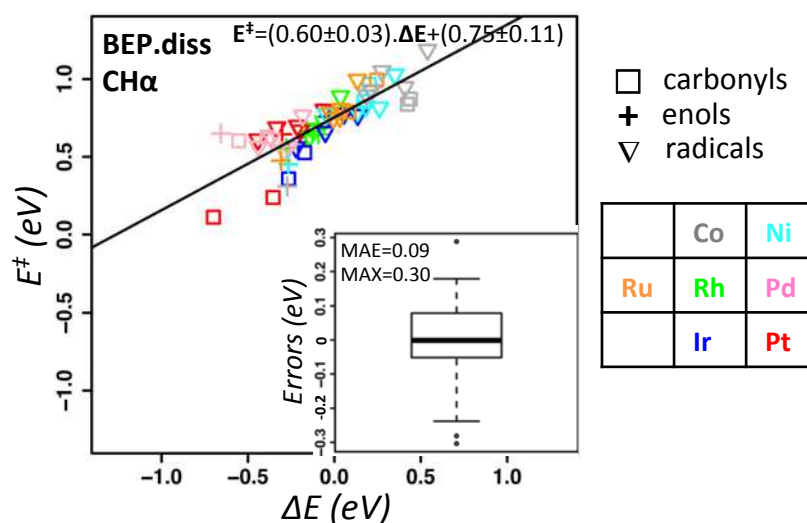


**Figure 3-10: BEP.diss relations for  $CH\alpha$  dissociations in monoalcohols on various transition metals and the corresponding error distributions.** The global model is obtained considering all the metals together (represented in various colors). The different symbols represent the formation of species with a different chemical nature.

All the points seem to fit well to the line except few points on the left of the graph. These points are mainly the reactions leading to carbonyls on Pt, Ir and Pd, and the reactions leading to enols. We will debate elsewhere in the chapter whether one should treat these points differently or not. Concerning the global error distribution, its amplitude is about of 0.45 eV

(from  $\sim -0.25$  to  $\sim +0.20$  eV), which is slightly higher than in the case of OH dissociation. Again, the parameters of the correlation have very tight confidence intervals and especially for the slope. This was not observed in Chapter 2 when we considered monoalcohols dehydrogenation on Rh, despite the good quality of the linear energy relations we had in that case. This is a direct effect of increasing the size of the sample by considering all the metals together, 56 points here *vs.* 12 in the case of Rh. This feature strengthens the validity of the model and of its prediction on the monoalcohols population.

## 2.2 Early and late TS: the impact on BEP-type relations

We evidenced that BEP.diss and TSS.diss.IS/IS are both good for OH dissociations, whereas only BEP.diss gives satisfying predictions for CH $\alpha$  dissociations when considering the whole set of metals. If we consider the BEP.diss for OH dissociations, we note that the slope (transfer coefficient) is  $0.11 \pm 0.03$ . The fact that this slope is close to 0 means that globally TS are early, and this whatever the metal. Concerning CH $\alpha$  dissociations, we observe a transfer coefficient of  $0.60 \pm 0.03$ . This value, intermediate between 0 and 1, suggests an intermediate nature of the TS related CH $\alpha$  scissions, meaning that the TS is as close to the reactant than to the product. Since both OH and CH breakings include exothermic and endothermic reactions (see **Figure 3-7**), thermodynamics argument is not sufficient to give a justification for the TS nature. However, the concept of early and late TS is at the root of the quality of a BEP-type relation.<sup>12</sup> Thus, it is important to find a way to discriminate between them. That is why we turned to geometrical considerations.

As we observed on **Figure 3-10**, some points look singular according to their positions with respect to the linear fit, in the CH $\alpha$  BEP.diss relation. The points corresponding to the formation of unsaturated species (carbonyls/enols) on Pt, Ir and Pd on the extreme left of the graph are especially striking (in particular for Pt and Ir). For each of them, we considered the TS and its immediate precursor and product. The precursor is the same initial state as the one considered in the linear relations, whereas the product is different. Indeed, to establish our linear energy relations we used a final state with the dissociated H on a distinct slab. However, this state is not the closest from the TS. In order to correctly look for similarities between the TS and its corresponding product, one should rather consider the coadsorbate state, meaning the dissociated molecular fragment with the dissociated H in its neighborhood.

Then, we calculated a Euclidian distance\* between the TS and its precursor on one side, and between the TS and its coadsorbate on the other side. If the TS-precursor distance is significantly smaller than the TS-coadsorbate one, then the TS is considered as early, else it is late (see **Table 3-5**). When the difference between the two distances is not very marked, we considered that the TS is not late of early but “intermediate”.

CH $\alpha$ scission	Pt				Ir				Pd			
	TS- reac	TS- prod	TS nature	$\epsilon$	TS- reac	TS- prod	TS nature	$\epsilon$	TS- reac	TS- prod	TS nature	$\epsilon$
Acetone	1.20	6.27	Early	0.23	2.06	5.58	Early	0.24	5.51	4.40	Interm.	0.11
Formaldehyde	1.73	2.65	Interm.	0.30	1.72	2.84	Interm.	0.12	5.82	1.76	Late	0.18
Enol	3.77	1.93	Late	0.07	2.66	2.60	Interm.	0.02	2.88	4.36	Early	0.29

**Table 3-5: TS nature according the some geometrical considerations.** “TS-reac” and “TS-prod” respectively refer to the Euclidian distance (in Å) between the TS and the reactant on one hand, and the TS and the product on the other hand. The TS nature is determined comparing TS-reac and TS-prod. The quantity “ $\epsilon$ ” denotes the absolute error (in eV) obtained by BEP.diss prediction for each point. In this table, we only considered carbonyls and enol stemming from CH $\alpha$  scission

As a consequence, unsaturated species stemming from CH breaking are related to the TS of different natures. Besides, many of them are intermediate between early and late, hence the intermediate value (between 0 and 1) of the transfer coefficient of the BEP relation. Now, let us focus on errors obtained *via* BEP predictions for the formation of those species, reported in **Table 3-5**. Concerning Pd and Ir, we observe that reactions related to intermediate TS correspond to the lowest errors. However, regarding Pt catalyst, errors are higher for carbonyl derivatives whatever the nature of their TS. These points appear at the very left extremity of the graph in **Figure 3-10**, and present the lowest reaction energy (meaning the highest exothermicity). As a result, we can find here the two major elements controlling the quality of a BEP relation, already reported by Vlachos and co-workers.<sup>13</sup> The nature of the TS must be similar among all the reactions that are considered. But moreover, the energetic range on which one the linear energy relation is plotted must be relatively restricted. That is why we observe clearly a V-shaped error distribution for the CH $\alpha$  BEP.diss relation (**Figure 3-10**). As appears on **Figure 3-11**, errors are lower at the center of the graph than at its extremities. Athermic and weakly exo/endothemic reactions may be treat together in the same predictive

\* We call “Euclidian distance”, the quantity  $d$  defined such that:

$$d = \sqrt{\sum_i (x_i^A - x_i^B)^2 + (y_i^A - y_i^B)^2 + (z_i^A - z_i^B)^2},$$

where  $(x_i^A, y_i^A, z_i^A)$  are the coordinates of the  $i^{\text{th}}$  atom of the structure  $A$ , and similarly for the structure  $B$ .

model. But highly exothermic and endothermic reactions must be treated separately due to their high errors.

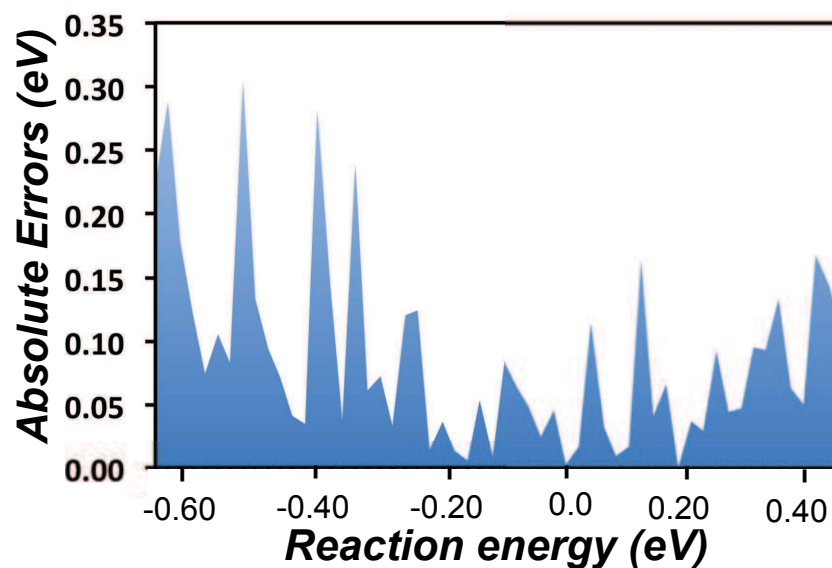


**Figure 3-11:** Absolute error distributions with respect to reaction energies, in the case of CHa BEP.diss relation. (See Figure 3-10.) A deep depletion is observed at the center of the graph, meaning for athermic reactions (and reactions with a weak reaction energy). Nevertheless, higher error values occur for highly exothermic and endothermic reactions, hence the V-shaped distribution.

To conclude, we saw in this section that while the performance of all the TSS relations are not equivalent, BEP relation always gives satisfying predictions, whatever the nature of the dissociated bond and whatever the metal. This phenomenon is due to the fact that TSS relations are very sensitive to the structural similarities between all the points that are considered. In the TSS paradigm, the TS must be close either to the FS or to the IS. To the opposite, BEP relation correlates activation energies and reaction energies, bringing together IS, FS and TS. That is why BEP relation can tolerate more discrepancies (up to a certain point) between the structures, as reported by Norskøv and coworkers.<sup>14</sup> Let us highlight that we did not reach the same conclusions for Rh (111) in Chapter 2. Indeed, we found there that all the BEP-type relations have equivalent performances. To resolve this apparent opposition, we must keep in mind that the energetic zone that is scanned is much larger considering all the metals together ( $-0.70 < \Delta E(\text{CH}\alpha) < 0.53$  eV), than restricting the analysis exclusively to Rh ( $-0.28 < \Delta E(\text{CH}\alpha) < 0.04$  eV), as depicted in **Figure 3-7**. As a result, on such a narrow area, it is difficult to observe any differences between the performances of all the BEP-type relations.

### 3 On the quality of the BEP predictions

As we just mentioned above, the quality of the BEP predictions depends on the chemical nature of the products. Some points, corresponding to the formation of unsaturated species, do not fit well to the BEP line, especially for CH $\alpha$  breaking. Hence it might be interesting to split the global relation according to the products. In this part we refer to the vocabulary and the methods described in the statistics section of Chapter 1. Besides let us mention that since we showed that the BEP.diss relation is the only one to be good both for OH and CH $\alpha$  dissociations, we will mainly focus on this one in the following.

#### 3.1 Reaction dependent models

The set of points we selected, contains reactions leading to radicals and to unsaturated species (carbonyls/enols). As confirmed by **Table 3-6**, unsaturated species often present the highest absolute errors when their activation energies are predicted *via* the global model, whatever the metal.

	BEP.diss	Co	Ni	Ru	Rh	Pd	Ir	Pt
CH $\alpha$ scissions	<i>Formaldehyde</i>	0.14	0.00	0.02	0.01	0.11	0.12	0.30
	<i>Acetone</i>	0.17	0.09	0.09	0.05	0.18	0.24	0.23
	<i>Enol</i>	0.28	0.14	0.09	0.03	0.29	0.02	0.07
	<i>MAX</i>	0.28	0.14	0.16	0.11	0.29	0.24	0.30
OH scissions	<i>Formaldehyde</i>	0.15	0.15	0.04	0.11	0.11	0.15	0.05
	<i>Acetone</i>	0.08	0.15	0.06	0.10	0.11	0.10	0.02
	<i>MAX</i>	0.18	0.15	0.12	0.11	0.15	0.15	0.05

**Table 3-6: Absolute errors (in eV) for the points corresponding to the carbonyls and enol formation.** These reactions are predicted via the CH $\alpha$  and OH global model in the BEP.diss definition. Their absolute errors are then compared to the maximal absolute error (MAX) obtained with the global models on each metal. Maximal errors on each metal are indicated in red

We can see that concerning CH $\alpha$  breaking, the maximal error is always reached by a carbonyl or an enol except for Ru and Rh. Similarly, for OH breaking carbonyls also present the

highest errors except for Ru. Thus, one can ask for OH and CH $\alpha$  scission if it could be preferable to split each global model, in two distinct models, one for mono- and di-radicals formation and one for unsaturated species (enol/carbonyls) formation. We tested this concept for BEP.diss, and we gathered the results in **Table 3-7**. In this table, we presented MAE and MAX obtained while predicting the formation of radicals using of one global model on one hand, and a model specific to the radicals, on the other hand. We added the MSE for the global model prediction. We proceeded in the same way for OH and CH $\alpha$  breaking, and for the prediction of the unsaturated molecules.

BEP.diss	Radicals		Unsaturated species	
	<i>Via global model</i>	<i>Via specific model</i>	<i>Via global model</i>	<i>Via specific model</i>
<b>CH<math>\alpha</math> scissions</b>	MAE 0.06	MAE 0.06	MAE 0.13	MAE 0.10
	MAX 0.16	MAX 0.14	MAX 0.30	MAX 0.27
	MSE +0.03		MSE -0.05	
<b>OH scissions</b>	MAE 0.07	MAE 0.06	MAE 0.10	MAE 0.03
	MAX 0.18	MAX 0.17	MAX 0.15	MAX 0.07
	MSE +0.04		MSE -0.10	

**Table 3-7: Errors analysis of the splitting of the global model according to the nature of the products.** For CH $\alpha$  and OH dissociations considered distinctly, one can imagine separating the reaction sample in two subsets: the radicals and the unsaturated species (enols and carbonyls) formation. A linear regression can be conducted within each of these subsets leading to two different specific models (one for radicals and one for unsaturated species). Predictions on these subgroups may be done either by the “global” model (no distinction between radicals and unsaturated species) or by one “specific” model. The quality of the prediction is assessed here by MAE, MAX and MSE when the prediction is performed with the global model, and only by MAE and MAX when one uses the two specific models.

We observe, concerning radicals that both for CH $\alpha$  and OH dissociations, almost no differences appear between the predictions from one global model and from one model specific to radicals. Indeed MAE and MAX are clearly not affected when considering all the points together. Besides, the MSE is lower than 0.05 eV. Then, we can deduce that including the carbonyls and enols in the set does not deteriorate at all prediction on radicals. Now, relating to unsaturated molecules, we can also see that the splitting has almost no effect for CH $\alpha$  scission. Yet, it is in that case that errors are the highest and that it would be interesting to reduce them. To the opposite, MAE and MAX are considerably lowered using a specific model is the case of OH dissociations. Nevertheless, these errors are still acceptable

(MAE=0.10 eV and MAX=0.15 eV) when the prediction is performed using the global model. Furthermore, the systematic shifts that are observed both for OH and CH $\alpha$  are on the same order of magnitude (0.05 and 0.10 eV), oriented in the same direction (both of them negative). This feature allows comparing together two different predictions obtained from BEP.diss for OH and CH $\alpha$  breaking. As a consequence, it does not appear necessary to split the global predictive model according to the nature of the products. However, one should just keep in mind that predictions are globally better for radicals than for unsaturated species especially for CH $\alpha$ . Also, since their MSE are not oriented in the same direction, it might be problematic to compare together radicals and unsaturated species. Similar conclusions are obtained for TSS relations.

## 3.2 Metal dependent models

### 3.2.1 BEP relation

Now that we addressed the question of reaction dependent models, one can ask if the quality of the prediction is equivalent for every metal. Besides, we wonder if it is worth splitting the global model according to the nature of the metal or not. In **Figure 3-12**, error distributions are depicted when predictions are performed *via* one global model (common to every metal) and when they are performed *via* distinct models, *i.e.* one per metal, still in the BEP framework. Concerning firstly CH $\alpha$  dissociations (see **Figure 3-12**, top panels), we can see here that using the global model significantly increases the error span for almost every metal. Only Ni, Rh and Pt are unaffected (the shifting down of the low “whisker” of the red box plot for Pt, is just a statistical effect due to the increase of the number of points). However, we can see that Ir and Pd predictions are affected by systematic deviations, that are non-negligible (around 0.10 eV) and going in opposite directions (negative for Ir and positive for Pd). This phenomenon increases the absolute errors obtained from the global model, and renders difficult any comparison between Ir and Pd. Similar observations arise from OH breaking, but the systematic deviation looks weaker (see **Figure 3-12**, lower panels). The only difference is that the benefit of using distinct predictive models is less obvious in that case. Indeed, error spans are rather close for Co, Ni and Ru when using the global model *vs.* the metal dependent models. The range of errors is increased by the global model for Rh and Pd, but it remains rather narrow for Ir and Pt. As a conclusion a global BEP.diss relation gives acceptable errors both for OH and CH $\alpha$  scissions. But the quality of the prediction may be considerably

improved on certain metals (especially for  $\text{CH}\alpha$  dissociations) by using metal dependent models, in particular for Pd and Ir.

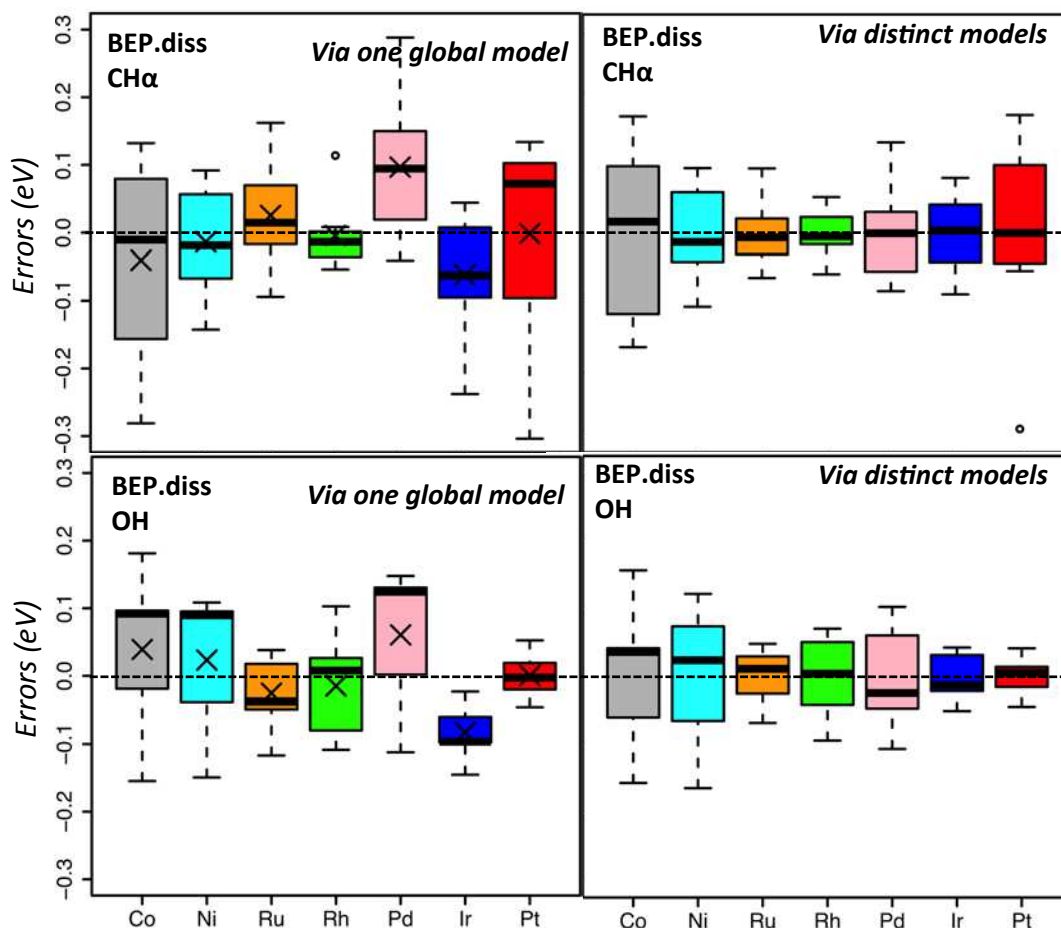


**Figure 3-12: Error distributions for the prediction of  $\text{CH}\alpha$  (top) and  $\text{OH}$  (bottom) dissociations with the BEP.diss relation.** On the left panel, prediction is performed by one global model (one for  $\text{CH}\alpha$  and one for  $\text{OH}$ ), common the whole set of metals. On the right panel, prediction is performed with seven distinct models, i.e. one per metal. The black cross on the left panel indicates the mean signed error (MSE).

In order to assess quantitatively the quality of the global BEP.diss relation, we gathered in **Figure 3-8**, the characteristic errors (MAE, MAX and MSE) obtained for each metal, using the global model. We observe that for  $\text{CH}\alpha$  breaking, predictions are much better for Ni, Ru and Rh. The other metals present higher errors close to 0.30 eV for the MAX. Concerning  $\text{OH}$  scission, the quality of the prediction is good and rather similar for every metal, with a MAX around 0.15 eV. Pt particularly stands out with a MAX of 0.05 eV and an MAE of 0.03 eV. Besides, Rh and Ru have also a low MAE, respectively 0.05 and 0.06 eV. As we noticed

above, Ir and Pd have non negligible and opposite MSE. However for a given metal, the sign of the MSE is the same for both CH $\alpha$  and OH dissociations. As a result we highlight that using the global model might be problematic only if it is necessary to compare these two metals together, but not if we consider them individually.

	BEP.diss	Co	Ni	Ru	Rh	Pd	Ir	Pt
CH $\alpha$ scissions	MAE	0.12	0.06	0.06	0.03	0.12	0.08	0.13
	MAX	0.28	0.14	0.16	0.11	0.29	0.24	0.30
	MSE	-0.04	-0.01	+0.03	0.00	+0.10	-0.06	0.00
OH scissions	MAE	0.11	0.11	0.05	0.06	0.12	0.08	0.03
	MAX	0.18	0.15	0.12	0.11	0.15	0.15	0.05
	MSE	+0.04	+0.02	-0.03	-0.02	+0.06	-0.08	0.00

**Table 3-8: Error analysis for CH $\alpha$  and OH prediction from the global BEP.diss relation.** MAE, MAX and MSE are given in eV for each metal. The highest errors are indicated in red in the case of CH $\alpha$  breaking.

### 3.2.2 TSS relations

To conclude, let us deal now with the TSS relations. According to our observations of section 2.1, the global TSS.diss.IS/IS definition gives satisfying predictions for OH breaking. However, no TSS relation valid for all the metals taken together can be found for CH $\alpha$  scission, except from the TSS.diss.FS/FS providing we exclude Pd. Hence, we will focus on the TSS.diss.IS/IS and TSS.diss.FS/FS definitions in the following. Concerning the first one, we do not notice any significant enhancement splitting the global model according to the metal nature both for CH $\alpha$  and OH bond (see **Table 3-9**). Only few differences appears for some metals such as CH $\alpha$  dissociations on Pd or OH dissociations on Pt. Regarding OH predictions, the quality was already acceptable considering all the metals together, and remains satisfying taking each metal separately. Then, relating to TSS.diss.FS/FS, it is patent according to **Table 3-10** that it is preferable to use one relation specific to each metal. The improvement is striking for almost every metal in the case of OH, and especially for Co and Pd in the case of CH $\alpha$ . Thus, we can think that there are too many discrepancies between the structures of every metal (both TS and FS) to mix all of them in a unique relation. Nevertheless, these divergences are attenuated while focusing on a unique catalyst, hence

explaining why individual TSS.diss.FS/FS relations lead to acceptable errors both for CH $\alpha$  or OH.

TSS.diss.IS/IS (MAE/MAX)		Co	Ni	Ru	Rh	Pd	Ir	Pt
CH $\alpha$	Global	0.26/0.41	0.16/0.32	0.14/0.36	0.06/0.12	0.10/0.24	0.11/0.32	0.17/0.59
	Specific	0.15/0.53	0.11/0.35	0.11/0.30	0.06/0.13	0.05/0.15	0.10/0.22	0.17/0.40
OH	Global	0.08/0.16	0.09/0.20	0.06/0.11	0.06/0.15	0.14/0.20	0.05/0.10	0.07/0.13
	Specific	0.08/0.17	0.09/0.19	0.03/0.05	0.06/0.15	0.10/0.19	0.04/0.05	0.04/0.07

**Table 3-9: Error analysis for every metal in the TSS.diss.IS/IS definition.** We present MAE and MAX (in eV) when the prediction is performed via the global model and via a metal dependent model.

TSS.diss.FS/FS (MAE/MAX)		Co	Ni	Ru	Rh	Pd	Ir	Pt
CH $\alpha$	Global	0.16/0.31	0.09/0.22	0.05/0.12	0.05/0.08	0.22/0.55	0.08/0.14	0.13/0.20
	Specific	0.06/0.10	0.06/0.13	0.04/0.09	0.02/0.06	0.12/0.25	0.04/0.10	0.06/0.17
OH	Global	0.44/0.61	0.25/0.42	0.28/0.44	0.08/0.21	0.14/0.34	0.39/0.55	0.54/0.68
	Specific	0.15/0.31	0.11/0.22	0.12/0.18	0.06/0.11	0.08/0.14	0.11/0.23	0.13/0.32

**Table 3-10: Error analysis for every metal in the TSS.diss.FS/FS definition.** We present MAE and MAX (in eV) when the prediction is performed via the global model and via a metal dependent model. We used the red color when the difference between the global absolute error and the specific absolute error is higher than 0.10 eV both for MAE and MAX.

## Conclusion

Starting from a restricted sample of reactions we established linear energy relations valid for a whole set of transition metals. In spite of the satisfying quality of the global linear energy relation, we showed that predictions are better for radicals than for unsaturated species (carbonyl derivatives and enols). Besides, the quality of the prediction depends on the metal, and sometimes metal-dependent linear relations can considerably lower the errors especially in the TSS.diss.FS/FS definition. These observations are related to the TS natures and to the wideness of the energetic zone that is scanned in the BEP relation.

Those relations enable addressing the question of alcohol reactivity, and may be possibly used also for polyalcohols. However, as explained in Chapter 2 on Rh, polyol reactivity can be significantly affected by intramolecular H-bonds. In order to mimic this effect, it could be interesting to introduce a water molecule in the neighborhood of the monoalcohol molecules and to see the effect on the correlations.

---

<sup>1</sup> P. Tereshchuk and J. L. F. Da Silva, *J. Phys. Chem. C*, **2012**, *116*, 24695-24705

<sup>2</sup> N. K. Sinha and M. Neurock, *J.Catal.* **2012**, *295*, 31-44

<sup>3</sup> Y. Ma, L. Hernandez, C. Guadarrama-Perez and P. B. Balbuena, *J. Phys. Chem. A*, **2012**, *116*, 1409-1416

<sup>4</sup> Y. Choi and P. Liu, *Catal. Today*, **2011**, *165*, 64-70

<sup>5</sup> M. Li, W. Guo, R. Jiang, L. Zhao and H. Shan, *Langmuir*, **2010**, *26*, 1879-1888

<sup>6</sup> G. Wang, Y. Zhou, Y. Morikawa, J. Nakamura, Z. Cai and X. Zhao, *J. Phys. Chem. B*, **2005**, *109*, 12431-12442

<sup>7</sup> J. E. Mueller, A. C. T. van Duin and W. A. Goddard III, *J. Phys. Chem. C*, **2010**, *114*, 20028-20041

<sup>8</sup> J. E. Sutton, P. Panagiotopouou, X. E. Veryldos and D. G. Vlachos, *J. Phys. Chem. C*, **2013**, *117*, 4691-4706

<sup>9</sup> B. Hammer and J. K. Nørskov, *Advances in Catalysis*, **2000**, *45*, 71-125

<sup>10</sup> G. Wang, J. Li, X. Xu, R. Li, and J. Nakamura, *Journal of Computational Chemistry*, **2005**, *26*, 871-878

<sup>11</sup> J. Wang, C.S. Lee and M.C. Lin, *J. Phys. Chem. C*, **2009**, *113*, 6681-6688

<sup>12</sup> R. A. van Santen, M. Neurock, and S. G. Shetty, *Chem. Rev.*, **2010**, *110*, 2005-2048

<sup>13</sup> S. Wang, V. Vorotnikov, J.E. Sutton, and D. G. Vlachos, *ACS Catal.*, **2014**, *4*, 604- 612

<sup>14</sup> S. Wang, V. Petzold, V. Tripkovic, J. Kleis, J. G. Howalt, E. Skúlason, E. M. Fernández, B. Hvolbæk, G. Jones, A. Toftelund, H. Falsig, M. Björketun, F. Studt, F. Abild-Pedersen, J. Rossmeisl, J. K. Nørskov and T. Bligaard, *Phys. Chem. Chem. Phys.*, **2011**, *13*, 20760-20765

# Chapter 4: Water-assisted dehydrogenation of monoalcohols on transition metals

---

## Introduction

In the previous chapter, we found linear energy relations to predict monoalcohol dehydrogenation on transition metals. However, the ultimate goal of this work is to predict polyol reactivity, which is affected by intramolecular H bonds hence impacting the BEP predictions. We can rationalize this effect by considering a water molecule, co-adsorbed on the surface with an alcohol molecule and assisting its dehydrogenation. Besides, transformation of biomass is generally performed in aqueous medium, and this study can give a first idea of the solvent effect on the dehydrogenation reaction.

In the first part of this chapter, we will present general considerations on the impact of water on monoalcohol reactivity. Afterwards, in a second part we will look for linear energy relations to predict activation barriers of such reactions.

## 1 Thermodynamics and reactivity

In this part, we want to probe the effect of water on the reactivity of monoalcohols. Thus, we considered dehydrogenation of few simple alcohols, namely, methanol, ethanol and isopropanol, co-adsorbed with one water molecule. For each of them we focused on the complete reaction path leading from the alcohol reactant, to the carbonyl product through two elementary dissociation steps ( $\text{CH}\alpha$  or  $\text{OH}$ ). We performed these calculations on the previous set of metals (Co, Ni, Ru, Rh, Pd, Ir and Pt). In the following, the non-water-assisted-dehydrogenation will be denoted “monoalcohol dehydrogenation”, and the water-assisted-dehydrogenation “dimer dehydrogenation”.

## 1.1 Configuration of water and co-adsorbates on metallic surfaces

In the previous chapter we presented adsorption modes of alcohols and some of their dehydrogenation products according to their chemical nature. We will show here that for some of them, the configuration on the surface is clearly affected by the presence of a water molecule in their neighborhood (see **Table 4-1**). Firstly, concerning alcohol molecules, in the “dimer situation” they are always H-bonded with the co-adsorbed water molecule and not directly connected to the surface. Regarding carbonyl derivatives, the adsorption mode is related to the substitution level. For low substituted species, such as formaldehyde or acetaldehyde, the C=O bond is generally adsorbed in top-bridge (C top - O bridge) as in the “monoalcohol situation”. However, in the “dimer situation”, high substituted species such as acetone are generally H-bonded to the water co-adsorbate, and not directly linked to the metal. Concerning alkoxy radicals, while they are usually in a hollow site, in the presence of water they move either to a top or to a bridge position for the most oxophilic metals such as Ni, Ru or Co.

Water co-adsorption effect, denoted “*coads effect*”, can be assessed as follows:

$$\text{coads effect} = E_{ads}^{dimer} - E_{ads}^{mono} - E_{ads}^{H_2O} \quad \text{Equation 4-1}$$

where  $E_{ads}^{dimer}$  and  $E_{ads}^{mono}$  are the adsorption energies of the species in the “dimer” and the “monoalcohol” situation, respectively, and  $E_{ads}^{H_2O}$  is the adsorption of the isolated water molecule on the metallic slab. All adsorption energies are referred toward the bare slab, the isolated water molecule and the species in the gas phase.

Water co-adsorption effect is generally stabilizing for all the structures whatever their nature, and is not strikingly different from one metal to another (globally oscillating between -0.10 and -0.30 eV). However, a clear dependence on the metallic nature is observed for alkoxy radicals. While this effect is destabilizing on Co or Ni (+0.20 and +0.10 eV), it is considerably stabilizing on Ir and Pt (around -0.45 eV). Indeed, on oxophilic metals, alkoxy radicals are in a hollow position in the “monoalcohol situation”. Yet, in the “dimer situation” the water co-adsorbate maintains them in a top or a bridge position. Hence, the stabilization induced by the H-bond is counterbalanced by the lack of Metal-O bonds. To the opposite, for non-oxophilic metals the hollow adsorption is not much more stable than the top one, the

hollow configuration being even unreachable for Pt. That is why, in these cases the stabilizing H-bond effect is not compensated, and the water co-adsorption effect is significant. These observations may have some consequences on the reactivity.

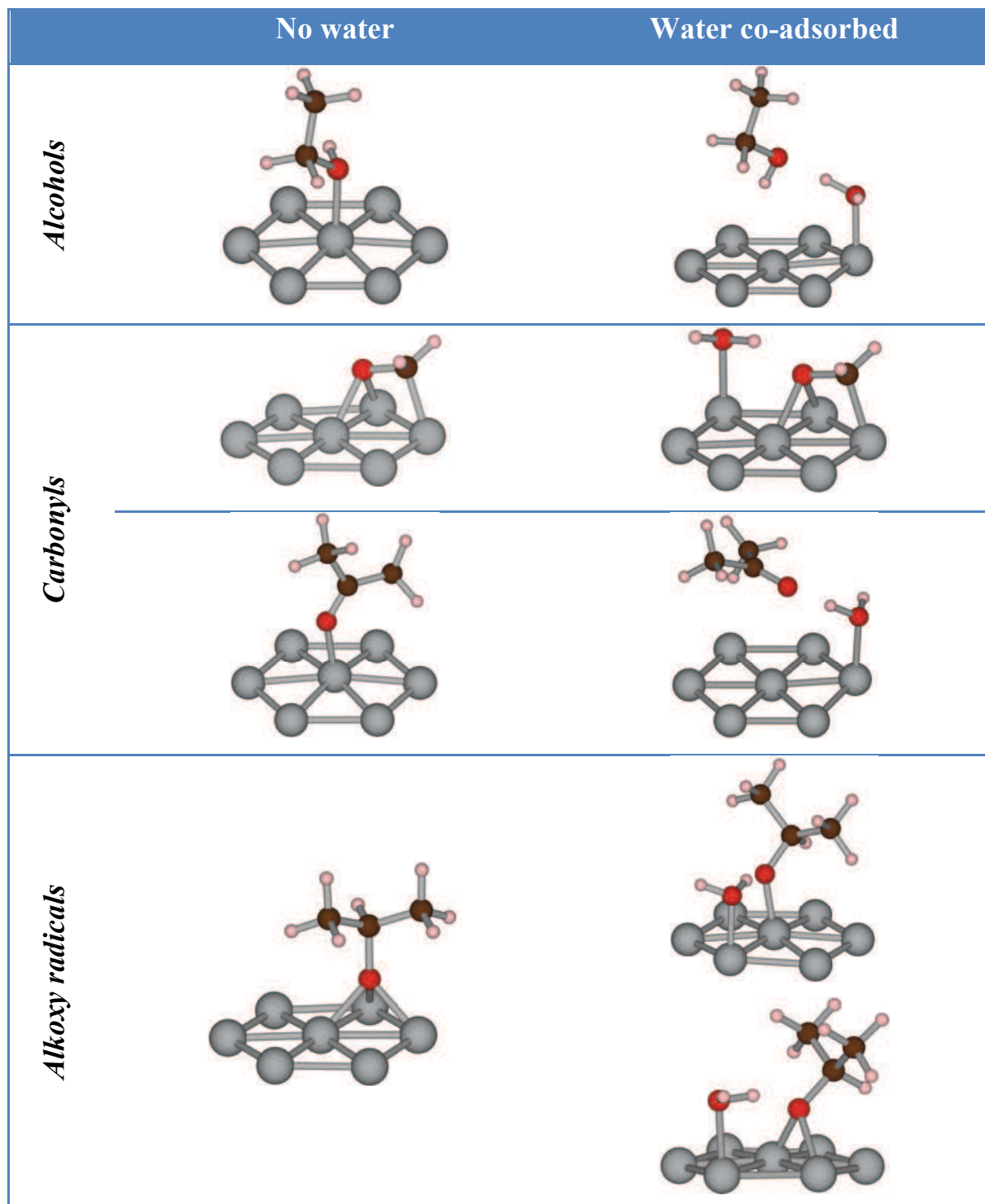
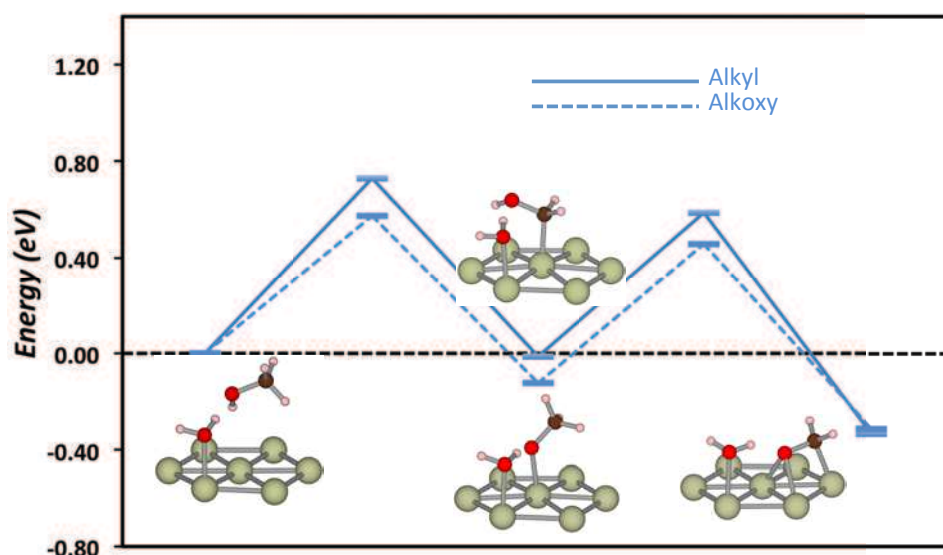


Table 4-1: Modification of the adsorption mode of some species in the presence of water. Grey: metal; Red: O; Brown: C; Pink; H

## 1.2 Water impact on monoalcohol reactivity

### 1.2.1 Basics

In order to appreciate the water assistance effect on monoalcohol reactivity, we will focus on methanol dehydrogenation toward formaldehyde. Formaldehyde can be obtained from two different routes. The reaction path can go through an alkyl radical intermediate ( $\text{CH}_2\text{OH}$ ); it is the “alkyl route”. But the reaction can also progress through an alkoxy radical intermediate ( $\text{CH}_3\text{O}$ ); it is the “alkoxy route”. The concept of water assistance means that a water molecule assists the dehydrogenation all along the reaction. In our situation, the water molecule is a spectator species and is not altered during the reaction, as depicted in **Figure 4-1**.



**Figure 4-1: Water-assisted dehydrogenation of methanol into formaldehyde on Rh.** The H-bond between the water molecule and the co-adsorbate is preserved all along the path. (We considered that the dissociated H diffused to the infinity.) Greenish: Rh, red: O, brown: C and pink: H

Inspired by the energetic span concept used to study catalytic cycles,<sup>1</sup> we will analyze the following reactions using their effective barriers ( $\delta E^\ddagger$ ). Considering a two-step reaction path,  $\delta E^\ddagger$  is defined as the maximum value between the first activation barrier, the second activation barrier and the sum of the first step reaction energy and the second step activation barrier. Three situations are especially important (see **Figure 4-2**):

- The first step has clearly the highest activation barrier.
- The second step has clearly the highest activation barrier.

- c) The second step barrier ( $E_2^\ddagger$ ) is lowest or equivalent to the first one ( $E_1^\ddagger$ ), but the first step is significantly endothermic (reaction energy:  $\Delta E_1 > 0$ ). If  $\Delta E_1 + E_2^\ddagger > E_1^\ddagger$ , then  $\delta E^\ddagger = \Delta E_1 + E_2^\ddagger$

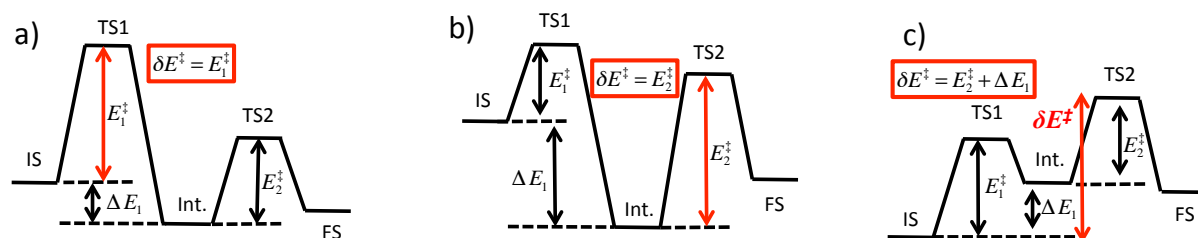


**Figure 4-2: Three important energetic profiles with their corresponding effective barriers  $\delta E^\ddagger$ .**  $E_1^\ddagger$  is the maximum barrier;  $E_2^\ddagger$  is the maximum barrier; or  $E_2^\ddagger + \Delta E_1$  is the maximum. IS: initial state, FS: final state, Int.: intermediate.

## 1.2.2 Methanol dehydrogenation

For each metal we considered successively the alkyl and the alkoxy routes, in the “monoalcohol situation” on one hand and in the “dimer situation” on the other hand. For each route, we calculated the corresponding effective barriers and we compared them together in order to select the lowest ones (see **Table 4-2**). We notice first that while in the “monoalcohol situation” the alkyl route is generally the most favorable, in the “dimer situation” the alkoxy route is globally preferred. This observation is related to the high stabilization effect of the water co-adsorbate on the alkoxy radical intermediate for certain metals as mentioned above. Concerning the “monoalcohol situation” we can see that Rh and Pd exhibit the lower effective barrier (0.70 eV), followed by Ru and Ir (0.78 eV), then Ni (0.82 eV) and Pt (0.84 eV), and finally Co (0.87 eV). In the absence of water, Rh and Pd are thus the most active catalysts for the methanol dehydrogenation into formaldehyde, whereas Co is the less efficient. Concerning the “dimer situation”, it is Ru and Rh whose present the lowest effective barriers (0.59 and 0.58 eV resp.), followed by Co (0.71 eV), Ni (0.75 eV) and Pd (0.79 eV), and finally Ir and Pt (0.90 and 0.91 eV resp.). In the presence of water, Ru and Rh are the most active, whereas Ir and Pt are the worst catalysts. The efficiency of Ru and Rh and the poor performance of Pd in aqueous medium are also found experimentally, in hydrogenation of biomass oxygenates on monometallic catalysts.<sup>2</sup> As a consequence, it appears clearly that water influences the catalyst activity, and can even invert the relative efficiency of some of them.

Water effect is different according to the metal and to the route that is considered (see **Table 4-3**). Concerning the alkyl paths, effective barriers are generally increased by about 0.10 eV, except for Rh and Ni. Rh is the less sensitive metal to water effect (effective barrier increase: +0.04 eV), whereas Ni is the most affected (effective barrier increase: +0.22). Relating to the alkoxy paths, while we observe a lowering of the effective barriers of a magnitude close to 0.20 eV for Ru, Rh, and Co, the effective barrier is decreased by a bit more than 0.10 eV on Ni and Pd. To the opposite, the alkoxy route is slightly disfavored by water on Ir and Pt, with an effective barrier increase of about 0.05 eV. As a result, water effect is globally similar and relatively weak on the majority of the metals regarding the alkyl route. However, the situation is much more dependent on the metallic nature for the alkoxy route. This is in agreement with the literature since the activation of OH scission and the slight inhibition of the CH breaking by water, are already reported for ethanol dehydrogenation on Rh (111).<sup>3</sup> It was also mentioned elsewhere<sup>4</sup> that the impact of the co-adsorbed water molecule is very weak for ethanol dehydrogenation on Pt (111).

			<b>Co</b>			<b>Ni</b>		
			$\delta E_{mono}^\ddagger$	0.87	Alkyl	$\delta E_{mono}^\ddagger$	0.82	Alkyl
			$\delta E_{dimer}^\ddagger$	0.71	Alkoxy	$\delta E_{dimer}^\ddagger$	0.75	Alkoxy
	<b>Ru</b>		<b>Rh</b>			<b>Pd</b>		
$\delta E_{mono}^\ddagger$	0.78	Alkyl	$\delta E_{mono}^\ddagger$	0.70	Alkyl	$\delta E_{mono}^\ddagger$	0.70	Alkyl
$\delta E_{dimer}^\ddagger$	0.59	Alkoxy	$\delta E_{dimer}^\ddagger$	0.58	Alkoxy	$\delta E_{dimer}^\ddagger$	0.79	Alkyl
			<b>Ir</b>			<b>Pt</b>		
			$\delta E_{mono}^\ddagger$	0.78	Alkyl	$\delta E_{mono}^\ddagger$	0.84	Alkyl
			$\delta E_{dimer}^\ddagger$	0.90	Alkoxy	$\delta E_{dimer}^\ddagger$	0.91	Alkyl

**Table 4-2: Effective barrier of methanol dehydrogenation into formaldehyde.** We reported here the most favorable route (Alkyl/Alkoxy) and its corresponding effective barrier for each catalyst, in the “monoalcohol” and the “dimer” situations.

	<b>Co</b>	<b>Ni</b>
	Alkyl +0.14	Alkyl +0.22
	Alkoxy -0.16	Alkoxy -0.13
<b>Ru</b>	<b>Rh</b>	<b>Pd</b>
Alkyl +0.08	Alkyl +0.04	Alkyl +0.09
Alkoxy -0.20	Alkoxy -0.24	Alkoxy -0.11
	<b>Ir</b>	<b>Pt</b>
	Alkyl +0.13	Alkyl +0.08
	Alkoxy +0.06	Alkoxy +0.07

*Table 4-3: Water effect on the effective barriers of methanol dehydrogenation into formaldehyde for both alkyl and alkoxy routes. The effect is measured by the difference between the effective barrier in the “dimer situation” and the effective barrier in the “monoalcohol situation”*

## 2 Linear energy relations for water-assisted dehydrogenation

Now that we addressed the question of water-assisted dehydrogenation in monoalcohols, we will see that it is possible to predict its activation barriers using BEP-type relations. Since above we focused on the formation of formaldehyde, in order to establish these linear energy relations we considered reaction paths leading to carbonyls from methanol, ethanol and isopropanol. Our sample of points is thus constituted by  $\text{CH}\alpha$  and OH dissociations, giving alkyl/alkoxy radicals and carbonyl derivatives (see **Figure 4-3**). Let us mention that we also included two diradicals for the OH scission.

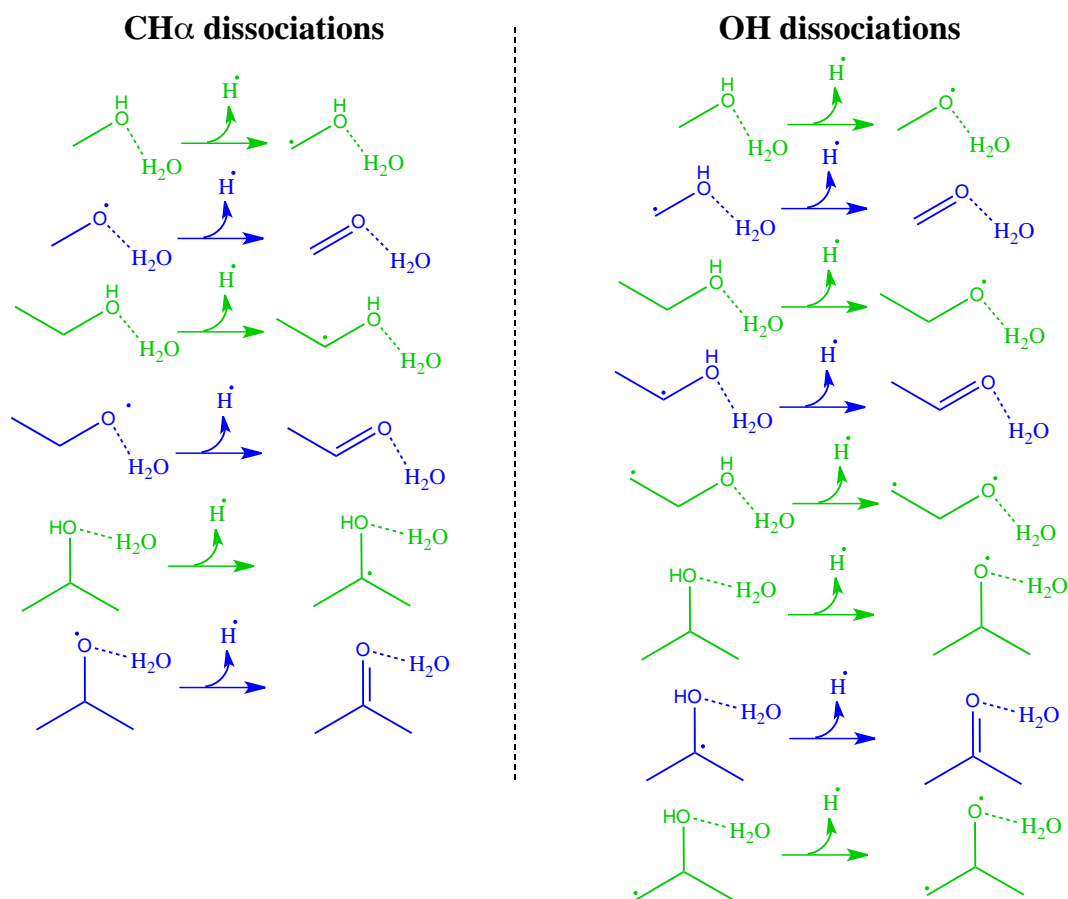


**Figure 4-3:** List of reactions used to establish BEP-type relations in the case of water-assisted dehydrogenation. The dissociated H is adsorbed on a separate slab. Blue color denotes the formation of carbonyls and green color is for radicals.

We will mainly deal with the BEP relation because in this paradigm, it is easy to get direct conclusions on the reactivity and on the chemistry of the system. As previously, we will design in the following the BEP relations that are related to water-assisted dehydrogenation by “dimer-BEP”, and we will use “monoalcohol-BEP” when they are related to the non-water-assisted dehydrogenation. Besides, as we did so far, we will continue to distinguish CH and OH scissions.

## 2.1 Metal and reaction dependent water effect

As mentioned in 1.2, water impact is different according to the metal and to the reaction. This can be rationalized taking into account the BEP.diss relations corresponding to  $\text{CH}\alpha$  and to OH breaking (see **Figure 4-4**). Concerning  $\text{CH}\alpha$  dissociation, we observe no major differences between the monoalcohol-BEP and the dimer-BEP lines, except for Pd. For the latter the slopes of the BEP line are very different in the two cases (close to zero in the dimer-BEP and close to 1 in the monoalcohol-BEP). This singularity of Pd will be debated further in this section. According to these observations,  $\text{CH}\alpha$  dissociations are globally not so much affected by water co-adsorption, and this whatever the metal that is considered. Regarding OH scission, we can see in **Figure 4-4** that the dimer-line (in blue) is clearly below the monoalcohol-line (in red) for Co, Ni, Ru and Rh. This is less striking for Pd, and concerning Ir and Pt the two lines overlap each other. This means that OH dissociations are clearly activated by water assistance on Co, Ni, Ru and Rh (activation energies are lowered), and a bit less on Pd. However, they are inhibited by water on Ir and Pt (activation energies are increased). The negative systematic deviation observed in Chapter 2, for the prediction of OH scission in glycerol on Rh, is directly related to this phenomenon. And that is why a negative systematic error is also expected for polyol prediction from monoalcohol BEP relations, on every metal except Ir and Pt. This point will be detailed in the last chapter.

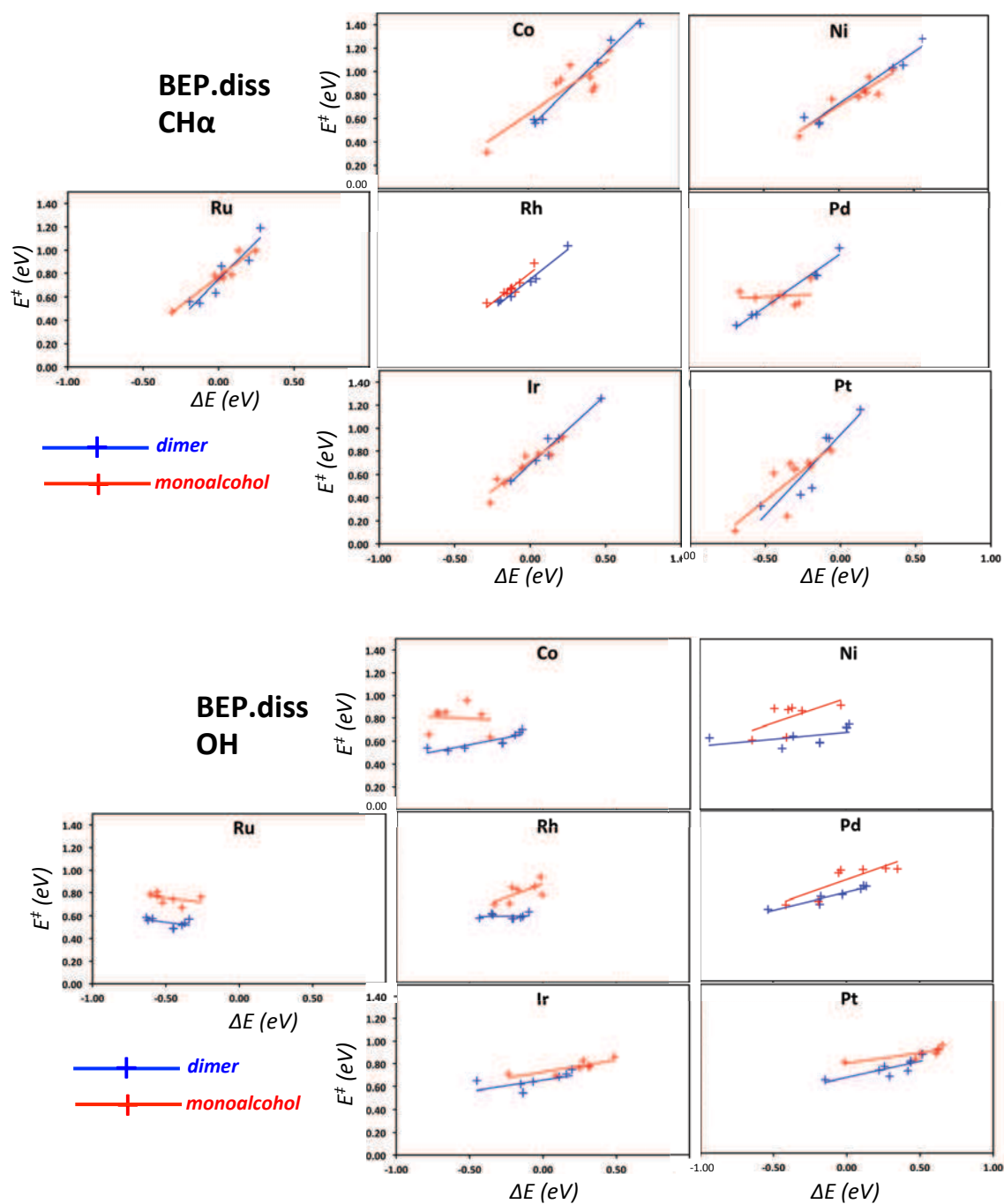
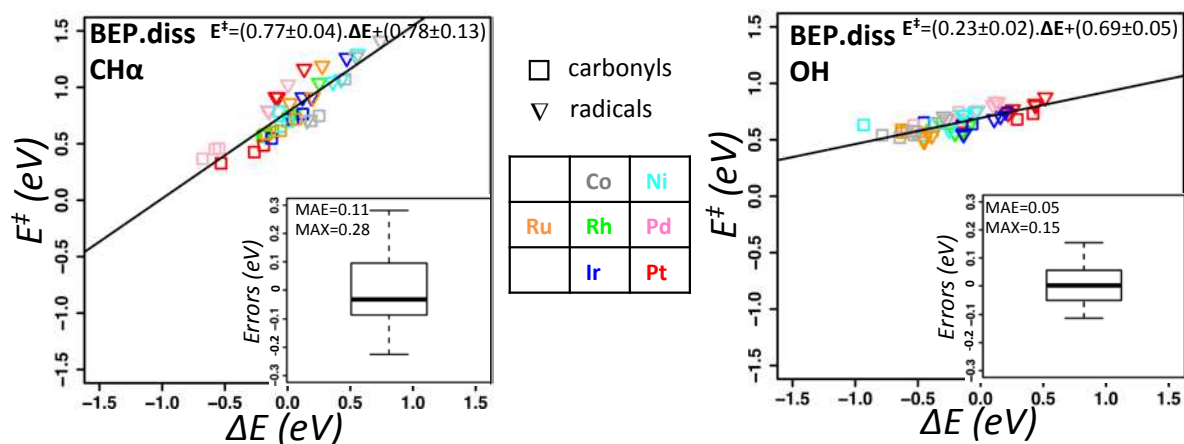


Figure 4-4: Comparison of BEP type relations in the case of “monoalcohol” and “dimer situation”. The relative position of the two models is compared for every metal between CH $\alpha$  and OH breaking.

## 2.2 On the quality of the BEP predictions

Now, we will assess the statistical quality of the predictive model in the BEP.diss definition. We will proceed as in Chapter 3, starting by analyzing the global linear relation common to every metal. Those relations are presented in **Figure 4-5**, in the case of CH $\alpha$  and OH scissions. We can see that errors are slightly higher for CH $\alpha$  dissociations than for OH, approximately ranging in the first case from -0.30 to +0.30 eV, and between -0.10 to +0.20 eV in the second case. Besides, we note here that in general, carbonyls fit well to the line. Indeed, unlike in the monoalcohol situation described in Chapter 3, we observed here in the dimer situation, that errors obtained for carbonyls are equivalent to errors obtained for radicals.



**Figure 4-5:** Global dimer-BEP.diss relations in the case of CH $\alpha$  and OH dissociations in monoalcohols on transition metals. The corresponding error distribution is depicted in the right bottom corner. MAE is the mean absolute error, and MAX is the maximum absolute error.

Then, let us have a look on the model performances metal per metal (see **Figure 4-6**). Concerning firstly CH $\alpha$  breaking (see top panels), we can see that the global model gives major errors for Co, Pt and Ru (error span > 0.3 eV). Errors are lower for Ni and Ir, and concerning Rh and especially Pd we note a significant systematic deviation (-0.04 and +0.13 eV resp.) in spite of the tightness of their ranges of errors. Non-negligible and opposite systematic errors also occur for Co and Pt (-0.09 and +0.06 eV resp.). The error span is strikingly lowered when using a specific model for each metal especially for Co, Ru, Ir and Pt. The opposite systematic deviation vanishes for Rh and Pd, and their error span remains

tight (from  $\sim -0.05$  to  $+0.05$  eV). Hence, it is obvious that in order to predict  $\text{CH}\alpha$  bond reactivity in the “dimer situation”, it is preferable to use metal-dependent models.

Regarding OH scission (see lower panels), we observe firstly much lower errors than for  $\text{CH}\alpha$ . Considering the global model, errors range approximately between  $-0.10$  and  $+0.10$  eV for every metal (slightly more for Ni). Low negative systematic deviations appear for Ru, Rh and Ir on the order of  $-0.05$  eV. The highest systematic shift is observed for Pd with a value of  $+0.08$  eV, in spite of its tight error distributions. Switching then to the prediction via metal dependent models, we notice only small differences, apart from the extinction of all the systematic deviation. As a result, for OH dissociations in the “dimer situation” the global predictive model gives satisfying results for every metal. The only problem might be to compare Pd with a different metal. In such case, one should use a model proper to each catalyst.

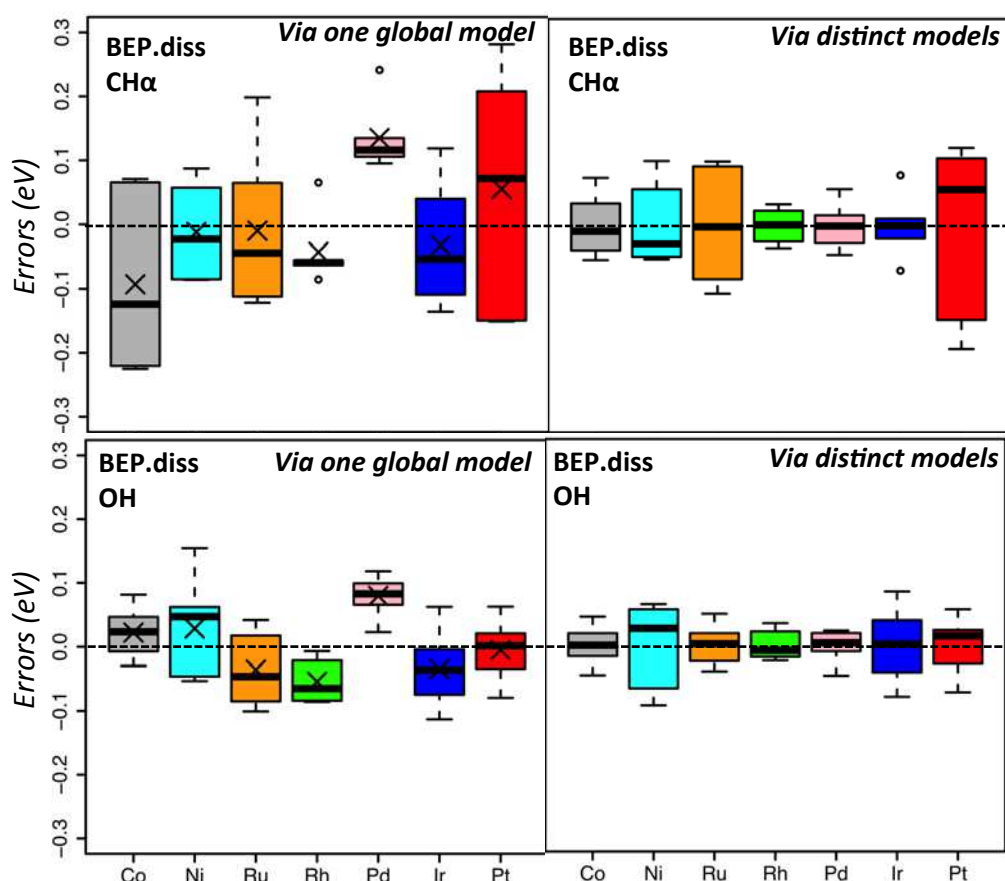


**Figure 4-6: Error distributions metal for water-assisted dehydrogenation BEP.diss relation.** Activation energies are estimated using the global model on one hand and using separate models (one for each metal) on the other hand. The black cross denotes the systematic deviation in the case of the global model predictions.

## 2.3 The consequences of water co-adsorption on the TS nature

As we can observe in **Figure 4-5**, the transfer coefficient of the BEP relation in the “dimer situation” is of 0.77 for CH $\alpha$  dissociations and of 0.23 for OH considering all the metal together. For comparison, in the “monoalcohol situation” (see Chapter 3) we found 0.60 for CH $\alpha$  and 0.11 for OH. As a consequence, water assistance increases the transfer coefficients of BEP relations. Some authors also achieve similar conclusion in the literature, concerning water-assisted OH scission on a set of various metals in the water molecule. Fajin *et al.*<sup>5</sup> already noted a close transfer coefficient (0.29). Moreover, Sautet and co-workers<sup>6</sup> also reported for this reaction an increase of the transfer coefficient due to water assistance (from 0.03 without water to 0.35 with water).

Hence, water co-adsorption renders the TS corresponding to OH breaking “less early”, and makes the TS related to CH $\alpha$  scission “later”. This tendency is confirmed when comparing together the corresponding transfer coefficient for the “monoalcohol” and the “dimer” situation in the case of CH $\alpha$  dissociations, for each metal taken individually (see **Table 4-4**). We observe that for every metal the transfer coefficient is clearly increased by water co-adsorption and become closer to 1. The effect is even more striking for Pd switching from 0.07 to 0.90. All the TS corresponding to water-assisted CH $\alpha$  scission are thus late and this has a consequence on the TSS relations.

Indeed, as mentioned in the previous chapter, it is not possible to find a global TSS.diss.FS/FS relation for CH $\alpha$  dissociations in the “monoalcohol situation”, especially because of Pd. However, now in the “dimer situation”, it is possible to considerably lower the absolute errors of the global relation, the MAX moving from 0.55 eV to 0.32 eV. Let us mention that still in this case, it is preferable to use distinct metal-dependent relations if one expects to compare two metals together. Indeed, high systematic deviations appear with the global model. Besides, each metal-dependent TSS.diss.FS/FS relation exhibits low errors with an MAE on the order of 0.05 eV and a MAX around 0.10 eV.

	<b>Co</b>	<b>Ni</b>
	Dimer 1.33±0.29 Mono 0.87±0.51	Dimer 0.88±0.32 Mono 0.80±0.36
<b>Ru</b>	<b>Rh</b>	<b>Pd</b>
Dimer 1.25±0.79 Mono 0.97±0.31	Dimer 1.03±0.24 Mono 1.02±0.39	Dimer 0.90±0.18 Mono 0.07±0.45
	<b>Ir</b>	<b>Pt</b>
	Dimer 1.20±0.34 Mono 0.99±0.35	Dimer 1.39±0.85 Mono 1.05±0.75

**Table 4-4: Transfer coefficients for CH $\alpha$  scission.** We compare for each metal the effect of water on the transfer coefficient.

## Conclusion

In this chapter, we evidenced the impact of water on alcohol reactivity, and its effect on the BEP correlation. H-bonds occurring between alcohol and water molecules activate OH scission, whereas no notable effect is observed on CH $\alpha$  dissociation. In the case of OH breaking, the influence of water is very dependent on the metallic nature. While activation energies are clearly decreased on oxophilic metals such as Co or Ni, they are less impacted on other metals such as Ir or Pt.

Satisfying linear energy relations were found for water-assisted dehydrogenation in monoalcohols. Such relations can be used to predict polyol reactivity, especially in the case of OH scission. Indeed, various intramolecular H bonds may exist in those species, and can potentially activate the OH breaking, thus acting as the water co-adsorbate for monoalcohols.

<sup>1</sup> S. Kozuch and S. Shaik, Account of Chemical Research **2011**, *44*, 101-110

<sup>2</sup> J. Lee, Y. Xu, and G. W. Huber, App. Catal. B: Env. **2013**, *140*, 98-107

<sup>3</sup> C. Michel, F. Auneau, F. Delbecq and P. Sautet, ACS Catal. **2011**, *1*, 1430-1440

<sup>4</sup> S. Chibani, C. Michel, F. Delbecq, C. Pinel and M. Besson, Catal. Sci. Technol., **2013**, *3*, 339-350

<sup>5</sup> J. L. C. Fajin, M. N. D. S. Cordeiro, F. Illas, and J. R. B. Gomes, J. Catal. 2010, *276*, 92-100

<sup>6</sup> C. Michel, F. Göttl and P. Sautet, Phys. Chem. Chem. Phys., **2012**, *14*, 15286–15290

# Chapter 5: Using BEP relations to address polyol reactivity on Rh and Pt

---

## Introduction

In Chapter 2, we showed that it is possible to predict glycerol reactivity on Rh from linear energy relations established on simple alcohols. However, this process leads to systematic errors, due to intramolecular H-bonds occurring in polyalcohols. In order to refine these results, we designed in chapter 3 and 4, BEP-type relations for monoalcohol dehydrogenation on various metallic surfaces, and we considered the influence of the H-bonds on such relations. Now, we can deal with the ultimate goal of this thesis: the prediction of polyol reactivity. We will focus in this chapter on two important polyols occurring in the mechanism of glycerol conversion into lactic acid, namely glycerol and 1,2-propanediol (1,2-PDO). Within the family of metals studied in the previous chapter, two metallic catalysts will be considered here, Rh and Pt. Our goal is to select by the means of BEP predictions, the most favorable dehydrogenation paths within a complex reaction network. These pathways could be eventually refined by DFT calculations if necessary.

After presenting the tools that are necessary to address polyol reactivity, we will use the BEP relations previously established on simple alcohols to predict glycerol and 1,2-PDO dehydrogenation. Then, we will be able to decide what is the best catalyst for glycerol conversion into lactic acid.

# 1 Predicting polyol reactivity: the tools and their limitations

## 1.1 Glycerol conversion on metallic catalysts: context of the project

In tight collaboration with experimentalists, Sautet's group of research is involved in an ongoing project aiming at producing lactic acid (LA) from glycerol using heterogeneous catalysis. Working initially on Rh, Sautet and co-workers evidenced that the reaction mechanism goes through a dehydrogenation in a first step<sup>1</sup> (see **Figure 5-1**). Glycerol is dehydrogenated into glyceraldehyde, giving an enol after dehydration in basic medium. Since the enol is not stable in aqueous solution, it is transformed into pyruvaldehyde (PAL) leading either directly to LA or to acetol. The latter is in equilibrium with PAL and 1,2-PDO through hydrogenation/dehydrogenation processes.

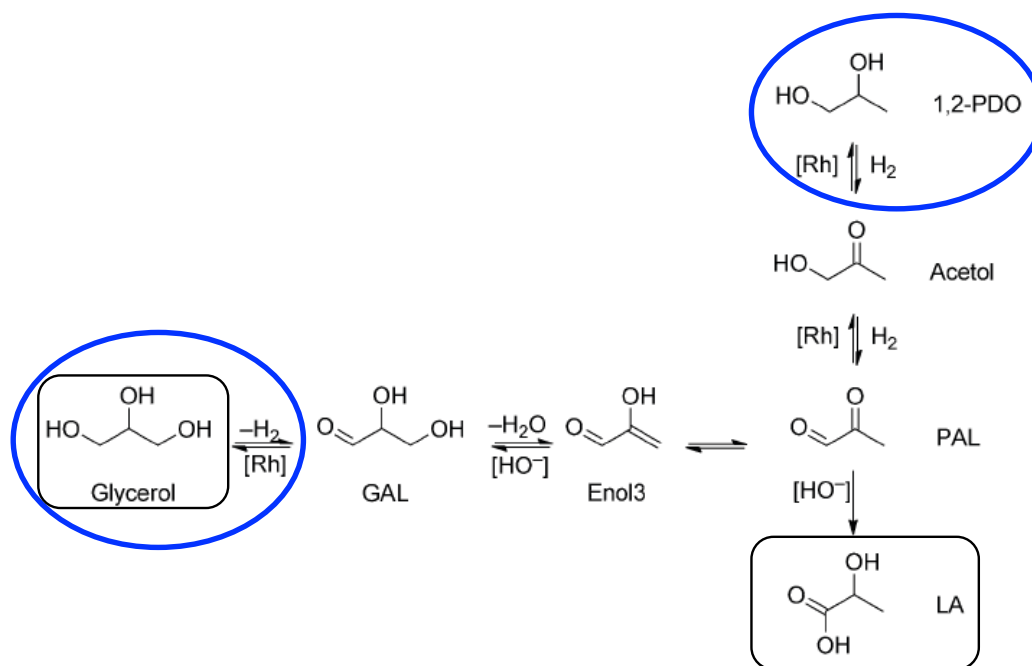


**Figure 5-1: Reaction mechanism from glycerol conversion to lactic acid (LA) on Rh in basic medium.** (Taken from Ref. [1]) GAL: glyceraldehyde, PAL: pyruvaldehyde, 1,2-PDO: 1,2-propanediol. Dehydrogenation explicitly occurs on glycerol and 1,2-PDO.

Since Pt is also commonly used for glycerol conversion,<sup>2,3</sup> our experimentalist collaborators have recently started to work with Pt. Assuming a reaction mechanism similar to the Rh one, we propose here to screen Pt reactivity by the means of our BEP-type relationships. Since dehydrogenation explicitly occurs on glycerol and 1,2-PDO (see **Figure 5-1**), we will focus in the following on CH and OH dissociations in these two polyalcohols. Let us mention that concerning CH breaking in 1,2-PDO, we only considered here CH bonds in  $\alpha$  position of a hydroxyl group. These results may be refined in a second stage considering every kind of CH bonds. However, in spite of the restricted part of mechanism that we decided to study, these polyols are still related to a large potential reaction network. As depicted in **Figure 5-2**, after monoradical intermediates, glycerol can lead to three unsaturated molecules (dihydroxyacetone-DHA, glyceraldehyde-GAL and one enol) and to various diradical species. Regarding 1,2-PDO, there are also three unsaturated species (acetol, lactaldehyde and one enol), but only three diradical intermediates.

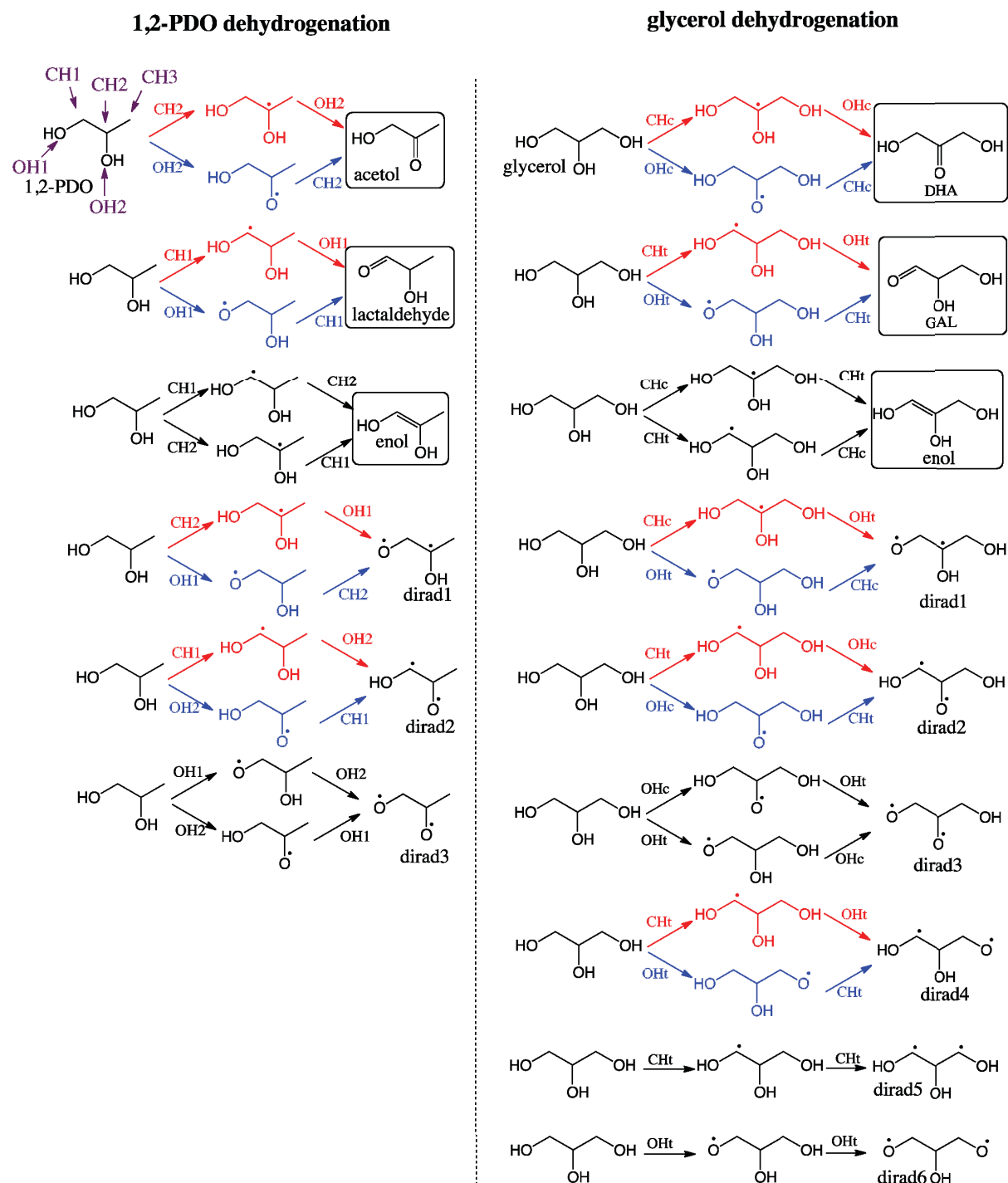


**Figure 5-2: Various dehydrogenation paths for 1,2-PDO and glycerol.** In both cases, after the formation of a monoradical intermediate, we get either unsaturated species (the surrounded molecules) or diradicals. When two routes are possible, we colored in red the alkyl path and in blue the alkoxy path. For glycerol CHc and CHt correspond respectively to central CH dissociation and terminal CH dissociation (and similarly for OH).

## 1.2 Improving the prediction of CH and OH dissociation barriers for glycerol

As explained in Chapter 2, predicting glycerol reactivity on Rh from monoalcohol BEP-type relationships leads to small systematic errors. These systematic deviations are opposite for CH and OH dissociations, hence rendering difficult any comparison between them. In this section, we wonder if it is possible to reduce these errors using the linear energy relations developed in the previous chapters. We applied them on Rh catalyzed dehydrogenation of glycerol, and we presented the corresponding error distributions on **Figure 5-3**. For both CH and OH bonds we compared in the BEP.diss definition, errors that are obtained by:

- The relation designed for Rh only (Chapter 2), in the case of non-water-assisted dehydrogenation (denoted “monoalcohol situation” in the following)
- The global relation established for a whole set of metals, in the “monoalcohol situation” (Chapter 3)
- The relations obtained in the case of water-assisted dehydrogenation, described in Chapter 4 (denoted “dimer situation” in the following)

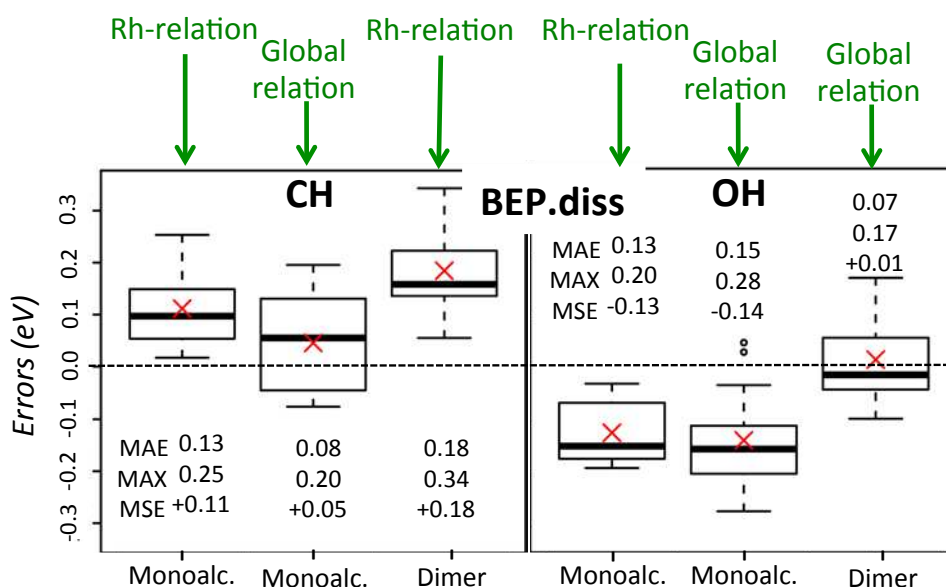


**Figure 5-3: Water-assistance effect on the prediction of glycerol reactivity from monoalcohol BEP.diss relation.** For both CH and OH breaking we compared the error distributions, using the “monoalcohol” Rh-relation (chapter 2), the “monoalcohol” global relation (chapter 3) and the “dimer” relation (chapter 4). Note that for the CH breaking in the “dimer situation” the global BEP relation is not efficient as explained in Chapter 4, and one must use a relation specific to Rh. The red cross represents the MSE.

Concerning CH dissociations, we observe in the “monoalcohol situation” that the global relation slightly decreases errors comparatively to the Rh-specific relation. The MSE in particular, moves from +0.11 to +0.05 eV, and the MAX from 0.25 to 0.20 eV. To the opposite, errors are clearly degraded using the “dimer” relation, with a MAX of 0.34 eV and an MSE of +0.18 eV. The global “monoalcohol” relation is thus preferable to predict CH scission in glycerol on Rh catalyst. Regarding OH breaking, we can see that in the “monoalcohol situation”, both the Rh-specific and the global relation lead to negative systematic deviations close to -0.15 eV. However, using the “dimer” relation allows eliminating the systematic shift and gives acceptable errors, with an MAE of 0.07 and a MAX of 0.17 eV. The global “dimer” relation is thus preferable to predict OH scission in glycerol on Rh catalyst. Hence, it is possible to extinct the systematic deviation, or at least to attenuate it for CH bond, and thus to compare CH and OH activation barriers stemming from BEP estimations.

OH bond is activated owing to intramolecular H-bonds present in glycerol and not in simple alcohols. However, let us mention that according to our previous discussions in Chapter 4, this effect is not similar for every metal.<sup>4,5</sup> As depicted in **Figure 5-4**, activation energies are clearly lowered on Rh by water assistance but much less for Pt. The “monoalcohol” and “dimer” relations are thus close for Pt. Besides, we can also expect a lower effect in 1,2-PDO than in glycerol. Indeed, only 1,2-H bonds (between two vicinal OH groups) can occur in 1,2-PDO, which is less favorable than 1,3 H-bonds in glycerol (between two terminal OH groups).<sup>6,7</sup> To conclude, let us remind that the positive systematic shift, appearing when predicting CH breaking in glycerol from simple alcohols, has likely a geometric origin. We think that the constraint imposed by the neighboring OH groups on the geometry of the chemisorbed glycerol imposes a deviation of the TS from that of the more free monoalcohol molecules, hence increasing the barrier. This constraint does not arise from intramolecular hydrogen bonding and is not described by the “dimer” models. This is hence fully normal and logical that the “dimer” relation does not improve the prediction of the CH bond dissociation process in glycerol. Having one less OH group, the chemisorbed 1-2, PDO structure is potentially less constrained than glycerol, and we can expect a better prediction from “monoalcohol” BEP-relation.

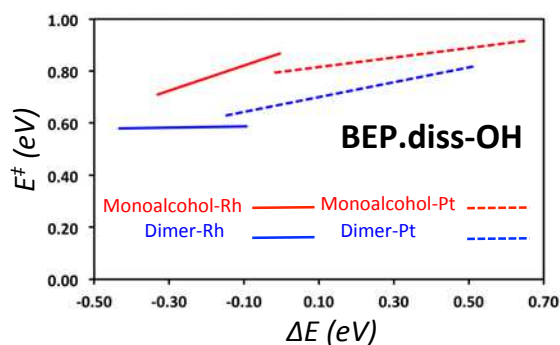


**Figure 5-4:** BEP.diss relation for OH dissociations in simple alcohols for the “monoalcohol” and the “dimer” situation. The two lines are very close to each other in the case of Pt.

### 1.3 Using the BEP relation to predict dehydrogenation paths

As depicted previously in **Figure 5-2**, glycerol dehydrogenates on Rh giving three main molecules (DHA, GAL and enol) and six diradicals. Diradicals cannot desorb and hence will remain as a dead-end on the surface or will be transformed further. Hence, either they poison the catalyst, or they continue to decompose on the metal, potentially undergoing subsequent C-C and C-O scissions. The selectivity branching between the unsaturated molecules and the diradical species is hence an important point for understanding of the catalytic activity. In order to check the consistency of BEP predictions with DFT calculations, we will compare here the glycerol dehydrogenation paths obtained by the two methods (BEP and DFT). The concept of effective barrier, developed in section 1.2.1 of Chapter 4, is central in this study. In the following of this chapter, we will use the equations presented in **Table 5-1**, to predict polyol (either glycerol or 1,2-PDO) reactivity both on Rh and Pt. Let us mention that we exclusively focused on the BEP.diss definition, since this relation established on a global set of metals, gives satisfying results both for CH and OH bond, either for Rh or for Pt as detailed in the previous chapters.

BEP.diss	
<b>CH<math>\alpha</math> (mono.global model)</b>	$E^\ddagger = 0.60 \cdot \Delta E + 0.75$
<b>OH (dimer-global model)</b>	$E^\ddagger = 0.23 \cdot \Delta E + 0.69$

**Table 5-1:** Equations used to predict polyol reactivity both on Rh and Pt. We used the “monoalcohol” model for CH dissociations and the “dimer” model for OH. In the case of Rh and Pt, the global predictive model obtained for “monoalcohols”, gives acceptable errors in the CH $\alpha$  dissociation, which are not significantly lowered using metal-dependent relations.

### 1.3.1 Level of confidence in the predictions

We must keep in mind that BEP estimations are only accurate up to a certain point. And thus, it is necessary to have a sufficient energy difference  $\delta E$  between two predictions in order to be confident in the relative position of the barriers. As mentioned above, CH and OH may be compared together since their MSE are both positive and close to zero. Hence, the only relevant parameters to take into account are MAE and MAX. If  $\delta E > MAX$ , we will consider the confidence level in the prediction as “high”. If  $MAE < \delta E < MAX$ , the prediction will be only “likely”. And if  $\delta E < MAE$ , it will be an “indeterminate” situation. We took MAX equal to 0.20 eV, meaning the highest value between CH and OH (see **Figure 5-3**), and similarly an MAE of 0.08 eV. The procedure is summed up in **Figure 5-5**. Besides, let us remind that the quality of the prediction is also related to the nature of the product. Indeed, as reminded in **Table 5-2**, unsaturated species (carbonyls/enols) stemming from CH scission (in second step) are expected to give the highest errors especially on Pt.

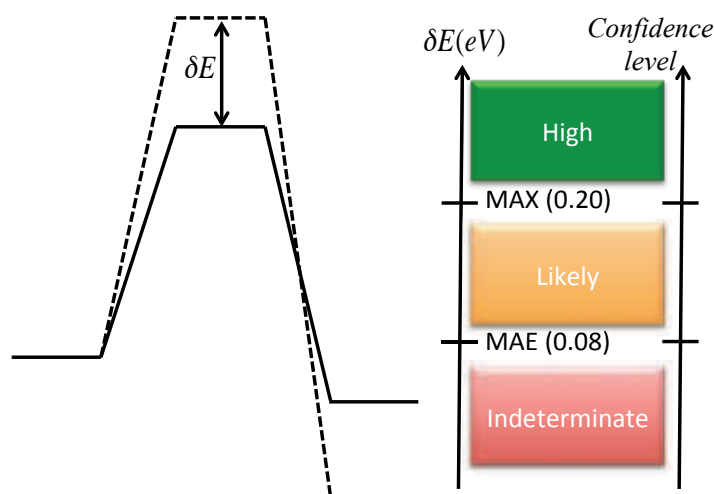


**Figure 5-5: Confidence level in the BEP prediction.** The higher the energetic difference between two estimations, the better the confidence on their relative positions is.

BEP.diss	Unsaturated species	Radicals
Simple alcohols	(MAE/MAX)	(MAE/MAX)
<b>CH via global-monoalc.</b>	0.13/0.30	0.06/0.14
<b>OH via global-dimer</b>	0.06/0.16	0.06/0.12

**Table 5-2: Errors (MAE and MAX) obtained for different nature of products.** The prediction is performed on simple alcohols using the global “monoalcohol” relation for CH scission, and the global “dimer” relation for OH breaking in the BEP.diss definition. The MAX of 0.30 eV corresponds to the formation of formaldehyde on Pt via CH breaking in last step. See Chapter 3 and 4 for details.

### 1.3.2 Glycerol on Rh: BEP predictions vs. DFT calculations

Let us first focus on DHA and GAL formation. These two carbonyl derivatives may result either from an alkyl route (CH dissociation followed by an OH scission), or from an alkoxy route (OH dissociation followed by CH scission). We can see on **Figure 5-6** (see the first row), that the alkyl and the alkoxy routes are very close to each other according to the DFT calculations, for both DHA and GAL. The enol can also stem from two different routes. Either the central CH bond is broken followed by terminal CH (noted “CHcCHt”), or the opposite (CHtCHc). Nevertheless these two paths are almost identical, according to DFT. These features are faithfully reproduced by the BEP relation as depicted on **Figure 5-6** (see the second row).

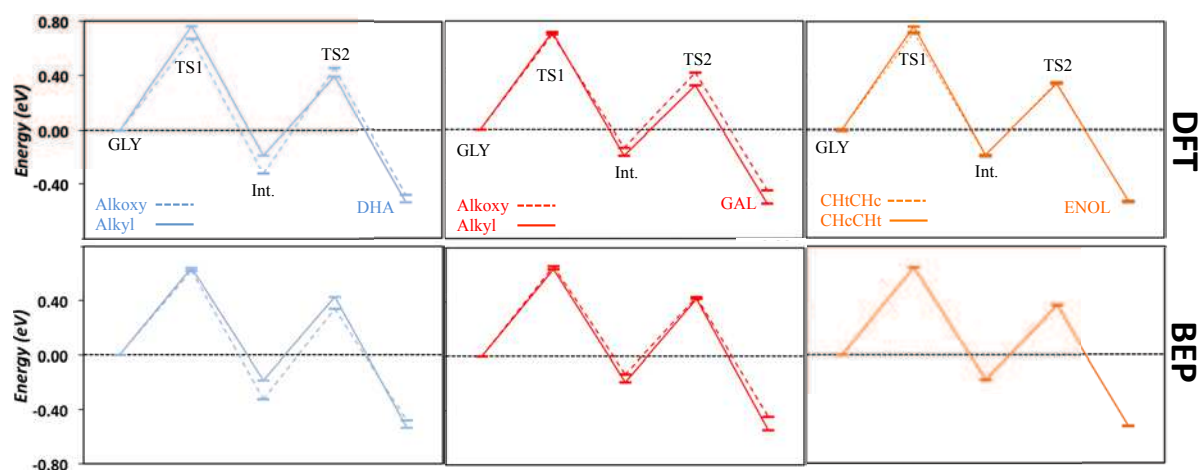


**Figure 5-6:** Glycerol (GLY) dehydrogenation toward dihydroxyacetone (DHA), glyceraldehyde (GAL) and ENOL. “Int.” denotes the monoradical intermediate. On the top row we represented the DFT calculations, and on the lower row, the BEP prediction. Let us precise that for DHA and GAL, the final product is not identical according to the dehydrogenation route (alkyl or alkoxy). We took in each situation a final product with a conformation corresponding to the radical intermediate.

Aiming at determining the most likely products that are obtained from glycerol dehydrogenation, we considered the effective barrier corresponding to each reaction path (including unsaturated molecules and diradicals). When two different routes (for example alkoxy/alkyl) are possible for a same compound, we selected the one with the lowest effective barrier. Then, we plotted together all the most favorable paths in **Figure 5-7**. Looking at BEP prediction, we notice first that all the routes are extremely close to each other at the first step, so that the BEP is not able to distinguish between them at this point. This is in full agreement with DFT that shows a small difference ( $\sim 0.15$  eV max) between the first step barriers. Concerning the second step, the span of BEP barriers is higher, but still limited. Thus, a safe

prediction would only conclude that the barrier leading to Dirad6 is the highest one. Similar observations appear for the DFT results, meaning some diradicals are kinetically disfavored. This is confirmed by the quantitative analysis of **Table 5-3**, presenting the BEP-estimated effective barriers. We can see that the difference between the minimum effective barrier (0.64 eV) and the maximum one (0.72 eV) is of 0.08 eV. This is typically an indeterminate situation. As a result, due to the closeness and the high similarity between all the energetic profiles, it is impossible to clearly conclude from the BEP (and from the full DFT as well) on the major kinetic pathway for glycerol reactivity on Rh. In such a situation, only thermodynamics considerations may be relevant. According to **Table 5-3**, the formation of unsaturated species, and especially of ENOL and DHA, presents the highest exothermicity and thus should be preferred.

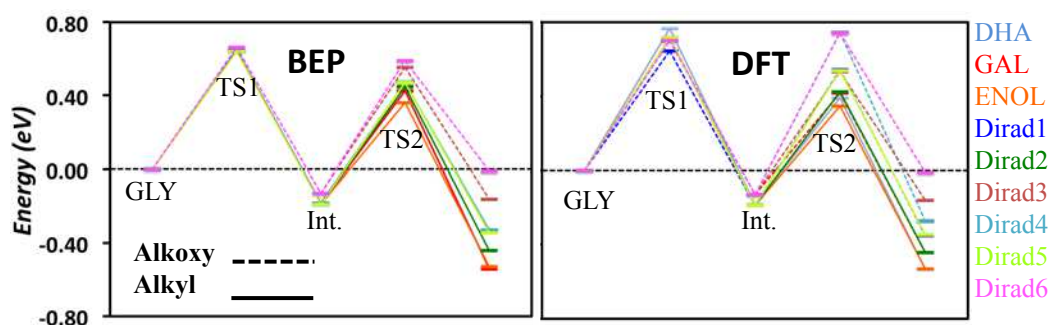


**Figure 5-7:** The most favorable routes for glycerol dehydrogenation on Rh. BEP estimations are presented on the left panel and DFT results on the right one. Alkyl paths are plotted in continuous line and alkoxy in dashed line. The products notation refers to **Figure 5-2**. GLY: glycerol, Int.: monoradical intermediate

Dehydrogenation Products	Lowest effective barriers (eV)	Overall reaction energies (eV)
<b>DHA</b>	0.64	-0.53
<b>GAL</b>	0.64	-0.44
<b>ENOL</b>	0.64	-0.53
<b>Dirad1</b>	0.65	-0.35
<b>Dirad2</b>	0.64	-0.44
<b>Dirad3</b>	0.69	-0.27
<b>Dirad4</b>	0.66	-0.16
<b>Dirad5</b>	0.66	-0.35
<b>Dirad6</b>	0.72	-0.01

**Table 5-3:** BEP-estimated effective barriers of the most favorable dehydrogenation routes presented in **Figure 5-7**, with their corresponding overall reaction energies. The lowest barrier is of 0.64 eV and the highest one is of 0.72 eV.

## 2 Predicting polyol dehydrogenation products on Rh and Pt

### 2.1 Glycerol dehydrogenation on Pt

Now, we will study glycerol dehydrogenation on Pt using the BEP relation. Let us focus firstly on the three unsaturated products (DHA, GAL and ENOL, see **Figure 5-8**). Contrary to Rh, we observe here that alkyl routes are clearly favored on Pt for DHA and GAL formation. ENOL formation seems to be more favorable, with a low second step activation barrier and an exothermic overall reaction energy. These observations suggest that CH dissociations are preferred on Pt, as mentioned by Greeley and coworkers.<sup>8</sup> This feature is related to the high instability of alkoxy radicals on Pt (see details in the first section of Chapter 3).

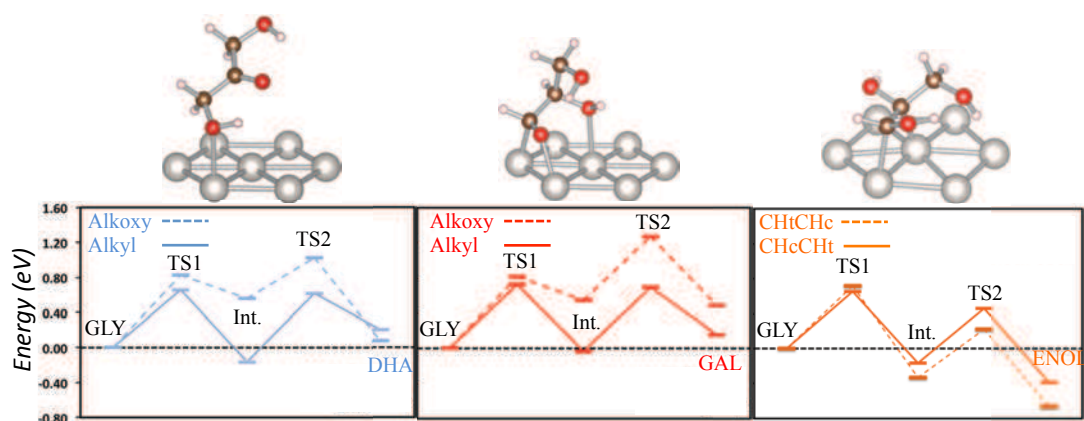


**Figure 5-8:** DHA, GAL and ENOL formation from glycerol (GLY) on Pt. “Int.” denotes the monoradical intermediate. The paths are predicted using the BEP relation. For each product we present the most stable structure adsorbed on Pt. Let us precise that for DHA and GAL, the final product is not identical according to the dehydrogenation route (alkyl or alkoxy). We took in each situation a final product with a conformation corresponding to the radical intermediate. Grey: Pt, brown: C, red: O, pink: H

Then, we proceeded as for Rh in 1.3.2, selecting the lowest effective barriers for every potential product. The corresponding energetic profiles are plotted in **Figure 5-9**, with their effective barriers and their overall reaction energies. While all the barriers are similar at the first step, we distinguish clearly several “packs” at the second step. Dirad3 and Dirad6 are obviously disqualified with “high” statistical probability, according to the confidence level classification described in section 1.3.1. These diradicals are obtained *via* two successive OH scissions, namely OHcOHc and OHtOHt (see **Figure 5-2** for the notations), leading thus to

alkoxy radicals, hence disfavored on Pt. To the opposite, ENOL and Dirad5 (CHtCHt) present the lowest effective barriers (0.66 and 0.68 eV respectively) and clearly the highest exothermicity (-0.39 and -0.54 eV resp.). This phenomenon was expected since alkyl radicals are preferred to alkoxy radicals on Pt.<sup>8</sup> Finally, we can see in the middle a clouded group, including DHA and GAL (with an effective barriers of 0.78 and 0.74 eV resp.) and some diradicals, all these reactions being endothermic. The discrepancies between these barriers are thin and we face here an “indeterminate” situation. However, it is worth noting that according to thermodynamics, DHA, GAL and Dirad1 are related to a lower endothermicity (0.15-0.20 eV) than Dirad2 and Dirad4 (0.46 and 0.52 eV resp.). As a conclusion, this BEP-screening of glycerol reactivity on Pt allows selecting five favorable pathways leading to: DHA, GAL, Dirad1, ENOL and Dirad5. Only these pathways should be refined by DFT calculations for a possible further analysis, keeping in mind that alkoxy routes are always disfavored on Pt.

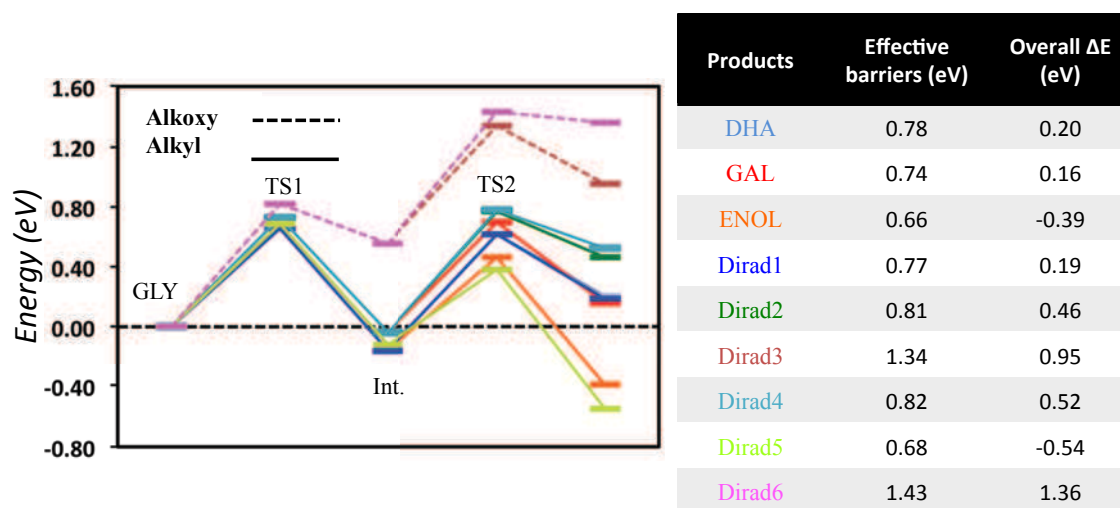


**Figure 5-9:** The most favorable routes for glycerol dehydrogenation on Pt, obtained from BEP prediction. Alkyl paths are plotted in continuous line and alkoxy in dashed line. In the right table be reported the corresponding effective barriers and the overall reaction energies. The notation of products refers to **Figure 5-2**. GLY: glycerol, Int.: monoradical intermediate

In order to be more confident in our predictions on Pt, we compared DFT results and BEP estimations for few activation energies (see **Table 5-4**). Concerning radical formation, we observe that best estimations are obtained for OH breaking (errors are close to zero), whereas CH scissions are regularly affected by a high and positive deviation ( $\sim +0.20$  eV) as observed on Rh in section 1.2. This means that CH activation energies are underestimated when they occur at first step, leading to alkyl monoradical intermediates. Therefore, we can assume that the effective barriers related to ENOL, Dirad1 and Dirad5 are underestimated. Regarding the

carbonyl formation, we notice high magnitude errors on the estimation of the second barrier for the alkoxy route (OHcCHc for DHA and OHtCHt for GAL). Besides these errors are not always oriented in the same direction, hence the difficulty to predict such reaction steps. This feature was already noticed for acetone and formaldehyde formation on Pt in Chapter 3. However, these errors are only related to the alkoxy route, which is disfavored on Pt. Hence, it does not impact our previous conclusions.

<b>BEP.diss vs. DFT</b>	<i>Dissociations</i>	<i>DFT-E<sup>‡</sup></i> (eV)	<i>BEP-E<sup>‡</sup></i> (eV)	<b>Errors (eV)</b>
<b>Radicals</b>	<i>CHc</i>	0.90	0.66	0.24
	<i>CHt</i>	0.98	0.73	0.25
	<i>OHc</i>	0.85	0.82	0.03
	<i>OHt</i>	0.88	0.82	0.06
<b>Carbonyls</b>	<i>OHcCHc (→DHA)</i>	0.20	0.47	-0.27
	<i>OHtCHt (→GAL)</i>	0.92	0.74	0.18

**Table 5-4:** DFT calculated activation barriers vs. BEP estimated barriers for some typical dissociations. “OHcCHc” means central OH scission followed by central CH breaking (and similarly for OHtCHt). Refer to **Figure 5-2** for more details.

## 2.2 1,2-PDO dehydrogenation

Now that we addressed the question of glycerol dehydrogenation, we will focus on 1,2-PDO. The BEP predictions are still performed using equations presented in **Table 5-1**. 1,2-PDO is another important intermediate occurring in the mechanism of glycerol conversion into lactic acid, on which one dehydrogenation happens (see **Figure 5-1**). Firstly, concerning the formation of acetol and lactaldehyde, we can see in **Figure 5-10** that alkoxy and the alkyl routes are very close to each other in the case of Rh, leading to an “indeterminate” situation. To the opposite, the alkyl route is clearly favored on Pt with a “high” confidence level. Let us mention that regarding ENOL, the two alkyl routes are equally probable both for Rh and Pt. Similar features were observed for glycerol dehydrogenation on Rh and Pt. Let us remind that according to the discussion of the section 1.3.2, we can be more confident in CH-predictions performed for 1,2-PDO than for glycerol.

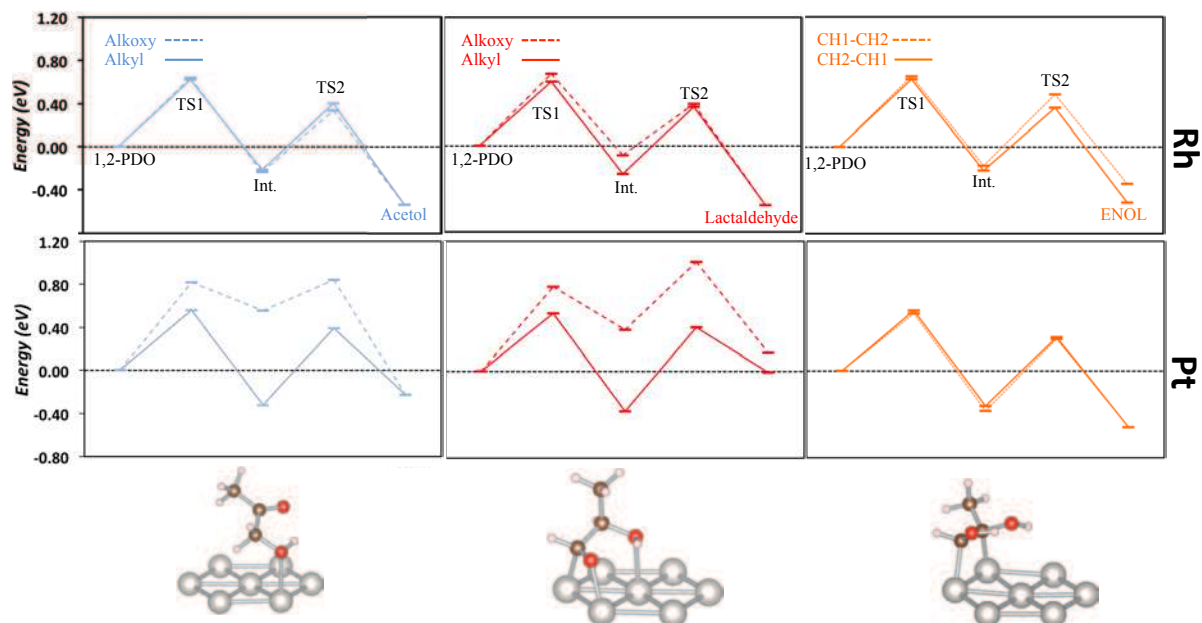


**Figure 5-10: 1,2-PDO dehydrogenation toward acetol, lactaldehyde and enol, predicted via the BEP relation.** “Int.” denotes the monoradical intermediate. On the top row we represented the reaction on Rh catalyst and on the lower one we considered the Pt catalyst. For each product we present the most stable structure adsorbed on Pt. Grey: Pt, brown: C, red: O, pink: H. Note that all the configurations are similar for Rh and Pt, except for ENOL. Concerning the latter, the C=C bond is in di- $\sigma$  on Pt and in  $\pi$  on Rh with the terminal OH linked to the metal. (See **Figure 5-2** for the CH1-CH2 notation on ENOL)

Then, we compared 1,2-PDO reactivity on Rh and Pt considering all the potential dehydrogenation products. As in the previous sections, we selected the most favorable route for each product, and we reported in **Table 5-5** the corresponding effective barriers and the overall reaction energies. Regarding first Rh catalyst, the discrepancies between all the barriers are too small to allow any conclusions. The only point is that thermodynamically, all the unsaturated species (acetol, lactaldehyde and ENOL) are favored comparatively to the diradicals. Now, let us focus on Pt catalyst. We observe that according to thermodynamics unsaturated species (exothermic reactions), and especially ENOL, are much more preferred to the diradicals (endothermic reactions). On the kinetics point of view it is obvious that Dirad3 (see **Figure 5-2** for the notations) is disfavored (confidence level: “high”), with an effective barrier of 1.21 eV. This diradical corresponds to 1,2-PDO undergoing two successive dehydrogenations of the two hydroxyl groups. The formation of this alkoxy diradical is thus unfavorable on Pt catalyst, consistently with previous observations on glycerol. The two other diradicals present lower effective barriers (0.79 and 0.85 eV) but still higher than some unsaturated species. Indeed, we notice that acetol and ENOL have the lowest effective barriers, respectively of 0.64 and 0.71 eV. The barrier difference with the diradicals is

sufficiently significant to consider that ENOL and acetol are favored on Pt (confidence level: “likely”). Finally, let us mention that even if its overall reaction energy is close to zero (athermic reaction), we cannot exclude the production of lactaldehyde. Indeed, its effective barrier is relatively low, even if the formation acetol and ENOL is clearly more favorable. As a conclusion, according to BEP-screening only three pathways leading to ENOL, acetol and lactaldehyde are potentially expectable on Pt for 1,2-PDO dehydrogenation, and should be refined by DFT for a possible further analysis. Concerning Rh, BEP estimations do not allow any confident conclusions on the kinetic point of view, but regarding thermodynamics the formation of unsaturated species is preferred.

1,2-PDO dehydrogenation	Rh		Pt	
	<i>Lowest effect. Barrier (eV)</i>	<i>Overall <math>\Delta E</math> (eV)</i>	<i>Lowest effect. Barrier (eV)</i>	<i>Overall <math>\Delta E</math> (eV)</i>
<i>Acetol</i>	0.63	-0.54	0.71	-0.23
<i>Lactaldehyde</i>	0.63	-0.55	0.78	-0.01
<i>ENOL</i>	0.63	-0.51	0.64	-0.52
<i>Dirad1</i>	0.67	-0.26	0.79	0.12
<i>Dirad2</i>	0.67	-0.34	0.85	0.31
<i>Dirad3</i>	0.68	-0.13	1.21	0.98

**Table 5-5: Overall reaction energies and BEP predicted effective barriers for 1,2 PDO dehydrogenation products on Rh and Pt.** We present in this table only the most favorable route for each product as we did for glycerol previously. For the notation of the products, see **Figure 5-2**.

### 3 Glycerol conversion into lactic acid: Rh or Pt?

According to the mechanism initially suggested on Rh (see **Figure 5-1**), we can distinguish two stages in conversion of glycerol into lactic acid (LA). At the first stage, glycerol is dehydrogenated into GAL, giving after various subsequent transformations pyruvaldehyde (PAL). At the second stage, an equilibrium is achieved between 1,2-PDO, acetol and PAL. Since LA results from PAL, it is important to shift the chemical equilibrium from 1,2-PDO towards acetol. Hence, two intermediate species are especially important in this mechanism: GAL and acetol.

We showed in this chapter that unsaturated species are thermodynamically favored on Rh and Pt. On the latter, this tendency is clearly confirmed by kinetics observations. While on both catalysts ENOL formation is clearly exothermic, this exothermicity is much higher than for the formation of carbonyl derivatives on Pt. As a result, we can suppose, at least for Pt catalyst, that GAL and acetol intermediates do not stem directly from glycerol and propanediol dehydrogenation. However, they should be rather obtained from subsequent rearrangements of ENOL within the solution, enol species being unstable in aqueous medium.

Those reaction processes occur at the interface metal/liquid. When a species is formed on the metallic surface, it must be able to desorb easily to undergo potential further transformations in solution. Thus, it is important to also consider adsorption/desorption energies of such species. Let us remind that adsorption energy is defined as the difference between the absolute energy of molecule adsorbed on the slab, and the sum of the bare slab and the molecule in the gas phase. We present in **Table 5-6** adsorption energies on Rh and Pt of glycerol and its main dehydrogenation products. Adsorption on Rh is globally stronger than on Pt, glycerol adsorption energy being of -0.61 eV on Rh and of -0.41 eV on Pt. Concerning Rh catalyst, ENOL and GAL present the lowest adsorption energies (-1.19 and -1.05 eV, respectively), DHA adsorption being slightly weaker (-0.85 eV). Regarding Pt catalyst, carbonyl derivatives are much less attached to the surface (-0.15 and -0.39 eV for DHA and GAL resp.) than ENOL (-1.05 eV).

Adsorption energies (eV)	Rh	Pt
<b>Glycerol</b>	-0.61	-0.41
<b>DHA</b>	-0.85	-0.15
<b>GAL</b>	-1.05	-0.39
<b>ENOL</b>	-1.19	-1.05

**Table 5-6: Adsorption energies of the main products stemming from glycerol dehydrogenation on Rh and Pt.**

As a consequence, when glycerol conversion occurs on Rh catalyst, reaction intermediates are too strongly bonded to the surface to easily desorb and undergo subsequent transformations within the solution. To the opposite, on Pt catalyst intermediate species are able to desorb easier than on Rh. That is why even if glycerol adsorption is weaker on Pt than on Rh, Pt is a better catalyst than Rh for glycerol conversion. This conclusion is in full agreement with experiments, as reported by Checa *et al.*<sup>3</sup> Besides, since carbonyl derivatives do not favorably link with Pt, PAL intermediate occurring in the last stage of the mechanism, and finally LA, will be easily findable in the solution rather than poisoning the metallic surface.

## Conclusion

Using BEP relations established for simple alcohols, we were able to address the reactivity of some complex alcohols such as glycerol and 1,2-PDO. We showed that taking into account the water assistance effect improves the quality of the predictions for OH scissions. However, we highlight that it is necessary to observe a certain gap between two barrier estimations in order to discriminate between them with a sufficient confidence level. We found that unsaturated species stemming from glycerol and 1,2-PDO dehydrogenation are preferred both on Rh and Pt catalysts, ENOL formation being particularly favorable on Pt. Besides, carbonyl intermediates being much less bonded on Pt than on Rh, glycerol conversion in liquid environment is expected to be better on Pt. Indeed, on the latter catalyst carbonyl derivatives can easily desorb and interact with the solution.

In this chapter, we screened a reaction mechanism focusing exclusively on CH and OH dissociations. Nevertheless, a complete reaction network also implies C-C and C-O breakings. Whether it is possible to predict dehydrogenation barriers of complex systems such as polyalcohols, from simple molecules, it is not obvious that a similar process can be applied to other reactions. Indeed, as suggested by Vlachos and co-workers<sup>9</sup> relating to C-C and C-O scissions on Pd, products resulting from the decomposition of furanic groups lead to higher errors than small species. This observation originates from the fact that C-C and C-O breakings induce structural deformations on the molecules, that are much more significant than CH or OH dissociations.

---

<sup>1</sup> F. Auneau, C. Michel, F. Delbecq, C. Pinel and P. Sautet, *Chem. Eur. J.* **2011**, *17*, 14288–14299

<sup>2</sup> A. M. Ruppert, K. Weinberg and R. Palkovits, *Angew. Chem. Int. Ed.* **2012**, *51*, 2564-2601

<sup>3</sup> M. Checa, F. Auneau, J. Hidalgo-Carrillo, A. Marinas, J. M. Marinas, C. Pinel and F. J. Urbano, *Catal. Today* **2012**, *196*, 91-100

<sup>4</sup> C. Michel, F. Auneau, F. Delbecq and P. Sautet, *ACS Catal.* **2011**, *1*, 1430-1440

<sup>5</sup> S. Chibani, C. Michel, F. Delbecq, C. Pinel and M. Besson, *Catal. Sci. Technol.*, **2013**, *3*, 339-350

<sup>6</sup> C. S. Callam, S. J. Singer, T. L. Lowary, C. M. Hadad, *J. Am. Chem. Soc.* **2001**, *123*, 11743–11754

<sup>7</sup> D. Coll, F. Delbecq, Y. Aray, P. Sautet, *P. Phys. Chem. Chem. Phys.* **2011**, *13*, 1448–1456.

<sup>8</sup> B. Liu, J. Greeley, *J. Phys. Chem. C*, **2011**, *115*, 19702–19709

<sup>9</sup> S. Wang, V. Vorotnikov, J. E. Sutton and D. G. Vlachos, *ACS Catal.*, **2014**, *4*, 604–612

## Summary and perspectives

---

In this thesis, we evidenced that polyalcohol reactivity can be predicted from BEP-type relations established on monoalcohols, with a satisfying accuracy. We proved the validity of this concept for glycerol dehydrogenation on Rh catalyst. However, this process may lead to small systematic errors in the prediction, originating from structural discrepancies between complex and simple alcohols. In the case of OH dissociation, we showed that intramolecular H-bonds occurring in glycerol are directly responsible for this deviation. Encouraged by those results, and aiming at screening the performance of various catalysts, we designed other linear energy relationships for a large set of late transition metals. Subsequently, simulating water-assisted-dehydrogenation, we assessed the influence of H-bonds on those relations. While in general no major effect was noticed for CH scission whatever the metal, it is obvious that OH breaking is activated under H-bond assistance. The latter observation is much more striking on oxophilic metals than on other ones. Finally, we applied those relations to a portion of a complex reaction network, implying the transformation of glycerol into lactic acid. Comparing Rh and Pt performances, we reached the same conclusion as experimentalists, meaning Pt catalyst is more efficient in the conversion of glycerol. These observations confirm the validity and the quality of our method.

Many perspectives may be considered:

1. In this thesis, we distinguished two situations concerning CH bonds, being either in  $\alpha$  position or in  $\beta$  position of the OH group. However, various authors do not make this distinction and treat them together in a unique relationship.<sup>1,2</sup> It can be interesting to consider CH $\beta$  dissociations, and also CH breaking occurring in small hydrocarbons, for the whole set of metals that we used in this thesis. In such a way, we would be able to see if it is possible or not, to establish on any metallic catalyst, a unique linear energy relation for all the CH bonds independently of their nature. This relation would be extremely useful, since it could be applied on any kind of alcohol, whatever its size and its number of OH groups.

2. During this project, we exclusively focused on dehydrogenation, showing that for such a reaction, reactivity of complex molecules may be deduced from simple molecules. However, it is not obvious that this conclusion remains valid whatever the kind of reaction that is considered, as suggested by Vlachos and co-workers.<sup>2</sup> Other types of bond breaking are necessary, in order to deal with a complex reaction network in its entirety. C-C and C-O scissions are especially important and were already extensively addressed in the literature for small species.<sup>3,4,5</sup> Yet, in spite of few studies related to complex molecules,<sup>6</sup> there is still a considerable lack of knowledge in the reactivity of such bonds in complex systems. It can be interesting to see in particular, how H-bonds present in polyalcohols influence those reactions according to the metals. And finally, one should also think about the possibility to predict C-C and C-O dissociations in polyols from monoalcohols.
  
3. In this work, we considered complex mechanisms involving several bond dissociations over metallic surfaces, and leading to various adsorbed intermediates and products. According to Hu and co-workers,<sup>7,8</sup> adsorption and desorption processes are determining for such multistep reactions, and can also be treated using linear energy relations. However, since biomass conversion is generally achieved in aqueous medium and not in the gas phase, those phenomena can be significantly impacted in a liquid environment. We think that it is important to deal with this issue in order to have a realistic insight of such reaction networks.
  
4. Another project could be to combine all those BEP-type relationships, to design microkinetic models for large molecular systems.<sup>9,10</sup> Such models bridge the gap between theory and experiment, and are necessary to have a complete overview of complex reaction processes.
  
5. The current study was performed on close-packed structures, yet open surfaces are known to be more reactive towards certain bond scissions.<sup>11</sup> To have an extensive comprehension of catalyst performances, generally composed of faceted particles, it is important to take account of the reactivity of its various facets. Even if linear energy relations should be valid independently of the surface, they can be differently affected on each of them according to the reaction nature.<sup>11</sup>

6. To conclude, in this project we only considered monometallic catalysts. However, other kinds of catalysts, such as bimetallics or metal oxides, are also widely used in biomass conversion.<sup>12</sup> Linear energy relations should also be applicable to such systems,<sup>13,14</sup> and thus can help to address their reactivity.

Even if this thesis focuses on glycerol, it must be also possible to conceive similar methods to study various carbohydrates, such as cellulose. For such complex molecular systems, *ab initio* calculations must be used in combination with linear energy relations, in order to address their reactivity in a reasonable time and to save computer memory. As a result, this work paves the way for the development of novel numerical techniques, allowing the computational design of solid catalysts for biomass conversion.

---

<sup>1</sup> J. E. Sutton and D. G. Vlachos, ACS Catal. **2012**, 2, 1624–1634

<sup>2</sup> S. Wang, V. Vorotnikov, J. E. Sutton and D. G. Vlachos, ACS Catal., **2014**, 4, 604–612

<sup>3</sup> P. Ferrin, D. Simonetti, S. Kandoi, E. Kunkes, J. A. Dumesic, J. K. Nørskov and M. Mavrikakis, J. Am. Chem. Soc. **2009**, 131, 5809–5815

<sup>4</sup> A. Michaelides, Z.P. Liu, C. J. Zhang, A. Alavi, D. A. King and P. Hu, J. Am. Chem. Soc. **2003**, 125, 3704–3705

<sup>5</sup> R. Alcalá, M. Mavrikakis, and J.A. Dumesic, J. of Catal., **2003**, 218, 178–190

<sup>6</sup> B. Liu, J. Greeley, J. Phys. Chem. C, **2011**, 115, 19702–19709

<sup>7</sup> B. Yang, R. Burch, C. Hardacre, G. Headdock, G. and P. Hu, ACS Catal. **2014**, 4, 182–186

<sup>8</sup> J. Cheng, P. Hu, P. Ellis, S. French, G. Kelly and C. M. Lok, J. Phys. Chem. C, **2008**, 112, 1308–1311

<sup>9</sup> J. K. Nørskov, F. Abild-Pedersen, F. Studt, and T. Bligaard, PNAS, **2011**, 108, 937–943

<sup>10</sup> M. Saliccioli, M. Stamatakis, S. Caratzoulas and D. G. Vlachos, Chem. Eng., **2011**, 66, 4319–4355

<sup>11</sup> J. K. Nørskov, T. Bligaard, B. Hvolbæk, F. Abild-Pedersen, I. Chorkendorff and C. H. Christensen, Chem. Soc. Rev., **2008**, 37, 2163–2171

<sup>12</sup> A. M. Ruppert, K. Weinberg and R. Palkovits, Angew. Chem. Int. Ed. **2012**, 51, 2564–2601

<sup>13</sup> A. Vojvodic, F. Calle-Vallejo, W. Guo, S. Wang, A. Toftelund, F. Studt, J. I. Martínez, J. Shen, I. C. Man, J. Rossmeisl, T. Bligaard, J. K. Nørskov and F. Abild-Pedersen, J. Chem. Phys., **2011**, 134, 244509

<sup>14</sup> C. Fan, Y. Zhu, Y. Xu, Y. Zhou, X. Zhou and D. Chen, J. Phys. Chem, **2012**, 137, 014703

# Appendix 1: Supplementary Information related to Chapter 2

---

## Linear energy relations as predictive tools for polyalcohol catalytic reactivity

Jérémie Zaffran, Carine Michel, Florian Auneau, Françoise Delbecq, Philippe Sautet\*

Université de Lyon, CNRS and Ecole Normale Supérieure of Lyon, 46 Allée d'Italie, 69364 Lyon Cedex 07, France

### Supplementary Information

#### Table of Contents

<b>1- Computational methods</b>	<b>2</b>
<b>2- Statistical approaches</b>	<b>2</b>
<i>The determination coefficient <math>R^2</math></i>	2
<i>The Mean Absolute Error (MAE), the Mean Signed Error (MSE) and the Maximal Error (MAX)</i>	3
<i>The box plots</i>	3
<i>Confidence intervals</i>	4
<b>3- Additional tables and figures</b>	<b>5</b>
<b>4- List of considered reactions for monoalcohols</b>	<b>10</b>
<i>CH<sub>α</sub> dissociations</i>	10
<i>CH<sub>β</sub> dissociations</i>	11
<i>OH dissociations</i>	12
<b>5- List of considered reactions for glycerol</b>	<b>13</b>
<i>CH dissociations</i>	13
<i>OH dissociations</i>	14
<b>6- Calculated structures for monoalcohols</b>	<b>15</b>
<i>CH<sub>α</sub> dissociations</i>	15
<i>CH<sub>β</sub> dissociations</i>	19
<i>OH dissociations</i>	21
<b>7- Calculated structures for glycerol</b>	<b>24</b>
<i>CH dissociations</i>	24
<i>OH dissociations</i>	28
<i>Structure and energy of most relevant configurations of glycerol on Rh(111) and of the main dehydrogenation products</i>	31

## **1- Computational methods**

The calculations presented in the current study were performed on periodic metallic slabs with VASP 4.36<sup>[1,2]</sup>, at the generalized gradient approximation (GGA) using the Perdew Wang 91 exchange-correlation functional<sup>[3]</sup> and the projector-augmented-wave method (PAW)<sup>[4]</sup>. For the expansion of the plane-wave basis set, a converged cutoff has been set to 400 eV and a (3×3×1) Monkhorst-Pack k-point mesh was chosen. Concerning the coverage, we considered a (3×3) supercell with 4 metallic layers and 5 vacuum layers (~10 Å).

For each X-H dissociation step, the most stable chemisorbed initial state (IS) and final state (FS) was searched, the dissociated H atom in the final state being considered at large distance from the molecular fragment and calculated on a separated unit cell. During the geometry optimization, the degrees of freedom of the adsorbate and the two uppermost metal layers have been relaxed while the two lowest metallic planes have been frozen in a bulk-like optimal geometry (distance (Rh-Rh)= 2.72 Å). Concerning the gas phase a box of 20×20×20 Å<sup>3</sup> was chosen and unrestricted calculations were performed for radicals. For every structure (both gas and adsorbate) the electronic energy convergence criterion was fixed to 10<sup>-6</sup> eV and the ionic force convergence criterion was fixed to 0.01 eV/Å. The transition states (TS) were precisely calculated by a combination of nudged elastic band method<sup>[5,6]</sup>, quasi-newton optimization and dimer method<sup>[7]</sup> and were characterized by the presence of a unique imaginary frequency corresponding to the reaction coordinate. Structures and energies for the IS and FS minima and for the TS are given below for the monoalcohol sample and for glycerol.

Special care was taken in the numerical accuracy of the calculated adsorption energies. The influence of the calculations parameters (number of K points, slab thickness) was tested on a subset of structures, with no significant change in the produced linear energy relationship. For example, in order to test the effect of the coverage, we calculated a set of points for glycerol including CH and OH scission both in with a 3x3 slab and a 4x4 slab. Very similar results were observed for correlation parameters (slope/intercept) and for error distributions.

## **2- Statistical approaches**

*All the statistical analysis was realized with the software R<sup>[8]</sup>*

A linear regression links two random variables,  $Y \in \{y_1, y_2 \dots y_n\}$  (dependent variable) and  $X \in \{x_1, x_2 \dots x_n\}$  (independent variable). The quality of the model can be assessed by various descriptors we will mention here.

***The determination coefficient  $R^2$***

$$R^2 = 1 - \frac{\sum_i (y_i - \hat{y}_i)^2}{\sum_i (y_i - \bar{y})^2},$$

where  $y_i$  is the value of the  $i^{th}$  dependent variable,  $\hat{y}_i$  is the linear model estimated value of the  $i^{th}$  dependent variable and  $\bar{y}$  is the mean of all the  $y_{i \in \{1,2,..n\}}$ . In our case  $y_i$  is the DFT value and  $\hat{y}_i$  is the BEP type relation estimated value.

**The Mean Absolute Error (MAE), the Mean Signed Error (MSE) and the Maximal Error (MAX)**

$$MAE = \frac{\sum_i |y_i - \hat{y}_i|}{N},$$

$$MSE = \frac{\sum_i (y_i - \hat{y}_i)}{N} \text{ and}$$

$$MAX = \max_{i \in \{1,2,..n\}} (y_i - \hat{y}_i)$$

where  $y_i$  is the value of the  $i^{th}$  dependent variable,  $\hat{y}_i$  is the linear model estimated value of the  $i^{th}$  dependent variable and  $N$  the size of the sample. While MAE is an absolute error, MSE is algebraic. In our case, the statistical error is thus defined as “DFT value – BEP type relation estimated value”.

**The box plots <sup>[9]</sup>**

Box plots (or box-and-whisker plots) are a way to depict data, which enable to directly visualize the points that are statistically representative. It is a practical method to represent error distributions of a linear regression (see figure S1).

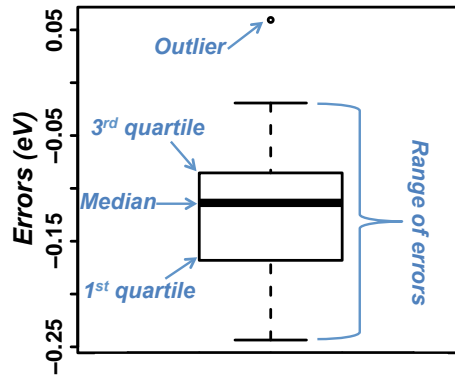


Figure S1:  
Example of a box plot

Representative data are contained between the “whiskers” of the box (range of errors). Those ones that are non-representative are named “outliers” and located outside the box and its whiskers.

### ***Confidence intervals***

The slope  $\alpha$  and the intercept  $\beta$  of the regression corresponding to a given population, are comprised inside an interval surrounding the slope  $a$  and the intercept  $b$  calculated for the sample from which it is extracted. For the slope (and similarly for the intercept), it can be calculated by the following simplified expression:

$$\alpha \in [a - t \cdot \sqrt{s_a^2}; a + t \cdot \sqrt{s_a^2}],$$

where  $s_a^2$  is the variance of the slope  $a$  and  $t$  is the “*Student coefficient*” depending on the expected confidence threshold (95% in general) and on the size of the sample.

### 3- Additional tables and figures

	TSS-diss.FS/FS				TSS-exo.FS/FS				BEP.assoc			
	$CH_\alpha$	$CH_\beta$	OH	all	$CH_\alpha$	$CH_\beta$	OH	all	$CH_\alpha$	$CH_\beta$	OH	all
A	1.00±0.02	1.05±0.04	1.03±0.04	1.03±0.04	1.02±0.02	0.94±0.06	1.02±0.05	0.99±0.03	0.09±0.30	0.43±0.07	0.49±0.37	0.61±0.25
B	0.81±0.06	0.84±0.13	1.04±0.14	0.89±0.11	0.83±0.05	0.67±0.11	1.01±0.15	0.81±0.08	0.78±0.04	0.68±0.01	0.87±0.07	0.76±0.04

	TSS-diss.FS/IS				TSS-exo.FS/IS				BEP.diss			
	$CH_\alpha$	$CH_\beta$	OH	all	$CH_\alpha$	$CH_\beta$	OH	all	$CH_\alpha$	$CH_\beta$	OH	all
A	1.01±0.03	0.99±0.11	1.05±0.07	1.03±0.06	0.99±0.04	0.99±0.06	1.03±0.04	1.03±0.03	0.91±0.30	0.57±0.07	0.51±0.37	0.39±0.25
B	0.81±0.06	0.66±0.21	1.02±0.13	0.87±0.11	0.79±0.09	0.71±0.21	1.00±0.10	0.91±0.08	0.78±0.04	0.68±0.01	0.87±0.07	0.76±0.04

	TSS-diss.IS/FS				TSS-exo.IS/FS				BEP.exo			
	$CH_\alpha$	$CH_\beta$	OH	all	$CH_\alpha$	$CH_\beta$	OH	all	$CH_\alpha$	$CH_\beta$	OH	all
A	0.98±0.05	0.93±0.03	0.96±0.02	0.96±0.02	1.00±0.04	1.01±0.08	0.95±0.03	0.97±0.03	0.87±0.40	0.45±0.16	0.52±0.39	0.53±0.36
B	0.63±0.12	0.48±0.10	0.60±0.07	0.60±0.07	0.68±0.10	0.63±0.12	0.68±0.10	0.63±0.07	0.78±0.06	0.68±0.03	0.87±0.07	0.77±0.06

	TSS-diss.IS/IS				TSS-exo.IS/IS				BEP.endo			
	$CH_\alpha$	$CH_\beta$	OH	all	$CH_\alpha$	$CH_\beta$	OH	all	$CH_\alpha$	$CH_\beta$	OH	all
A	1.07±0.05	0.95±0.14	1.02±0.08	1.03±0.05	1.02±0.07	0.99±0.05	1.00±0.05	1.02±0.03	0.13±0.40	0.55±0.16	0.48±0.39	0.47±0.36
B	0.79±0.10	0.61±0.25	0.83±0.13	0.77±0.09	0.71±0.15	0.56±1.17	0.80±0.11	0.75±0.08	0.78±0.06	0.68±0.03	0.87±0.07	0.77±0.06

*Table S1:*

Correlation parameters and their confidence intervals for the 12 BEP type relationships for 29 CH and OH dissociation elementary steps of the considered monoalcohol family, considering separately  $CH_\alpha$ ,  $CH_\beta$  and OH dissociations and also the whole set of dehydrogenations (“all”)

	TSS-diss.FS/FS			TSS-exo.FS/IS			BEP.diss		
	MAE	MAX	$R^2$	MAE	MAX	$R^2$	MAE	MAX	$R^2$
<b>All</b>	0.09	0.23	1.00	0.08	0.17	1.00	0.07	0.18	0.29
<b><math>CH_\alpha</math></b>	0.03	0.06	1.00	0.03	0.09	1.00	0.03	0.07	0.82
<b><math>CH_\beta</math></b>	0.04	0.09	1.00	0.06	0.07	1.00	0.01	0.02	0.99
<b>OH</b>	0.06	0.11	0.99	0.05	0.15	0.99	0.05	0.10	0.56

*Table S2:*

Error analysis (Mean Absolute Error, MAE, Maximal absolute error, MAX, and determination coefficient,  $R^2$ ) for the 29 CH and OH dissociation elementary steps of the considered monoalcohol family on Rh (111), considering the global sample (All) or subfamilies ( $CH_\alpha$ ,  $CH_\beta$ , OH).

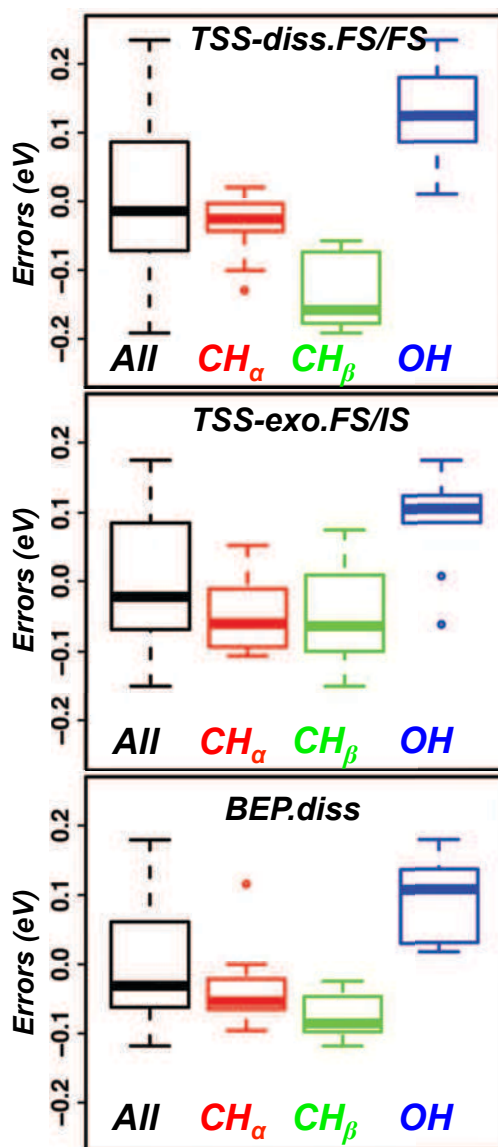
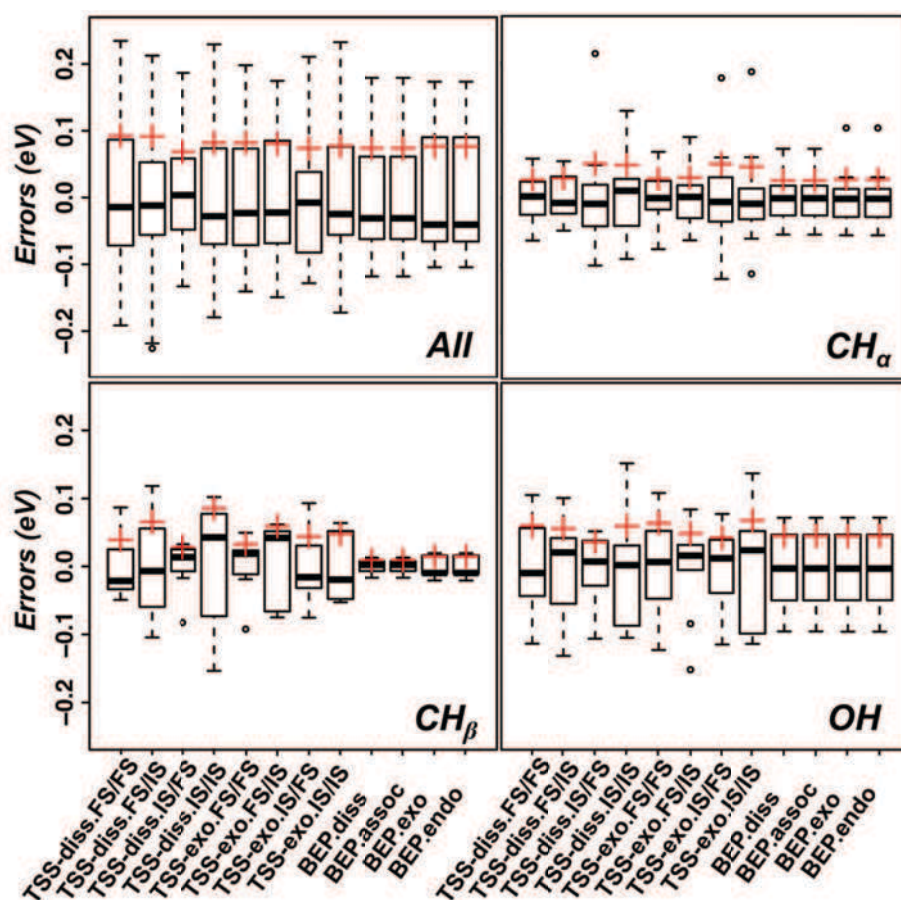


Figure S2:

Errors distribution for the 3 main relationships in the case of monoalcohol dehydrogenation, considering all the points together and using the so-established model to predict  $CH_\alpha$ ,  $CH_\beta$  and  $OH$  respectively. As indicated in the paper, systematic deviations are seen, especially for the  $OH$  bond cleavage.



**Figure S3:**  
 Errors distributions for the 12 linear energy relationships in the case of the dehydrogenation on Rh (111) for the monoalcohol sample, considering all the points together and the 3 subsets  $CH_\alpha$ / $CH_\beta$ / $OH$  separately. Red crosses depict the mean absolute error (MAE) for each relationship.

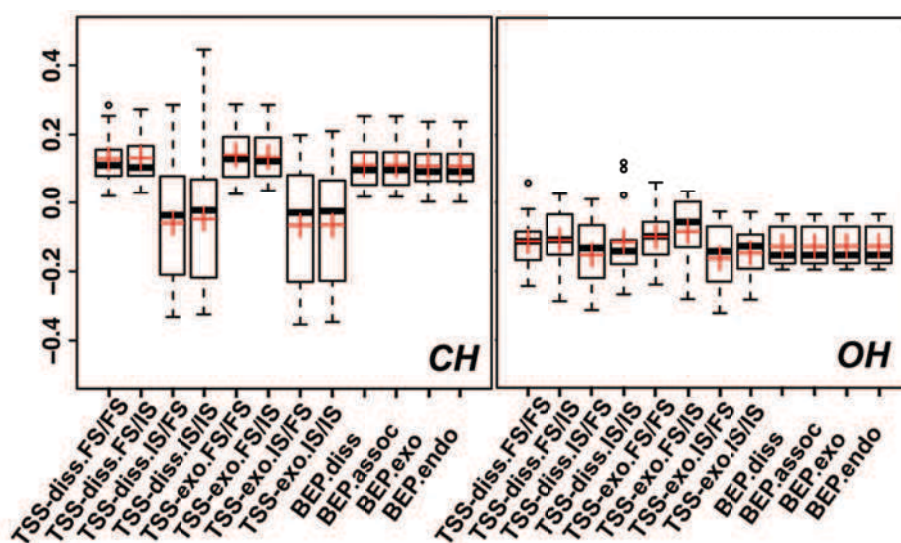


Figure S4:  
 Errors distributions for the prediction of glycerol CH and OH dissociations using the linear energy relationship established with the monoalcohol sample. 12 definitions of the correlation are compared. Red crosses depict the mean signed error (MSE) for each relationship.

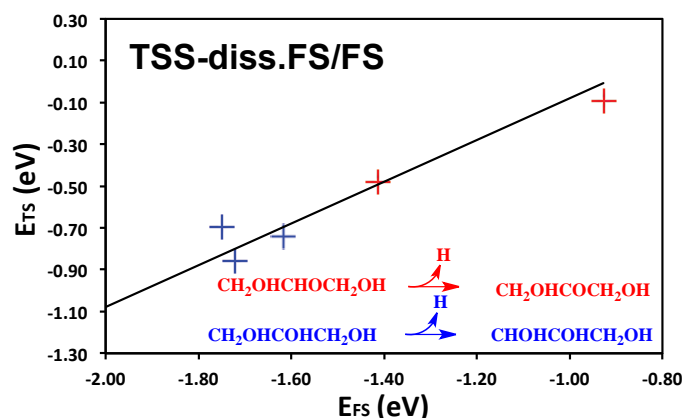


Figure S5:

In the case of glycerol (or its dehydrogenation products), due to the high number of conformations, several TS can be envisaged for one given reaction leading to different conformations of the same product on the surface. In order to enforce the validity of our predictive model we included many of these points in the correlation. We represented this situation on this figure for two specific reactions. The straight black line is the TSS-diss.FS/FS correlation obtained directly from glycerol. One observes that for dihydroxyacetone (in red) formation the lowest FS is associated with the most stable the TS. However for the enol formation (blue) the relation is not strictly verified. Indeed, the point corresponding to the most stable FS corresponds to the least stable TS. Nevertheless energies are not so different and these points correctly fit with the whole correlation within given statistical errors.

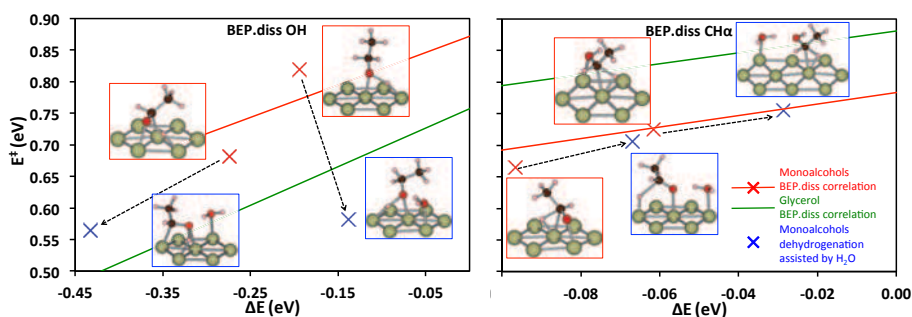


Figure S6:

Effect of water assistance on the BEP.diss relationship for OH dissociation on the left panel and for CHa dissociation on the right one. On both of them, glycerol and simple alcohols linear energy relationships are plotted. Two points, related to ethanol dehydrogenation, are selected for CHa and OH dissociation to evidence the deviation in activation energy and in reaction energy caused by water co-adsorption. The “balls & sticks” pictures depict the transition states associated to each chosen reaction step. As shown on the graphics, hydrogen bonds with water shift the points of monoalcohols towards the “glycerol area” for OH dissociation but not for CHa ones.

#### 4- List of considered reactions for monoalcohols

For each elementary step, the calculated reaction energy and activation energy are listed in eV. The dissociation occurs on the Rh(111) surface and in the product H is considered on a separate slab in hollow position.

##### *CH<sub>α</sub> dissociations*

			$\Delta E$ (eV)	$E^\ddagger$ (eV)
CH <sub>3</sub> OH		CH <sub>2</sub> OH	-0.11	0.68
CH <sub>3</sub> O		CH <sub>2</sub> O	-0.16	0.64
CH <sub>3</sub> CH <sub>2</sub> OH		CH <sub>3</sub> CHOH	-0.06	0.73
CH <sub>3</sub> CH <sub>2</sub> O		CH <sub>3</sub> CHO	-0.10	0.66
CH <sub>2</sub> CH <sub>2</sub> OH		CH <sub>2</sub> CHOH	-0.28	0.55
CH <sub>2</sub> CH <sub>2</sub> CH <sub>2</sub> OH		CH <sub>2</sub> CH <sub>2</sub> CHOH	-0.12	0.67
CH <sub>3</sub> CHCH <sub>2</sub> CH <sub>2</sub> OH		CH <sub>3</sub> CHCH <sub>2</sub> CHOH	-0.14	0.63
CH <sub>3</sub> CHOHCH <sub>3</sub>		CH <sub>3</sub> COHCH <sub>3</sub>	0.04	0.89
CH <sub>3</sub> CHOCH <sub>3</sub>		CH <sub>3</sub> COCH <sub>3</sub>	-0.09	0.65
CH <sub>2</sub> CHOHCH <sub>3</sub>		CH <sub>2</sub> COHCH <sub>3</sub>	-0.24	0.61
CH <sub>2</sub> CH <sub>2</sub> CHOHCH <sub>3</sub>		CH <sub>2</sub> CH <sub>2</sub> COHCH <sub>3</sub>	-0.07	0.73
CH <sub>2</sub> CH <sub>2</sub> (Me)CHOHCH <sub>3</sub>		CH <sub>2</sub> CH <sub>2</sub> (Me)COHCH <sub>3</sub>	-0.08	0.67

***CH<sub>β</sub> dissociations***

			<b>ΔE (eV)</b>	<b>E<sup>‡</sup> (eV)</b>
CH <sub>3</sub> CH <sub>2</sub> OH		CH <sub>2</sub> CH <sub>2</sub> OH	0.04	0.69
CH <sub>3</sub> CH <sub>2</sub> O		CH <sub>2</sub> CH <sub>2</sub> O	0.25	0.83
CH <sub>3</sub> CHOH		CH <sub>2</sub> CHOH	-0.21	0.57
CH <sub>3</sub> CHOHCH <sub>3</sub>		CH <sub>2</sub> CHOHCH <sub>3</sub>	0.01	0.67
CH <sub>2</sub> CHOHCH <sub>3</sub>		CH <sub>2</sub> CHOHCH <sub>2</sub>	0.01	0.70
CH <sub>3</sub> COHCH <sub>3</sub>		CH <sub>2</sub> COHCH <sub>3</sub>	-0.26	0.54
CH <sub>3</sub> CHOCH <sub>3</sub>		CH <sub>2</sub> CHOCH <sub>3</sub>	0.25	0.83

**OH dissociations**

			<b><math>\Delta E</math> (eV)</b>	<b><math>E^\ddagger</math> (eV)</b>
$\text{CH}_3\text{OH}$		$\text{CH}_3\text{O}$	-0.17	0.82
$\text{CH}_2\text{OH}$		$\text{CH}_2\text{O}$	-0.23	0.70
$\text{CH}_3\text{CH}_2\text{OH}$		$\text{CH}_3\text{CH}_2\text{O}$	0.01	0.87
$\text{CH}_2\text{CH}_2\text{OH}$		$\text{CH}_2\text{CH}_2\text{O}$	-0.19	0.82
$\text{CH}_3\text{CHOH}$		$\text{CH}_3\text{CHO}$	-0.27	0.68
$\text{CH}_3\text{CHOHCH}_3$		$\text{CH}_3\text{CHOCH}_3$	-0.21	0.84
$\text{CH}_2\text{CHOHCH}_3$		$\text{CH}_2\text{CHOCH}_3$	-0.02	0.93
$\text{CH}_3\text{COHCH}_3$		$\text{CH}_3\text{COCH}_3$	-0.33	0.69
$\text{CH}_3\text{CH}_2\text{CHOHCH}_3$		$\text{CH}_3\text{CH}_2\text{CHOCH}_3$	-0.05	0.85
$\text{CH}_3\text{CH}_2\text{CHOHCH}_2$		$\text{CH}_3\text{CH}_2\text{CHOCH}_2$	0.00	0.77

## 5- List of considered reactions for glycerol

For each elementary step, reaction energy and activation energy are listed in eV. The dissociation occurs on a surface and H is considered on a separate slab in hollow position. In some cases various transition states corresponding to different reactants and products were found for one given reaction. In these situations we listed several activation and reaction energies for the corresponding reaction.

### CH dissociations

			$\Delta E$ (eV)	$E^\ddagger$ (eV)
CH <sub>2</sub> OHCHOHCH <sub>2</sub> OH		CHOHCHOHCH <sub>2</sub> OH	-0.19, -0.12	0.72, 0.75
CH <sub>2</sub> OHCHOCH <sub>2</sub> OH		CHOHCHOCH <sub>2</sub> OH	-0.06	0.87
CH <sub>2</sub> OHCHOHCH <sub>2</sub> O		CHOHCHOHCH <sub>2</sub> O	-0.32, 0.19	0.70, 1.00
CH <sub>2</sub> OHCHOHCHOH		CHOHCHOHCHOH	-0.24	0.65
CH <sub>2</sub> OCHOHCH <sub>2</sub> OH		CHOCHOHCH <sub>2</sub> OH	-0.42	0.45
CH <sub>2</sub> OHCOHCH <sub>2</sub> OH		CHOHCOHCH <sub>2</sub> OH	-0.34, -0.24, -0.25	0.52, 0.64, 0.80
CH <sub>2</sub> OHCHOHCH <sub>2</sub> OH		CH <sub>2</sub> OHCOHCH <sub>2</sub> OH	-0.18, -0.45	0.77, 0.63
CH <sub>2</sub> OCHOHCH <sub>2</sub> OH		CH <sub>2</sub> OCOHCH <sub>2</sub> OH	-0.15	0.74
CHOHCHOHCH <sub>2</sub> OH		CHOHCOHCH <sub>2</sub> OH	-0.47, 0.64, -0.60	0.35, 0.35, 0.32
CH <sub>2</sub> OHCHOCH <sub>2</sub> OH		CH <sub>2</sub> OHCOCH <sub>2</sub> OH	-0.61, -0.39	0.32, 0.44

**OH dissociations**

			<b><math>\Delta E</math> (eV)</b>	<b><math>E^\ddagger</math> (eV)</b>
<chem>CH2OHCHOHCH2OH</chem>		<chem>CH2OHCHOHCH2O</chem>	-0.13	0.70
<chem>CH2OCHOHCH2OH</chem>		<chem>CH2OCHOHCH2O</chem>	0.12	0.87
<chem>CH2OHCOHCH2OH</chem>		<chem>CH2OHCOHCH2O</chem>	-0.20	0.60
<chem>CHOHCHOHCH2OH</chem>		<chem>CHOHCHOHCH2O</chem>	-0.19	0.61
<chem>CH2OHCHOCH2OH</chem>		<chem>CHOHCHOCH2O</chem>	0.12	0.89
<chem>CH2OHCHOHCHOH</chem>		<chem>CH2OHCHOCHO</chem>	0.08, 0.31	0.80, 0.56
<chem>CH2OHCHOHCH2OH</chem>		<chem>CH2OHCHOCH2OH</chem>	-0.32, -0.03	0.67, 0.67
<chem>CH2OHCHOHCH2O</chem>		<chem>CH2OHCHOCH2O</chem>	-0.03	0.66
<chem>CH2OHCOHCH2OH</chem>		<chem>CH2OHCOCH2OH</chem>	-0.26	0.67
<chem>CHOHCHOHCH2OH</chem>		<chem>CHOCHOHCH2OH</chem>	-0.35, 0.51	-0.30, 0.52

## 6- Calculated structures for monoalcohols

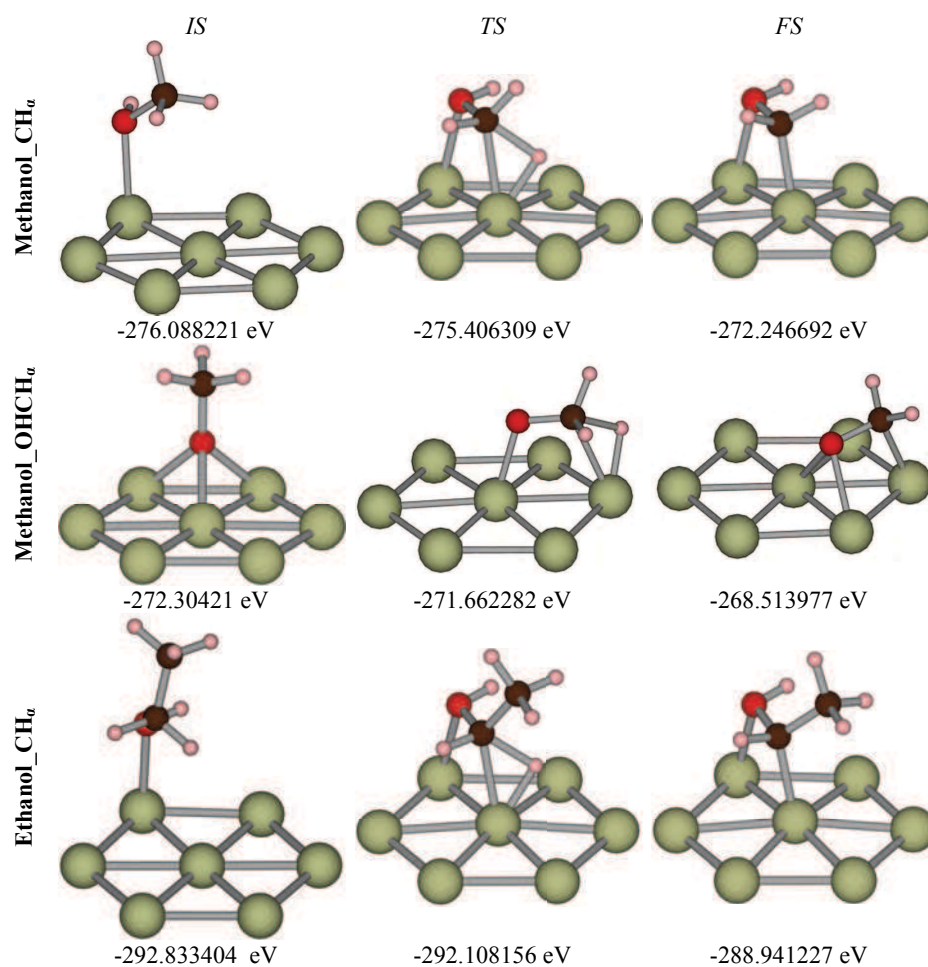
We list here IS, TS and FS structures for the CH or OH dissociation of the sample of monoalcohol molecules on Rh(111) together with their obtained total energies (12  $\text{CH}_\alpha$ , 7  $\text{CH}_\beta$  and 10 OH dissociations).

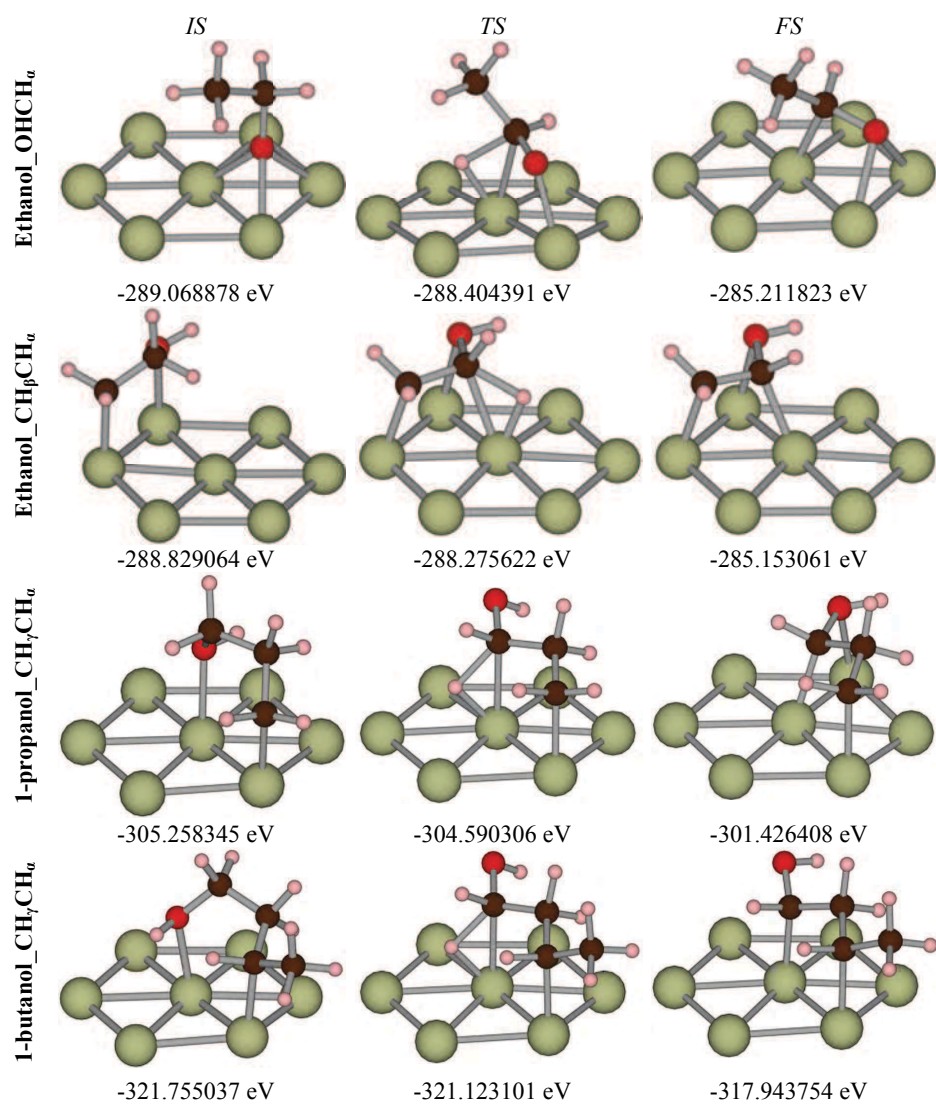
H is on a separate slab in *FCC* position (-249.277433 eV).

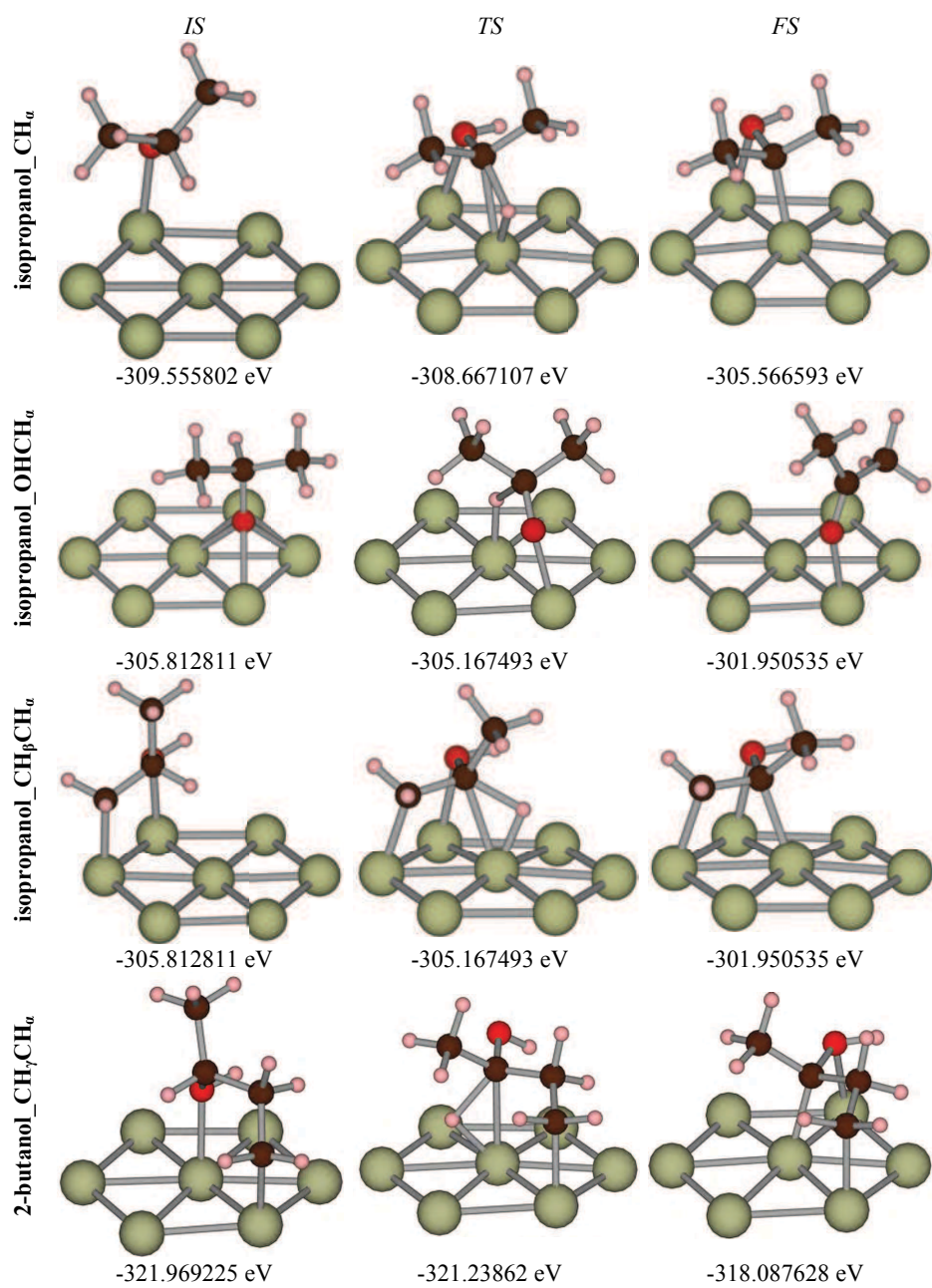
Each TS is confirmed by a unique imaginary frequency.

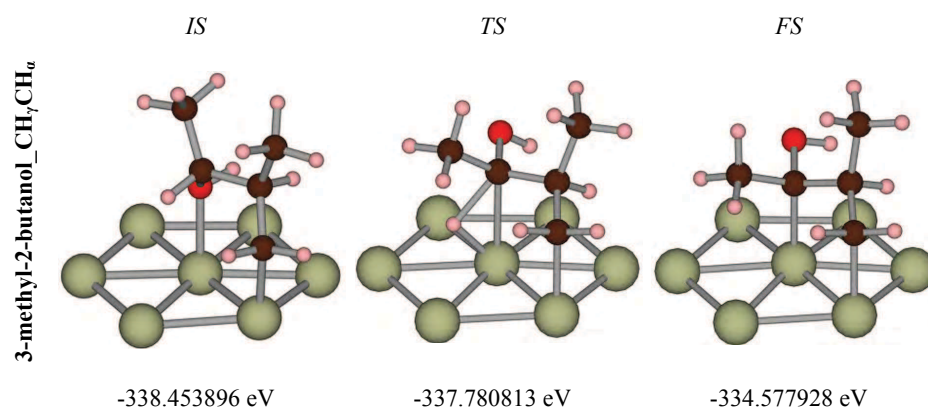
The notation we adopted is such that “methanol\_ $\text{CH}_\alpha$ ” means “dissociation of the CH which is in  $\alpha$  of the OH group in methanol” and “ethanol\_ $\text{CH}_\alpha\text{OH}$ ” means “dissociation of the OH in ethanol that underwent a dissociation of the  $\text{CH}_\alpha$  before”

### $\text{CH}_\alpha$ dissociations

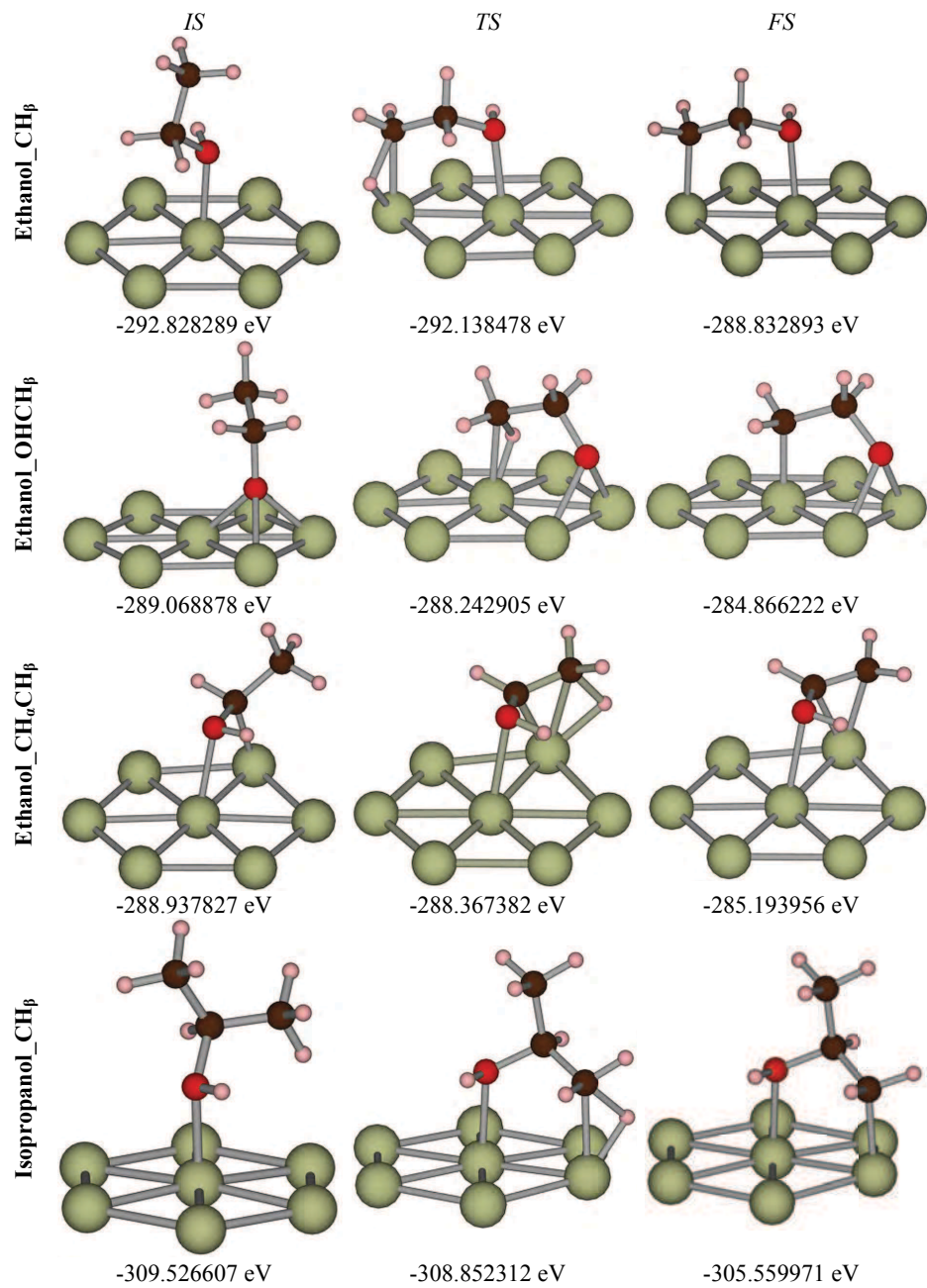


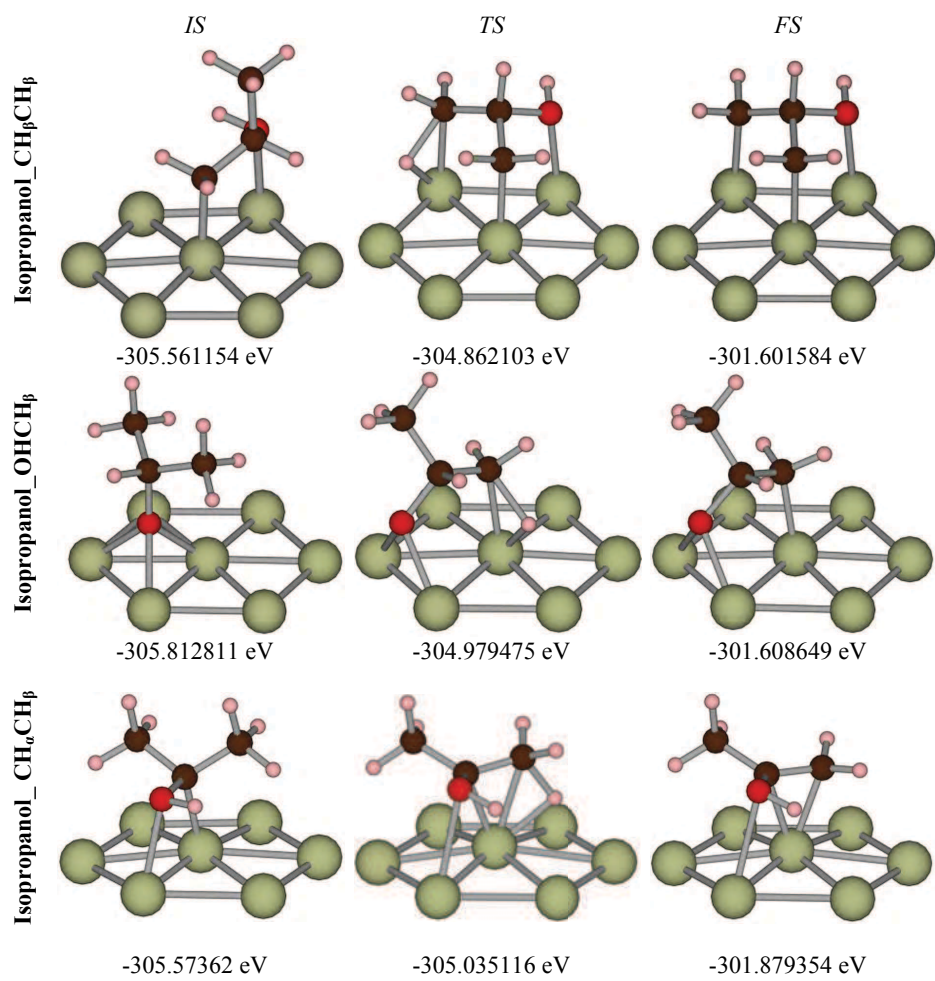




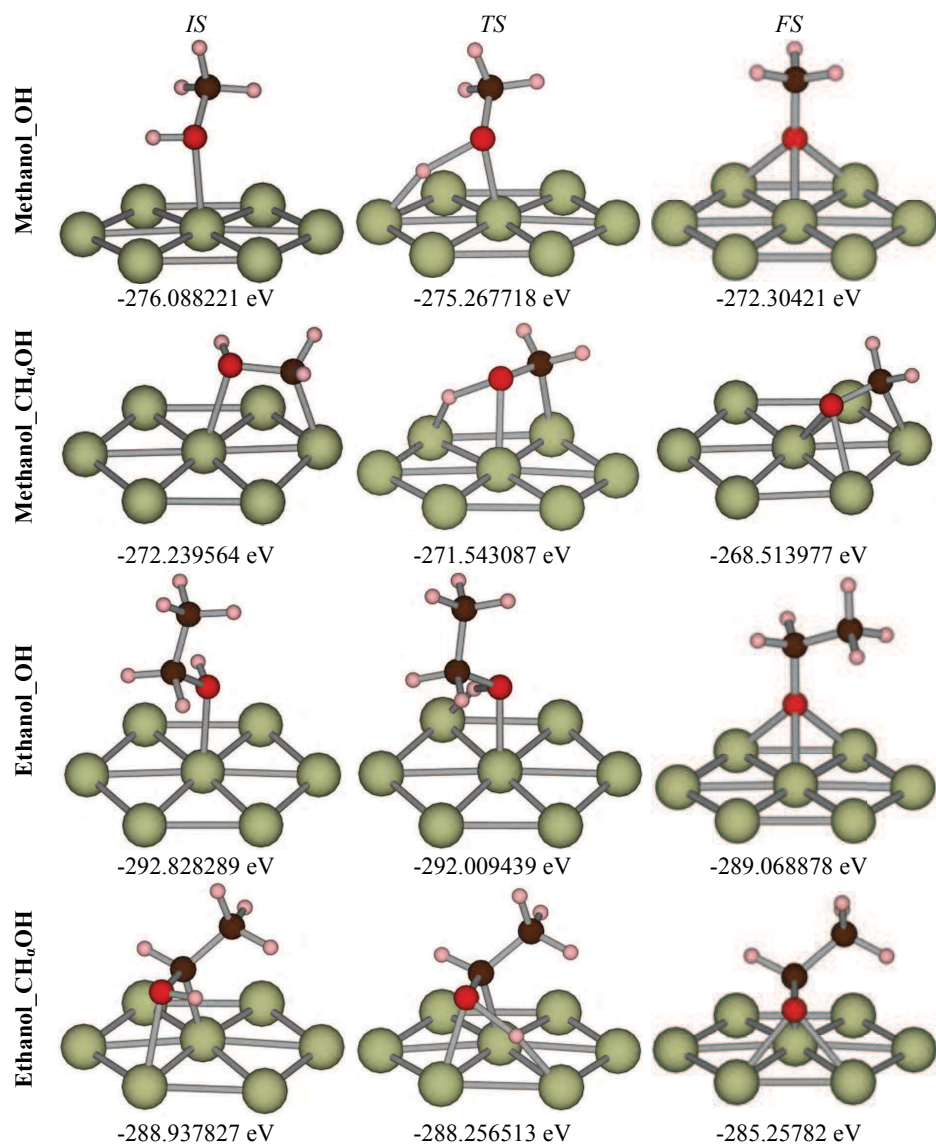


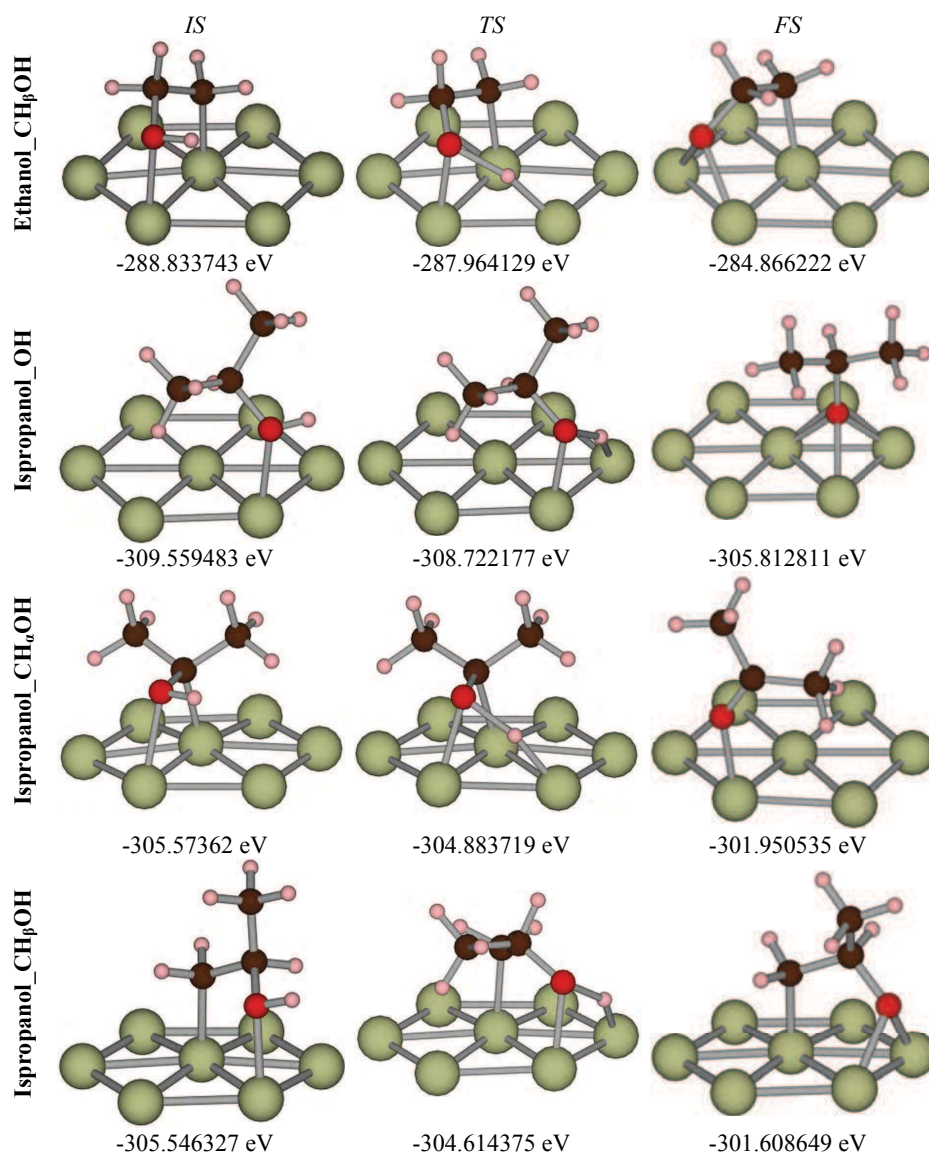
**CH<sub>6</sub> dissociations**

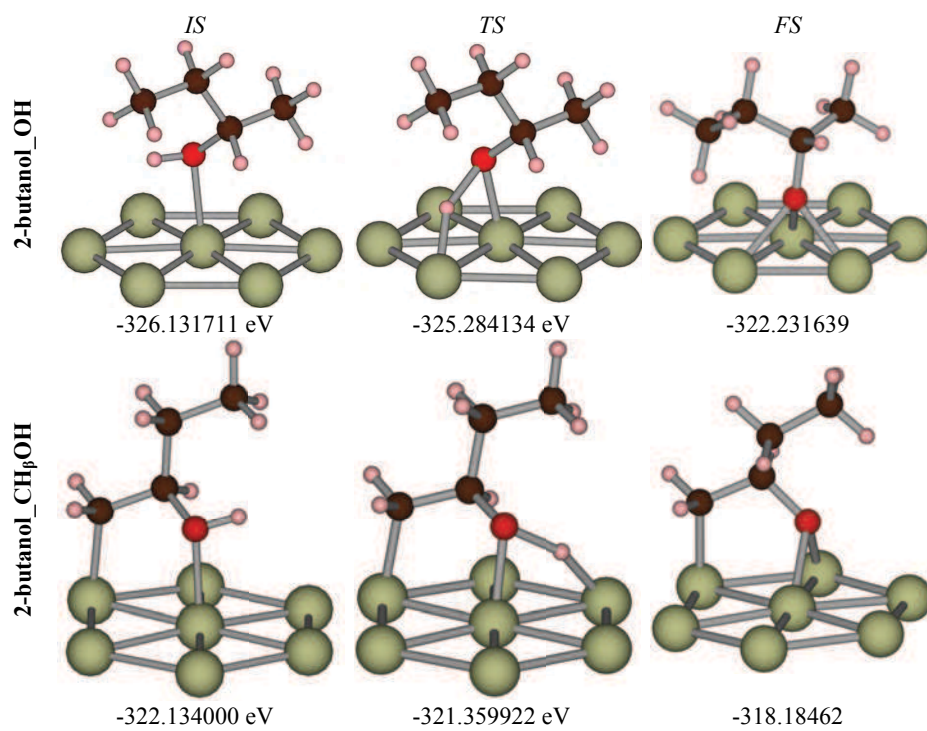




**OH dissociations**







## 7- Calculated structures for glycerol

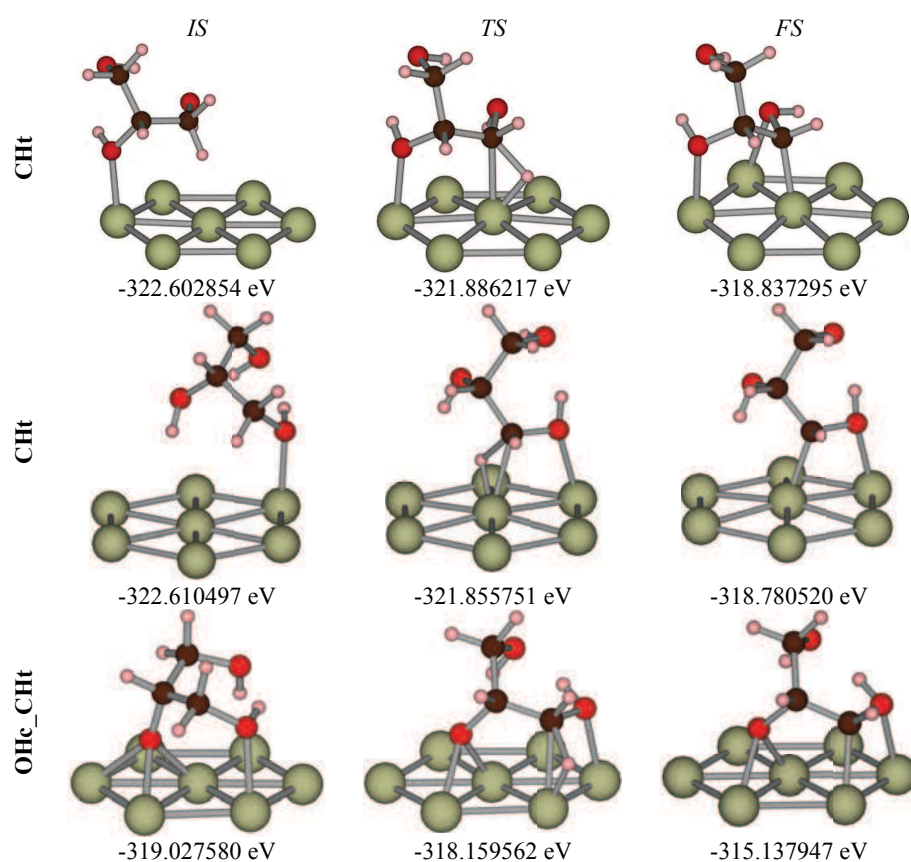
We list here IS, TS and FS structures for the CH or OH dehydrogenation of glycerol on Rh(111) together with their obtained total energies (18 C-H and 12 O-H activations).

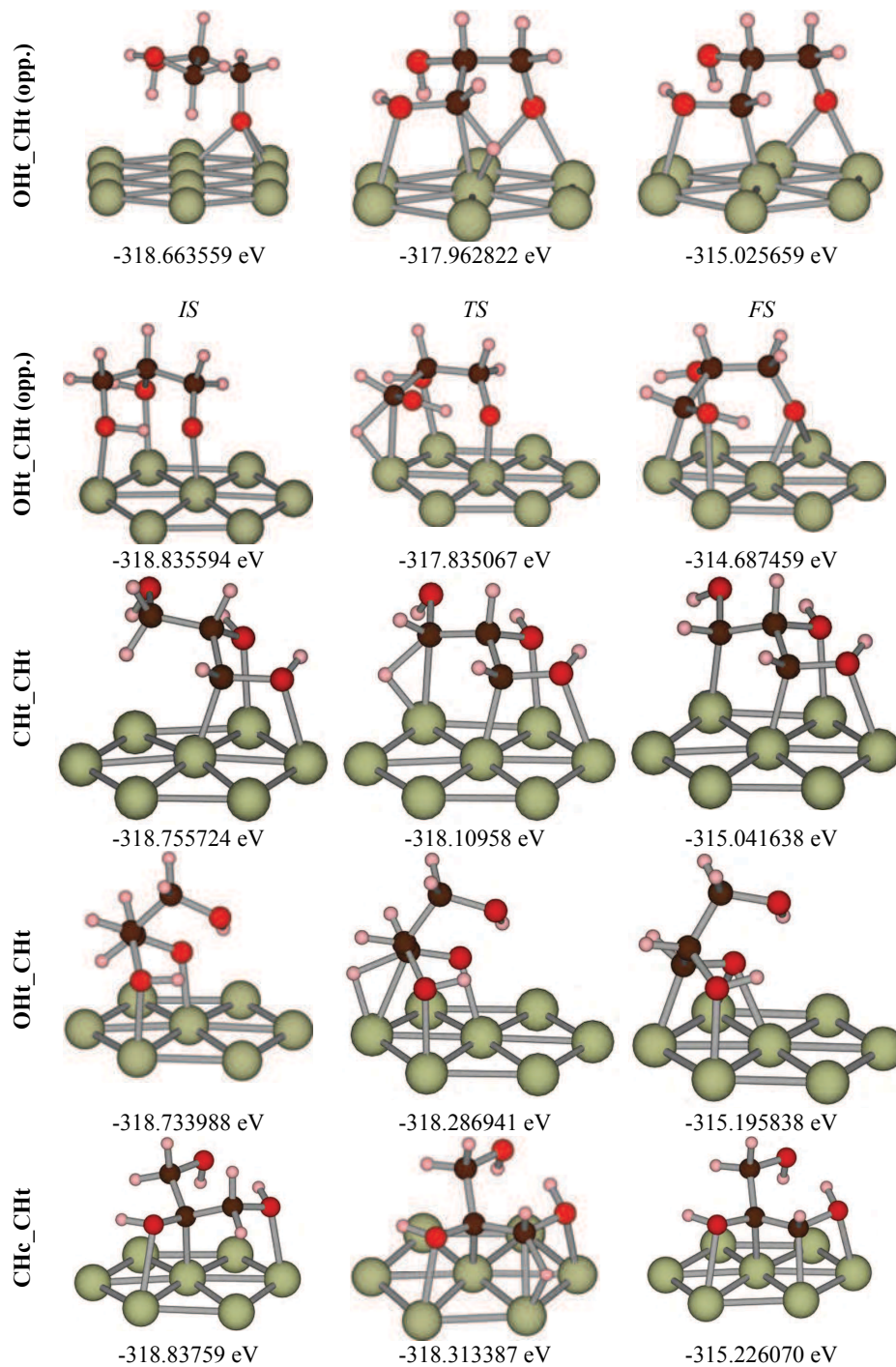
H is on a separate slab in *FCC* position (-249.277433 eV).

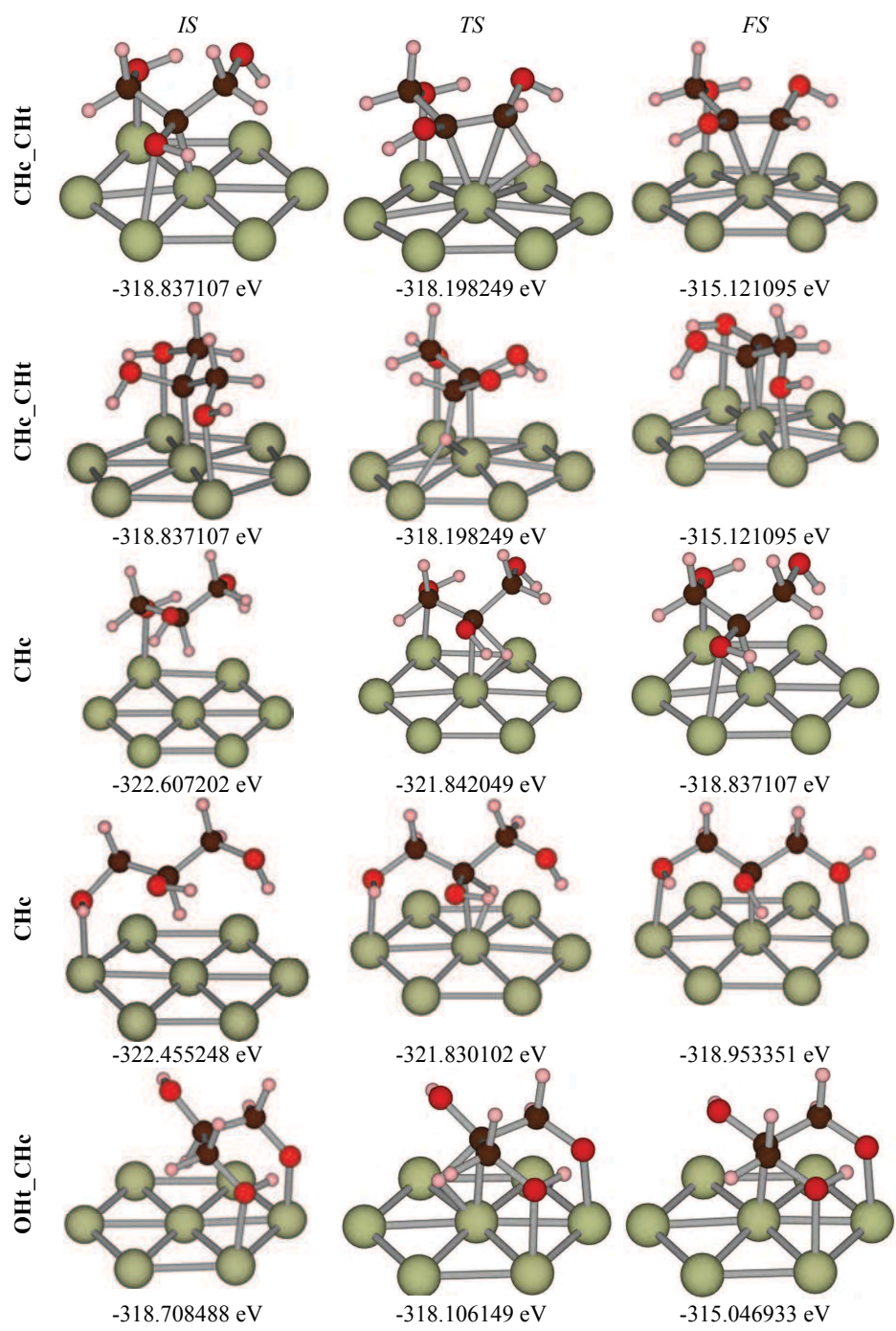
Each TS is confirmed by a unique imaginary frequency.

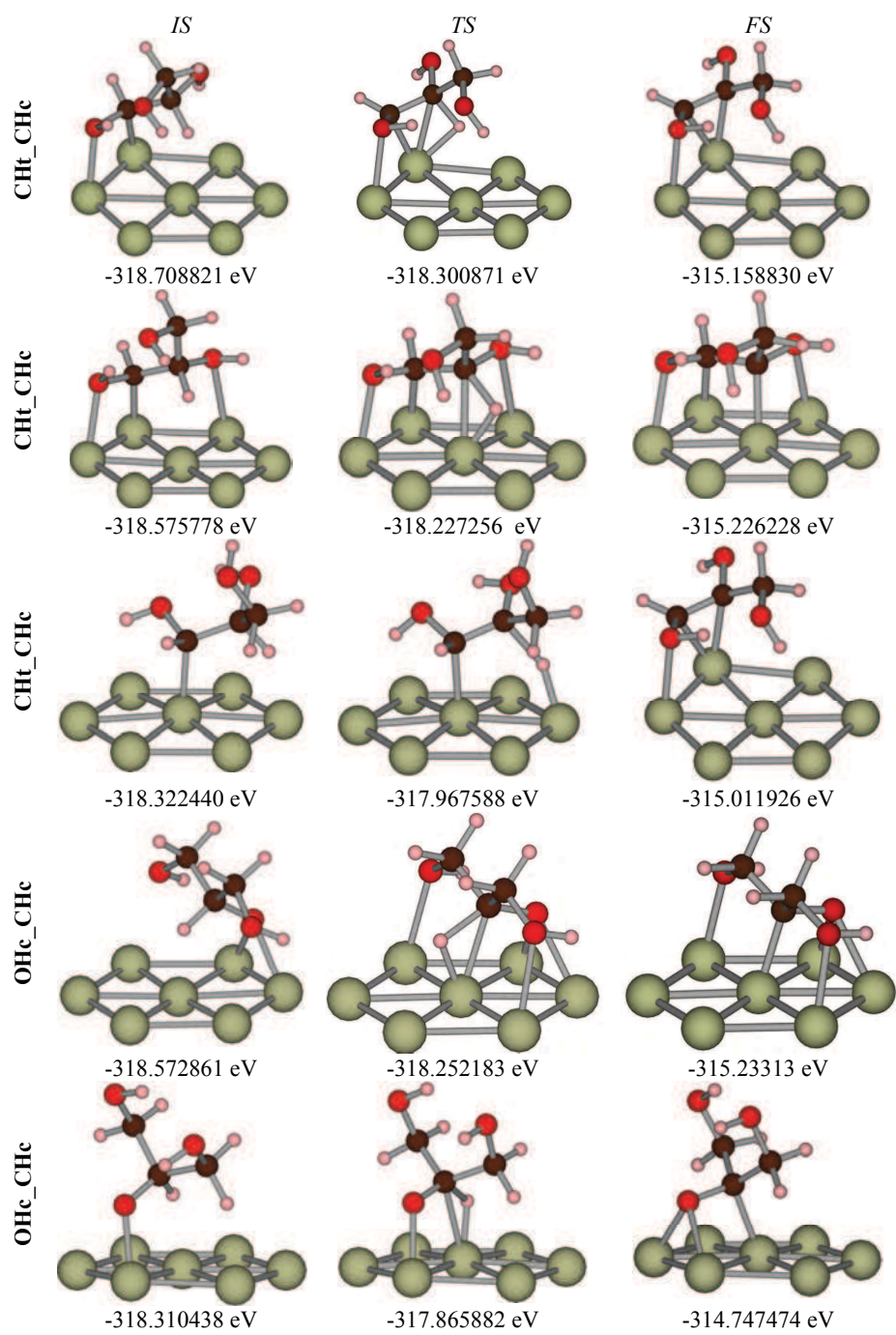
The notation we adopted is such that “CHt” means “dissociation of the terminal CH” and “CHt\_OHc” means “dissociation of the central OH in the glycerol that underwent a dissociation of the terminal CH before”

### CH dissociations

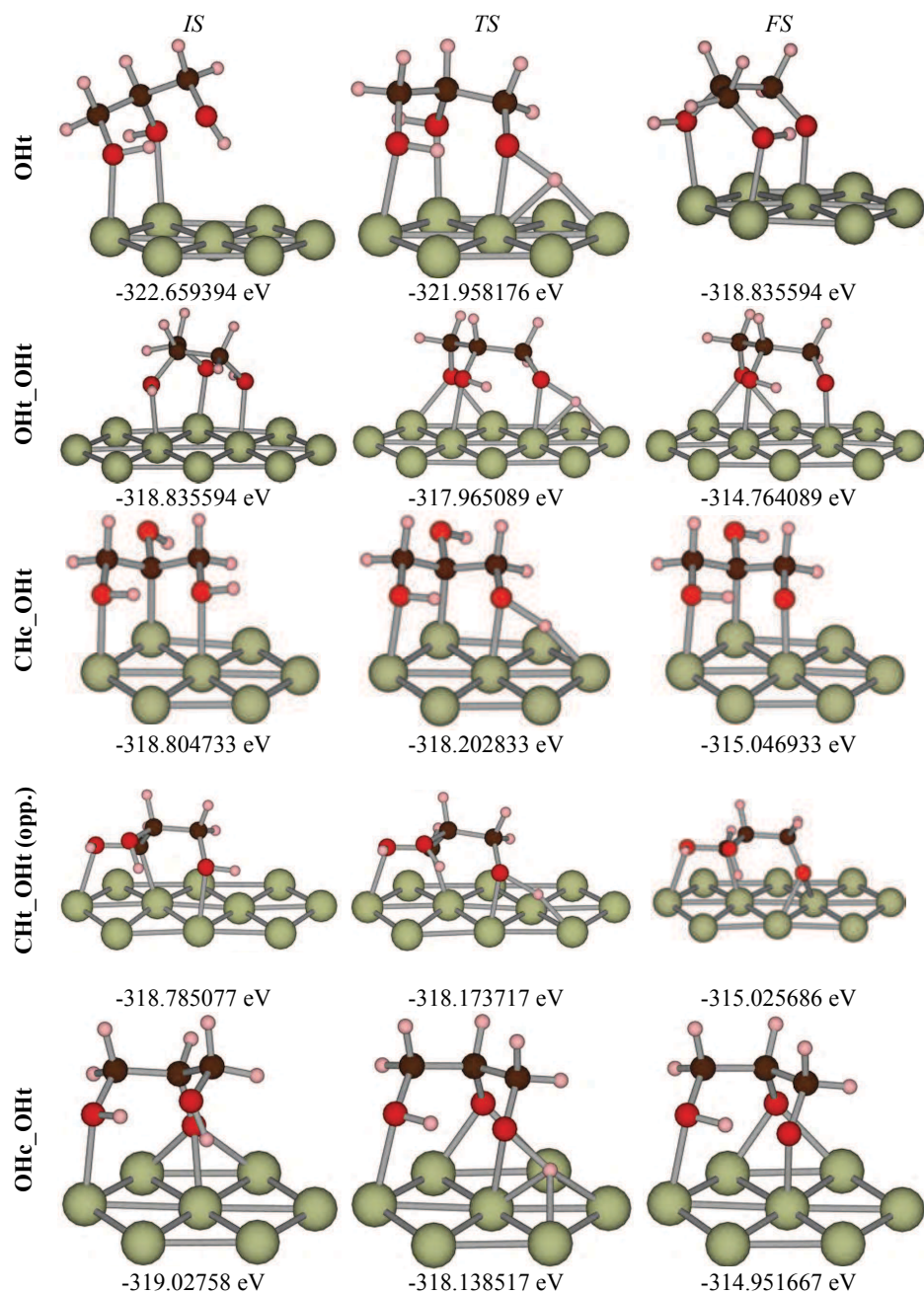


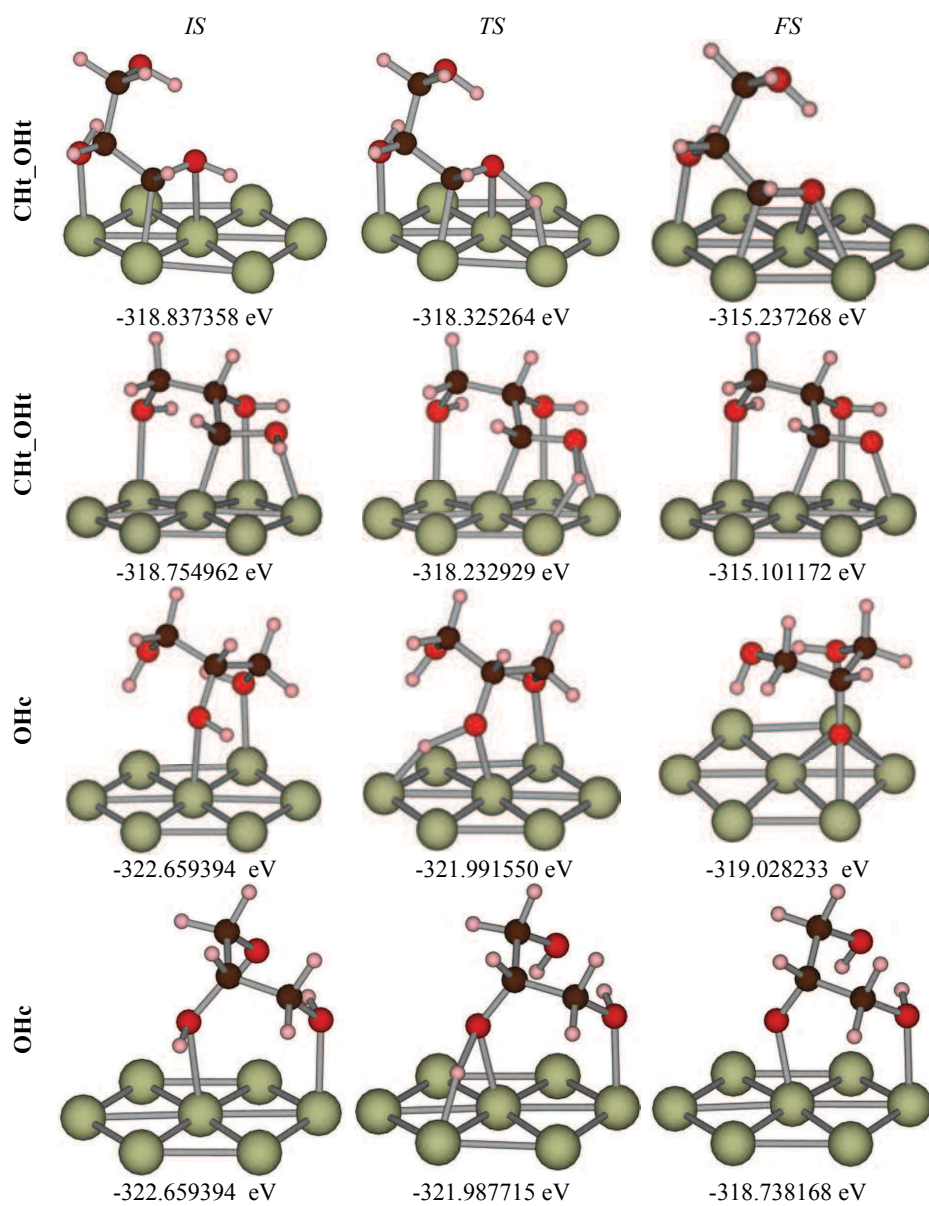


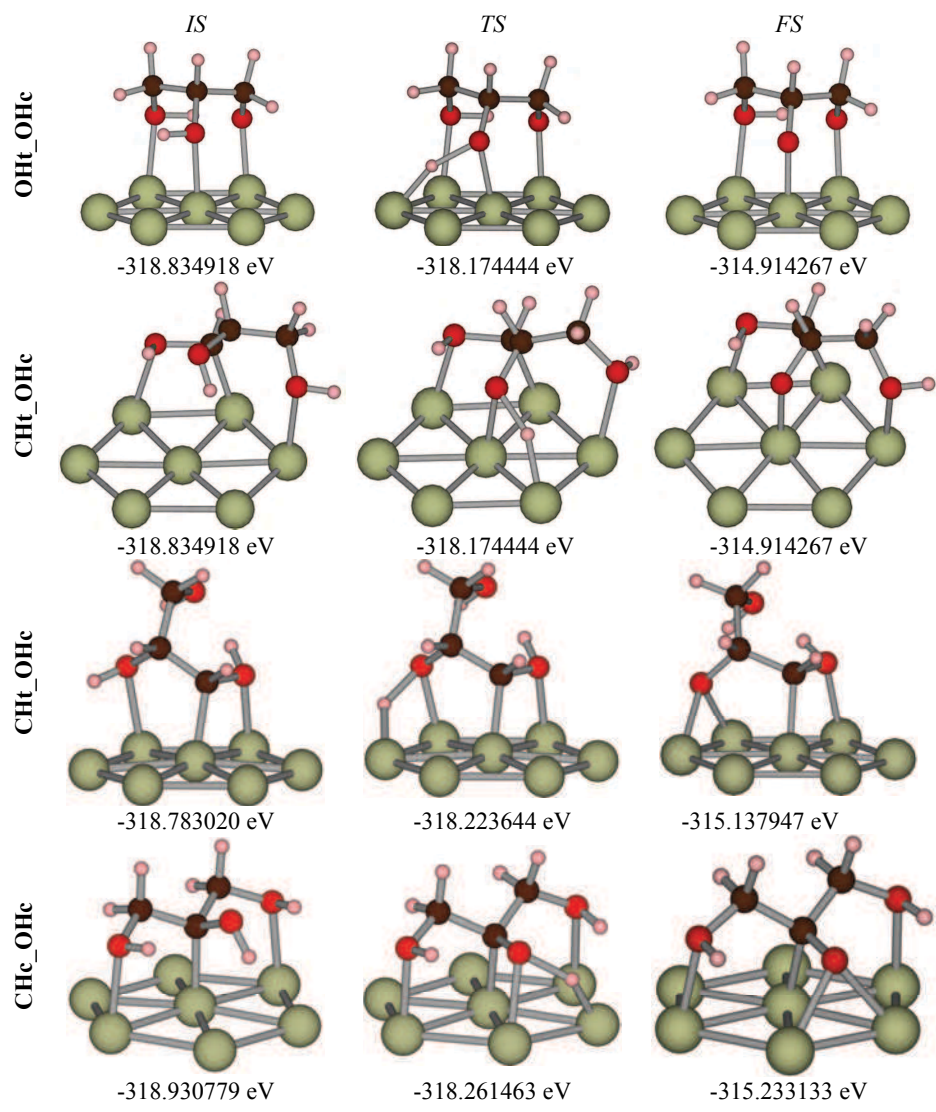




**OH dissociations**

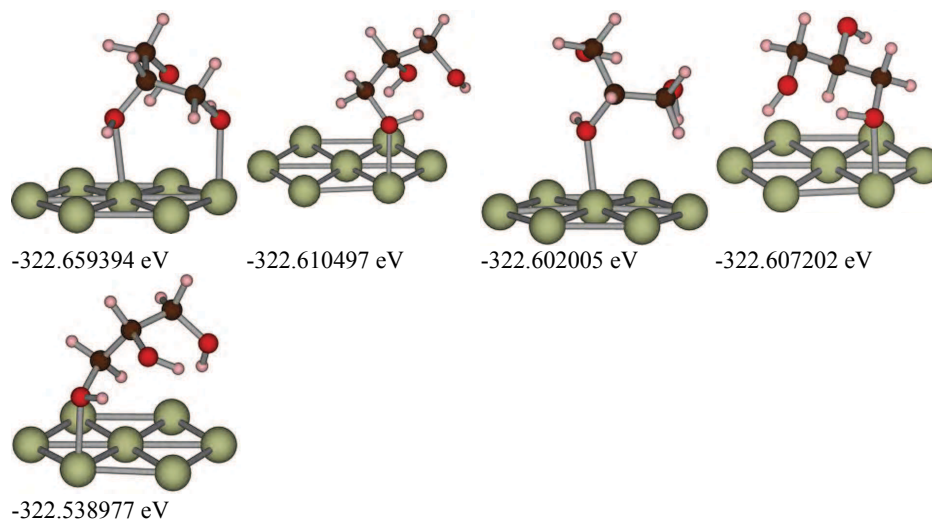




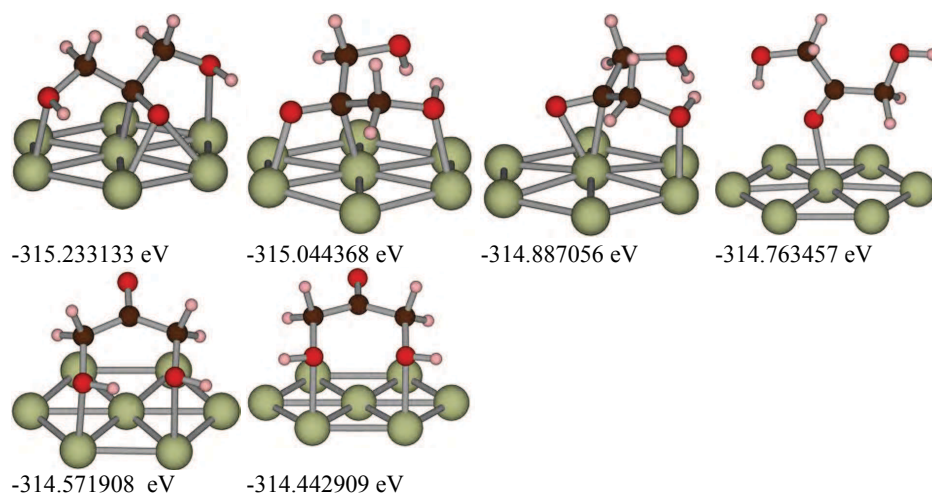


**Structure and energy of most relevant configurations of glycerol on Rh(111) and of the main dehydrogenation products**

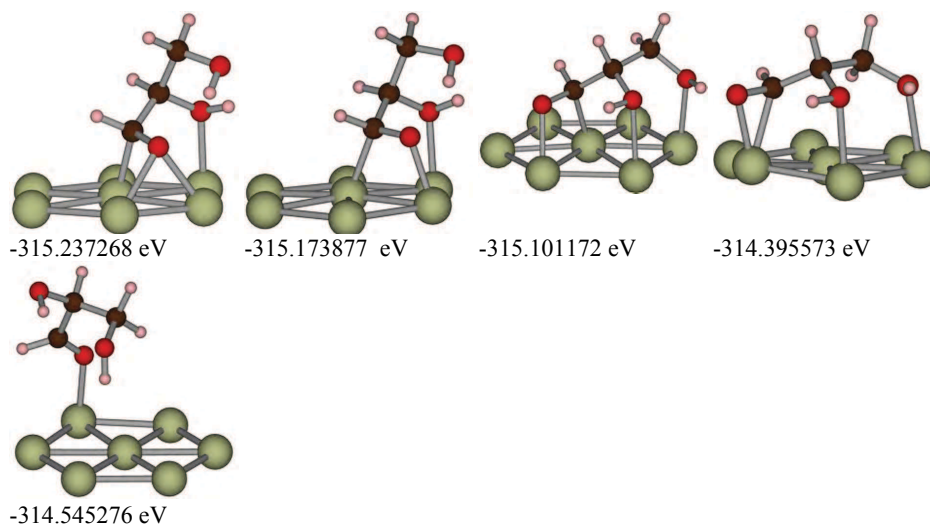
**Glycerol**



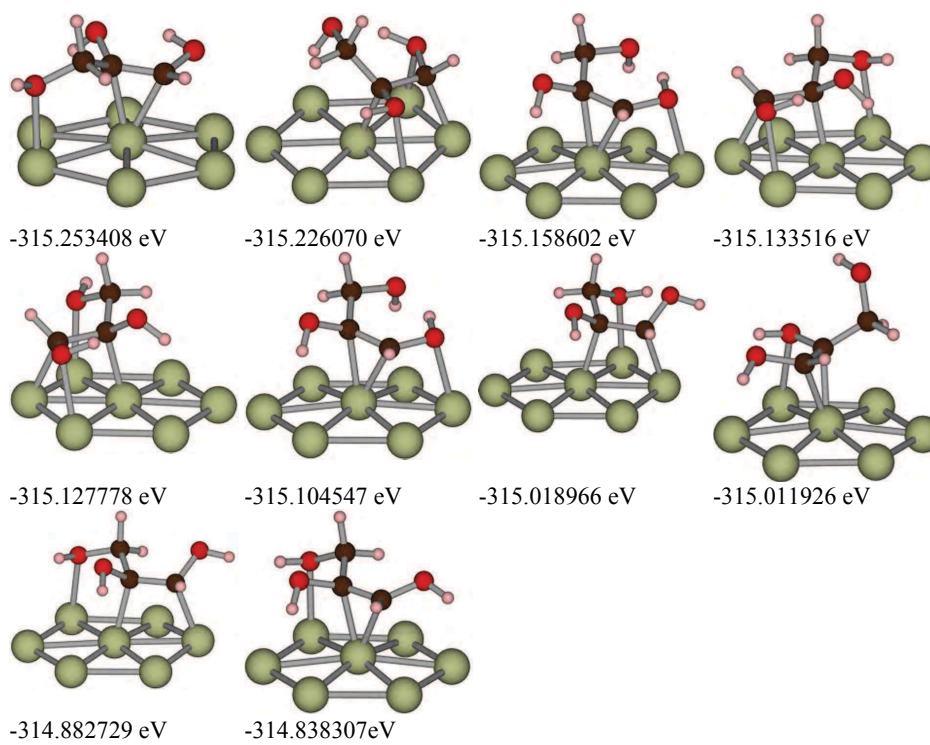
**Dihydroxyacetone**



**Glyceraldehyde**



**Enol**



---

## References

- <sup>1</sup> Kresse, G.; Hafner, J. *Phys. Rev. B* **1993**, *47*, 558-561.
- <sup>2</sup> Kresse, G.; Furthmüller, J. *Phys. Rev. B* **1996**, *54*, 11169-11186.
- <sup>3</sup> Perdew, J.P.; Wang, Y. *Phys. Rev. B* **1992**, *45*, 13244-13249.
- <sup>4</sup> Kresse, G.; Joubert, D. *Phys. Rev. B* **1999**, *59*, 1758-1775.
- <sup>5</sup> Henkelman, G.; Uberuaga, B.P.; Jónsson, H. *J. Chem. Phys.* **2000**, *113*, 9901-9904.
- <sup>6</sup> Henkelman, G.; Jónsson, H. *J. Chem. Phys.* **2000**, *113*, 9978-9985.
- <sup>7</sup> Heyden, A.; Bell, A. T.; Keil, F. J. *J. Chem. Phys.* **2005**, *123*, 224101.
- <sup>8</sup> Crawley, M.J *The R book*, 2<sup>nd</sup> ed.; John Willey & Sons: West Sussex, 2013.
- <sup>9</sup> Spatz, C. *Basic Statistics: Tales of Distributions* , 10<sup>th</sup> ed.; Wadsworth Cengage learning, 2010.

*Contact information:*

J r mie Zaffran

[zaffran.j@gmail.com](mailto:zaffran.j@gmail.com)